Lawrence Berkeley National Laboratory

Recent Work

Title
ACCELERATING THE LOOP EXPANSION

Permalink
https://escholarship.org/uc/item/9zr901d5

Author
Ingermanson, R.

Publication Date
1986-07-01

Lawrence Berkeley Laboratory
UNIVERSITY OF CALIFORNIA

Physics Division

ACCELERATING THE LOOP EXPANSION

R. Ingermanson
(Ph.D. Thesis)

July 1986

DISCLAIMER

Accelerating the Loop Expansion[1]

Randall Ingermanson

Department of Physics

and

Lawrence Berkeley Laboratory

University of California

Berkeley, California 94720, U.S.A.

Ph.D. Thesis

ABSTRACT

This thesis introduces a new non-perturbative technique into quantum field theory. To illustrate the method, I analyze the much-studied ϕ^4 theory in two dimensions. As a prelude, I first show that the Hartree approximation is easy to obtain from the calculation of the one-loop effective potential by a simple modification of the propagator that does not affect the perturbative renormalization procedure. A further modification then suggests itself, which has the same nice property, and which automatically yields a convex effective potential. I then show that both of these modifications extend naturally to higher orders in the derivative expansion of the effective action and to higher orders in the loop-expansion. The net effect is to re-sum the perturbation series for the effective action as a systematic "accelerated" non-perturbative expansion. Each term in the accelerated expansion corresponds to an infinite number of terms in the original series. Each term can be computed explicitly, albeit numerically. Many numerical graphs of the various approximations to the first two terms in the derivative expansion are given. I discuss the reliability of the results and the problem of spontaneous symmetry-breaking, as well as some potential applications to more interesting field theories.

Acknowledgements

At several points in the preparation of this thesis, I was tempted to abandon the whole idea. I would like to thank three people who helped prevent me from doing so. Dae Sung Hwang convinced me that the original idea was not nonsense. Orlando Alvarez's timely advice enabled me to make a midcourse adjustment. My wife Eunice forced me to repeatedly explain a certain difficulty to her, until I finally saw the way around it. I am grateful for technical advice, discussion and encouragement from fellow graduate students Z. Bern, H.S. Chan, O. Cheyette, M. Golden, J. Mañes, S. Mahajan, J. Yamron, as well as from members of the theory group at LBL, K. Bardakci, I. Hinchliffe and A. Niemi. I also thank the many relatives and friends whose personal support has made the past six years of graduate school more than just an academic exercise.

Contents

I   Introduction

1   The Effective Action

The classical action has played a crucial role in theoretical physics for over a century. In field theory, the dynamics of classical fields can be described by a local action functional

$$S = \int_x \mathcal{L}(\phi_x) \, .$$

(For simplicity, I consider a theory of one scalar field. Spacetime dependence is shown by a subscript: ϕ_x means $\phi(x)$. It is easy to generalize to spinors and vector particles as well as internal degrees of freedom.) $\mathcal{L}$ is a Lorentz-invariant function of ϕ_x and of a finite number of its derivatives. The equations of motion are then determined by the variational principle

$$\frac{\delta S}{\delta \phi_x} = 0 \, .$$

In quantum field theory, the classical action is supplanted by the "effective action", via the following somewhat circuitous route. Define

$$\sigma[J] \equiv S + \int_x J_x \phi_x \, .$$

It is extremely convenient to define the partition functional $Z[J]$ by the path integral formula

$$Z[J] \equiv e^{iW[J]} \equiv \int [d\phi] e^{i\sigma[J]/\hbar} \, .$$

(Hereafter, I will set $\hbar = 1$.)

In terms of Z we then have a simple formula for the correlation functions in the presence of the source J:

$$\underbrace{\langle \phi_x \phi_y \ldots \phi_z \rangle_J}_{n \text{ fields}} = \frac{1}{Z[J]} \int [d\phi] \, \phi_x \phi_y \ldots \phi_z \, e^{i\sigma[J]}$$

$$= e^{-iW[J]} (-i)^n \frac{\delta^n}{\delta J_x \delta J_y \ldots \delta J_z} e^{iW[J]} .$$

(1.1)

If we have some means of calculating $W[J]$, then (1.1) allows us to compute the vacuum correlation functions by taking $J \to 0$.

Instead of following this approach, it is sometimes convenient to perform a Legendre transformation on $W[J]$. Denote the mean field by

$$\Phi_x[J] \equiv \langle \phi_x \rangle_J$$

$$= \frac{\delta W}{\delta J_x} .$$

(1.2)

Then the effective action Γ is defined by

$$\Gamma[\Phi] \equiv W[J] - \int_x J_x \Phi_x .$$

Note that

$$\frac{\delta \Gamma}{\delta \Phi_x} = \int_y \frac{\delta W}{\delta J_y} \frac{\delta J_y}{\delta \Phi_x} - J_x - \int_y \frac{\delta J_x}{\delta \Phi_x} \Phi_y$$

$$= -J_x .$$

(1.3)

Furthermore,

$$\frac{\delta \Phi_z}{\delta J_y} = \frac{\delta^2 W}{\delta J_z \delta J_y} \qquad (1.4)$$

$$\frac{\delta J_z}{\delta \Phi_y} = -\frac{\delta^2 \Gamma}{\delta \Phi_z \delta \Phi_y}.$$

So

$$\int_y \frac{\delta^2 W}{\delta J_z \delta J_y} \frac{\delta^2 \Gamma}{\delta \Phi_y \delta \Phi_z} = -\delta_{zz}. \qquad (1.5)$$

Jona-Lasinio [1] showed long ago that $\Gamma[\Phi]$ gives the truncated one-particle-irreducible Feynman diagrams.

In contrast to the classical action, the effective action $\Gamma[\Phi]$ is non-local. One can expand it as

$$\Gamma[\Phi] = \int_z \Gamma_z^{(1)} \Phi_z + \tfrac{1}{2} \int_{z,y} \Gamma_{zy}^{(2)} \Phi_z \Phi_y + \dots$$

where

$$\Gamma_{z\dots y}^{(n)} \equiv \left[\frac{\delta^n}{\delta \Phi_z \dots \delta \Phi_y} \Gamma[\Phi] \right]_{\Phi=0}.$$

This is useful when computing scattering amplitudes, but there is another expansion which is better for studying the low-energy content of the theory. The derivative expansion is given by

$$\Gamma[\Phi] = \int_z \left[-V(\Phi_z) + \tfrac{1}{2} Z(\Phi_z)(\partial_\mu \Phi_z)^2 + \dots \right], \qquad (1.6)$$

where V and Z are ordinary functions. Since Γ is non-local, there are an infinite number of terms in this expansion. $V(\Phi)$ is called the effective potential. $Z(\Phi)$ should not be confused with the partition functional $Z[J]$.

2 · On the Effective Potential

Consider the case where the source is translationally invariant:

$$J_x = \hat{J} = \text{constant}.$$

Then $\Phi[J]$ must also be translationally invariant and we can define $\hat{\Phi}(\hat{J}) \equiv \Phi[\hat{J}]$, which is also a constant. So all the derivative terms in the expansion (1.6) of Γ vanish and

$$\Gamma[\hat{\Phi}] = -V(\hat{\Phi}) \cdot \left(\int_x\right),$$

where $\left(\int_x\right)$ = volume of spacetime. Similarly, $W[\hat{J}] = -E(\hat{J}) \cdot (\int_x)$, where $E(\hat{J})$ is the energy of the system. One can easily show [2] that $V(\hat{\Phi})$ is the work/$(\int_x)$ required to move from the vacuum state ($J = 0$) to the state determined by $J_x = \hat{J}$. V and E are related by

$$V(\hat{\Phi}) = E(\hat{J}) + \hat{J}\hat{\Phi}. \tag{1.7}$$

Also, we have the relations, which follow from (1.2) and (1.3),

$$\hat{\Phi}(\hat{J}) = -\frac{dE}{d\hat{J}}$$

$$\hat{J}(\hat{\Phi}) = \frac{dV}{d\hat{\Phi}}. \tag{1.8}$$

Two important features of the effective potential are that 1) V is real, and 2) V is convex [3]. The fact that V is real follows from (1.7). A simple proof that V is convex is given by Calloway and Maloof [4], where it is

shown that

$$\frac{d^2V}{d\hat{\Phi}^2} \geq 0.$$

I will return to these important points after discussing briefly the common methods for computing $V(\hat{\Phi})$.

First, let me point out what is the main "industrial" use for $V(\hat{\Phi})$. Since the vacuum is the lowest energy state, the vacuum value of $\hat{\Phi}$ minimizes $V(\hat{\Phi})$:

$$\left.\frac{dV}{d\hat{\Phi}}\right|_{\hat{\Phi}=\hat{\Phi}_{vac}} = 0.$$

Thus, we compute $V(\hat{\Phi})$ as a test for spontaneous symmetry breaking.

This test was introduced by Coleman and Weinberg [5], using a somewhat cumbersome version of the loop-expansion. Jackiw [6] then showed how to simplify the computations of the loop-expansion, in an elegant paper which tamed the combinatorial jungle inherent in the Coleman-Weinberg approach.

Jackiw's paper is still the standard reference for practical calculations. In principle, however, one *could* do much better. Cornwall, Jackiw and Tomboulis [7] (CJT) showed how to extend this method to composite operators. As a bonus, this extension allows one to formally rewrite Jackiw's loop-expansion much more compactly. Each diagram in this formal expansion corresponds to an infinite number of diagrams in Jackiw's expansion! Unfortunately, this beautiful development is difficult or impossible to use in

practical calculations, except to lowest order in the coupling constant. In this case, one finds the same results as can be obtained by the Hartree approximation, which for scalar theories gives the same results as a variational calculation using a Gaussian wavefunctional [8]. See Jackiw's lectures [9] for a review of all of these approximations.

The Hartree approximation (hereafter called simply the Gaussian approximation) is non-perturbative, since it basically sums up all the "easy" diagrams in Jackiw's loop-expansion to all orders in perturbation theory. Unfortunately, procedures for systematically improving the Gaussian approximation are hard to come by. CJT's method is impractical; a suggestion due to Stevenson [10] has not yet been carried out; another approximation using the "coupled cluster approximation" [11, 12, 13] looks interesting, but involves complicated and unfamiliar techniques. In quantum mechanics, the Gaussian approximation works very well [10]. However, it is not clear how good the approximation is for field theory. In scalar theories, it includes all one-loop diagrams, but not all two-loop diagrams. (Furthermore, there is a technical complication called "examining the end-points" [14], which can muddy the waters. If this complication is ignored, then one may find the wrong vacuum (as pointed out in [14]), or no vacuum at all [15], or may be forced to restrict the range of definition of the effective potential [12, 16].)

Despite these disadvantages, the Gaussian approximation has some very

nice features. It can be extended to soliton systems rather straightforwardly [17, 18]. Recently, it has also been used to compute higher-order terms in the derivative expansion of the effective action [12].

One test of the validity of the loop-expansion (and also of the Gaussian approximation) is the following pair of questions. Is the resulting effective potential real? Is it convex? The answers are somewhat disappointing.

The loop-expansion yields a real effective potential if and only if the classical potential $U(\phi)$ is convex: $U''(\phi) \geq 0$. For all values of ϕ at which U is not convex, the perturbative effective potential is complex to every finite order in the loop-expansion. (Yet, the sum of the series is real. For a very nice discussion of the reality and convexity of the effective potential from the functional viewpoint, see [19].) Furthermore, the perturbative expansion does not necessarily yield a convex effective potential.

The Gaussian effective potential performs somewhat better. It is always real; however, it is not necessarily convex.

It has been argued that the convexity property is "silly" [10]. I disagree; it is no more silly than the reality property. Convexity is an important non-perturbative property that powerfully constrains the effective potential. Any computation that yields a non-convex effective potential is wrong. (Though not necessarily wrong everywhere. It may be wrong over only a small domain, as we shall see later.)

If convexity is not silly, it is nonetheless annoying. Naively, it appears to rule out the double-well type of potential so familiar in spontaneous symmetry-breaking. Much of modern particle physics relies on symmetry-breaking: pion physics, electro-weak breaking via the still-unseen Higgs boson, GUT breaking to the standard $SU(3) \times SU(2) \times U(1)$ and the resulting inflationary universe. Yet symmetry-breaking apparently depends on the fragile concept of a non-convex potential. How can convexity be harmonized with symmetry-breaking? The answer is that the double-well vanishes (in a sense), but the symmetry-breaking remains [20]. But more of this in due time.

I can now explain the purpose of this thesis. I have found two new systematic approximations for computing the effective potential (as well as higher-derivative terms in the effective action). Both approximations improve on the loop-expansion (and also on the Gaussian approximation). Both can be regarded as being intermediate between Jackiw's loop-expansion and the much improved formal expansion of CJT.

The first approximation I will describe is simply a combination of the loop-expansion and the Gaussian approximation. It enables one to do an infinite number of diagrams at each stage of the loop-expansion, by a simple modification of the propagator. I call this approximation the n-loop Gaussian approximation. The one-loop version of this approximation is just the recently revived Gaussian approximation [10, 14, 21, 22]. Unfortunately,

the resulting effective potential is not necessarily convex.

The second approximation is an improvement on the n-loop Gaussian approximation and automatically yields a convex effective potential. Again, the method requires only a slight modification of the propagator. Despite this, the effect on the resulting effective potential can be dramatic. For reasons to be explained later, I call this approximation the n-loop self-consistent approximation.

An important property of both of these approximations is that the familiar perturbative techniques (Feynman diagrams, loop integrals, renormalization) can be imported wholesale.

3 A Preview

This thesis is organized as follows.

For the sake of concreteness, I will analyze in some detail the ϕ^4 model in two dimensions. Although this model actually describes some physical systems rather well, (e.g., polyacetylene [23]), I will ignore any real-world applications. I choose to study ϕ_2^4 because the model is simple enough to make calculations easy, (especially renormalization), but rich enough to exhibit the nice features of the self-consistent approximation. In addition, there are a number of rigorous facts known about the model, which enable me to check qualitatively my approximations.

In Section 2, I will review some of these facts, and show how previous calculations measure up against these rigorous results. I will anticipate points where the self-consistent approximation improves on previous calculations. Last, I will discuss briefly the fate of the classical double-well potential.

An important technical tool which I will use extensively in this thesis is the Schwinger-Dyson equation. In Section 3, to establish my notation, I will derive this equation for ϕ_2^4 and give the standard graphical interpretation. This leads naturally to the loop-expansion. I will then exhibit a special case of the Schwinger-Dyson equation which describes the effective potential non-perturbatively.

The first real calculation comes in Section 4. I calculate the well-known one-loop effective potential in a way that makes it natural to generalize to both the Gaussian approximation and the self-consistent approximation. Using the Schwinger-Dyson equation, I then motivate and carry out these generalizations. Finally, I compare the results, exhibiting a number of computer-generated graphs.

In Section 5, I show how similar calculations can be done straightforwardly for higher-derivative terms in the effective action, again using the Schwinger-Dyson equation. Results are plotted for the first term in the derivative expansion.

The problem of generalizing the Gaussian approximation and the self-

consistent approximation to n loops is straightforward, and requires only the standard techniques of Feynman diagram calculation. I demonstrate this in Section 6 by doing an explicit computation for two loops. Continuation to higher loops is then obvious, though increasingly tedious. I also consider the question of the reliability of our results, and propose a tentative answer. Finally, I show that a further improvement is possible at two loops and beyond; more graphs are displayed, showing the effects of this improvement.

In Section 7, I consider the problem of spontaneous symmetry-breaking. The computations of Section 4 are modified to the broken-symmetry phase and the various approximations to the effective potential are compared.

I summarize the basic ideas in Section 8, and state conclusions. Also, I suggest some obvious (and some speculative) ideas for continuing the line of research for which this thesis is the first step.

II · A Review of ϕ_2^4

1 The Classical Model

The model we will investigate is described by the Lagrangian

$$\mathcal{L} = \tfrac{1}{2}(\partial_\mu \phi)^2 - U(\phi),$$

where U is the classical potential

$$U(\phi) \equiv \tfrac{1}{2}m^2\phi^2 + \frac{\lambda}{24}\phi^4.$$

If $m^2 > 0$, then $U(\phi)$ has a unique minimum at $\phi = 0$. I will call this situation the *symmetric phase*.

If $m^2 < 0$, then $U(\phi)$ has degenerate minima at $\phi = \pm F$, where

$$F^2 \equiv \frac{-6m^2}{\lambda}. \tag{2.1}$$

It is then preferable to expand U about one of the minima, say $+F$. Up to a constant, U is given by

$$U(\phi) = \frac{\lambda F^2}{6}(\phi - F)^2 + \frac{\lambda F}{6}(\phi - F)^3 + \frac{\lambda}{24}(\phi - F)^4$$

$$= \frac{M^2}{2}(\phi - F)^2 + \frac{g}{6}(\phi - F)^3 + \frac{\lambda}{24}(\phi - F)^4,$$

where

$$M^2 \equiv \tfrac{1}{3}\lambda F^2 = U''(F)$$

$$g \equiv \lambda F = U'''(F)$$

$$\lambda = U''''(F).$$

I have chosen to eliminate m^2 in favor of M^2 above, with an eye toward future renormalization. We will see that M^2 requires a log-divergent counterterm, while g and λ are only finitely renormalized.

The case $m^2 < 0$ is called the *broken-symmetry phase*, or more simply, the broken phase.

Note that we go from one phase to the other by sending m^2 through zero. For simplicity of notation, I will denote the physical mass by m_R, defined as:

$$m_R^2 = \begin{cases} m^2, & \text{if } m^2 \geq 0; \\ M^2 \quad (= -2m^2), & \text{if } m^2 < 0. \end{cases}$$

So classically, the phase transition is attained only by sending m_R^2 down to zero and then bringing it up again. This trivial fact has important consequences. Observe that the dimensions of m_R^2, g and λ are all $[\text{mass}]^2$. Also

$$g = \begin{cases} 0, & \text{(symmetric phase)} \\ \sqrt{3\lambda m_R^2}, & \text{(broken phase)} \end{cases}$$

so only m_R^2 and λ are independent quantities. Either one of these can be

used to set the scale. The only truly independent quantity is the ratio

$$\tilde{\lambda} \equiv \frac{\lambda}{m_R^2}.$$

Now, perturbation theory will be unreliable in the limit $\lambda \to \infty$, (at fixed m_R), or equivalently, $\tilde{\lambda} \to \infty$. Clearly, this means that perturbation theory is also unreliable for λ fixed and $m_R \to 0$. (This fact is well-known [24].) This apparently means that perturbative methods are completely untrustworthy near the phase transition. This argument has a possible flaw, however. The conclusion depends on the (classical) premise that the phase transition occurs at $m_R = 0$. It can be rigorously shown that this premise is correct at the quantum level. (See [25] for a synopsis.) We conclude that a perturbative analysis of the phase transition is risky business.

2   Rigorous Results

In axiomatic field theory, Simon and Griffiths [26] showed that our model cannot have a first-order phase transition. This means that, *if there is a phase transition*, then the vacuum expectation value of ϕ must vary continuously through the transition. For example, in the classical model, the phase transition satisfies this criterion. From (2.1), we see that ϕ_{min} is continuous, where

$$\phi_{min} = \begin{cases} 0, & m^2 \geq 0 \\ \sqrt{-6m^2/\lambda}, & m^2 < 0 \end{cases}$$

is the value of the field at which the potential is minimized.

On a slightly less rigorous level, Chang [25] showed that there *is* a phase transition by means of the following trick. Above, we defined $\tilde{\lambda} = \lambda/m_R^2$, a dimensionless constant, which uniquely specifies the model. (Actually, one must also specify the *phase* of the model, either broken or symmetric.) For our purposes, however, $\tilde{\lambda}$ is not quite appropriate. Define $\hat{\lambda} = \lambda/\mu^2$, where μ is some parameter with dimensions of [mass]. Start with a classical Hamiltonian, in either the broken or the symmetric phase, and normal-order it with respect to μ. Up to scale, the resulting quantum Hamiltonian is specified completely by the phase and by $\hat{\lambda}$. Now consider two Hamiltonians, one of which is classically in the symmetric phase, specified by $\hat{\lambda}_S$, the other which is classically in the broken phase, specified by $\hat{\lambda}_B$. A priori, there is no relation whatsoever between the two Hamiltonians, not even if $\hat{\lambda}_S = \hat{\lambda}_B$. Chang showed that it is possible that the two Hamiltonians are *identical*, after normal-ordering, if $\hat{\lambda}_B$ and $\hat{\lambda}_S$ satisfy a particular relation. The method of proof was to use Coleman's re-normal-ordering formulae [15]. Equality holds if and only if $\hat{\lambda}_B$ and $\hat{\lambda}_S$ satisfy

$$\hat{\lambda}_S \exp\left(\frac{-8\pi}{\hat{\lambda}_S}\right) = \hat{\lambda}_B \exp\left(\frac{4\pi}{\hat{\lambda}_B}\right). \tag{2.2}$$

(I have altered the form of Chang's equation (2.14) slightly.)

(2.2) can be solved numerically. I have plotted $\hat{\lambda}_S$ versus $\hat{\lambda}_B$ in Fig. (2.1). Not surprisingly, large $\hat{\lambda}_B$ corresponds to large $\hat{\lambda}_S$. As $\hat{\lambda}_B$ decreases.

$\hat{\lambda}_S$ decreases down to the point where $\hat{\lambda}_B = 4\pi$, $\hat{\lambda}_S \simeq 54.270$. Decreasing $\hat{\lambda}_B$ further is equivalent to *increasing* $\hat{\lambda}_S$. (Thus, we need only consider $\hat{\lambda}_B \leq 4\pi$. For $\hat{\lambda}_B > 4\pi$, the model is equivalent to some other model with $\hat{\lambda}_B \leq 4\pi$, and both are equivalent to a third model with $\hat{\lambda}_S$ determined by Fig. (2.1).) As $\hat{\lambda}_B \to 0$, $\hat{\lambda}_S \to \infty$. For $\hat{\lambda}_B$ sufficiently small, the model will be in the broken phase. Hence, for some $\hat{\lambda}_{S,crit} \geq 54.270$, corresponding to some $\hat{\lambda}_{B,crit} \leq 4\pi$, the model undergoes a phase transition from the symmetric to the broken phase.
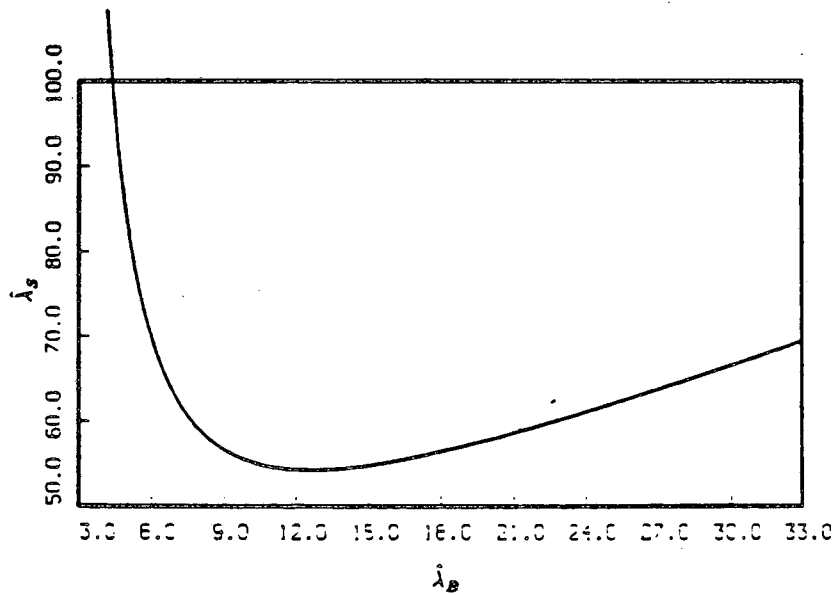
Figure (2.1): Plot of $\hat{\lambda}_B$ versus $\hat{\lambda}_S$ given by equation (2.2).

3 Perturbative Results

I will review the calculation of the perturbative effective potential in Section 4. What we will find is the following:

1. In the symmetric phase, the model undergoes a first-order phase transition as $\tilde{\lambda}$ increases, in both the one-loop and two-loop approximations. The effective potential is real, but not necessarily convex.

2. In the broken phase, a first-order phase transition is inferred from the fact that there is a minimum possible value for F. The effective potential is complex for $\Phi^2 < \frac{1}{3}F^2$, and is not convex.

4 Variational Results

The Gaussian approximation is basically a variational method, in which trial wave-functionals are Gaussian [8]. Chang [27] computed the Gaussian effective potential; it is real, but not necessarily convex. The effective potential always has a local minimum at $\hat{\Phi} = 0$. There is a first-order phase transition. (Stevenson [10] found similar results for the models in one, two and three dimensions, as well as a new "precarious" field theory in four dimensions.)

Drell, Weinstein and Yankielowicz [28] duplicated some of Chang's results. They also performed a different variational calculation, on the lattice, in which they showed that a relatively simple family of ground state wave-functionals lead to a *second-order* phase transition. In the broken phase, for small F^2, (i.e., near the phase transition), they showed that solitons are light and play an important role.

5   Lattice Results

Calloway and Maloof [4] analyzed ϕ^4-theory using Monte Carlo methods on a 4^4 lattice. They first presented a qualitative dimension-independent analysis of the *continuum* ϕ^4 model, which concluded that the effective potential should be a flat-bottomed well. (I will give a quick demonstration of this fact in the next subsection, using a different method.)

Calloway and Maloof then computed $\hat{\Phi}(\hat{J})$ numerically, on the lattice. Inverting this to find $\hat{J}(\hat{\Phi})$, they integrated our equation (1.8) to obtain $V(\hat{\Phi})$:

$$V(\Phi) = \int_0^\Phi d\hat{\Phi}\, V'(\hat{\Phi}) = \int_0^\Phi d\hat{\Phi}\, \hat{J}(\hat{\Phi}). \qquad (2.5)$$

For a finite lattice, the result of this calculation is necessarily analytic. Thus, it is impossible to obtain a true flat-bottomed well. However, their numerical results for large coupling constant show a distinctly flattened out single-well potential.

6   On the Fate of the Double-well

Suppose that the classical potential is a double-well, as shown in Fig. (2.2).
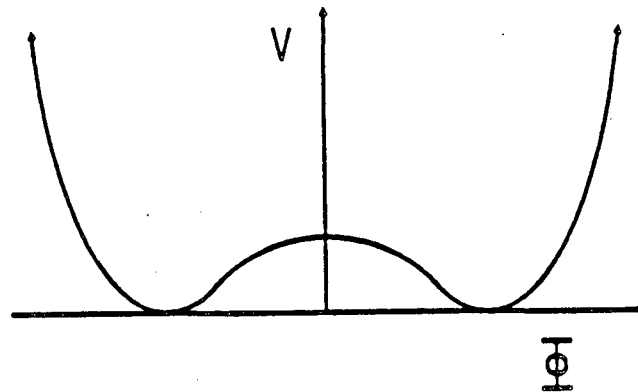
Figure (2.2): Typical double-well potential.

The question is: what happens to the effective potential? The perturbative and Gaussian results suggest that the potential will have at least two isolated minima. We can dispense with this idea, thanks to the convexity requirement. The potential must be a single well. What form will it take?

After taking account of quantum effects, the symmetry will either remain broken or be restored.

If the symmetry is restored, then there is a single minimum at $\Phi = 0$.

If the symmetry is broken, then there are two orthogonal vacuum states $|\Omega_{\pm}\rangle$ satisfying

$$\langle \Omega_{\pm}| \phi_x |\Omega_{\pm}\rangle = \pm F.$$

Adding a constant to the Hamiltonian such that

$$\langle \Omega_{\pm}| H |\Omega_{\pm}\rangle = 0,$$

we define the one-parameter family of states

$$|\Omega_t\rangle = \sqrt{\tfrac{1}{2}(1+t)}\,|\Omega_+\rangle + \sqrt{\tfrac{1}{2}(1-t)}\,|\Omega_-\rangle ,$$

where $-1 \leq t \leq 1$. Then we have

$$\langle\Omega_t|\,H\,|\Omega_t\rangle = 0,$$

$$\langle\Omega_t|\,\phi_z\,|\Omega_t\rangle = tF.$$

So qualitatively, the effective potential looks as shown in Fig. (2.3).
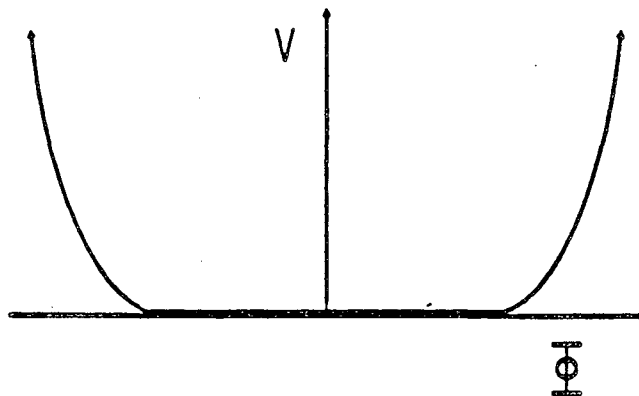
Figure (2.3): Qualitative form of effective potential when symmetry is broken.

The above line of reasoning is fairly well-known [20]. Different arguments which lead to the same conclusion are given in [2, 19].

As we already noted, the flat-bottomed potential well is non-analytic at $\hat{\Phi} = \pm F$. The perturbative and Gaussian approximations for the region

$|\hat{\Phi}| \leq F$ should be regarded as analytic continuations of $V(\hat{\Phi})$ from the region $|\hat{\Phi}| \geq F$. These are useful in the sense that they give the potential energy density of metastable field configurations [29]. Furthermore, they give an approximation to the zero-momentum scattering amplitudes, information which is already available from the non-flat part of $V(\hat{\Phi})$.

We can now see how symmetry-breaking can be harmonized with the convexity of V. Symmetry breaking requires only that the vacuum expectation value of the field be non-zero, which is clearly consistent with the convex, flat-bottomed potential sketched in Fig. (2.3).

III   Schwinger-Dyson Equations

1   The Main Equation

In this section, I will review the derivation of the quantum equation of motion, the Schwinger-Dyson equation [30]. For ϕ_2^4, the only divergence we need worry about is the mass term. Both the coupling constant and the wave-function renormalization are finite. I will not renormalize the coupling constant but I *will* compute the wave-function renormalization.

The Lagrangian will be rewritten as

$$\mathcal{L} = \tfrac{1}{2}K^2(\partial_\mu\phi)^2 - U(\phi)$$

$$U(\phi) \equiv \tfrac{1}{2}m^2K^2\phi^2 + \frac{\lambda K^4}{24}\phi^4.$$

Here, ϕ is the renormalized quantum field, m is the bare mass, λ the bare coupling and K (usually denoted $\sqrt{Z_\phi}$) is the bare wave-function renormalization.

As before, $S = \int_x \mathcal{L}(\phi_x)$ and one finds

$$-\frac{\delta S}{\delta\phi_x} = K^2(\partial_x^2 + m^2)\phi_x + \frac{\lambda K^4}{6}\phi_x^3.$$

The classical equation of motion states that this quantity vanishes. The quantum equation of motion follows from the fact that the integral of a

derivative is trivial:

$$0 = -i \int [d\phi] \frac{\delta}{\delta \phi_z} e^{i\sigma[J]}$$

$$= \int [d\phi] \left(J_z + \frac{\delta S}{\delta \phi_z} \right) e^{i\sigma[J]}$$

$$= \left[J_z + \frac{\delta S}{\delta \phi_z} \bigg|_{\phi_z = -i \frac{\delta}{\delta J_z}} \right] \underbrace{\int [d\phi] e^{i\sigma[J]}}_{e^{iW[J]}} .$$

One then finds that

$$J_z = e^{-iW[J]} \left(-\frac{\delta S}{\delta \phi_z} \bigg|_{\phi_z = -i \frac{\delta}{\delta J_z}} \right) e^{iW[J]} \tag{3.1}$$

$$= K^2 (\partial_z^2 + m^2) \frac{\delta W}{\delta J_z} + \frac{\lambda K^4}{6} \left[\left(\frac{\delta W}{\delta J_z} \right)^3 - 3i \left(\frac{\delta^2 W}{\delta J_z^2} \right) \frac{\delta W}{\delta J_z} - \frac{\delta^3 W}{\delta J_z^3} \right] .$$

This is the Schwinger-Dyson equation, expressed in terms of J and $W[J]$.

As in Section 1, we perform a Legendre transform

$$\Gamma[\Phi] = W[J] - \int_z J_z \Phi_z ,$$

where

$$\Phi_z \equiv \frac{\delta W}{\delta J_z} .$$

It is convenient to simplify the functional derivative notation:

$$\Gamma_z \equiv \frac{\delta \Gamma}{\delta \Phi_z}$$

$$\Gamma_{zy} \equiv \frac{\delta^2 \Gamma}{\delta \Phi_z \delta \Phi_y} \qquad \text{etc.,}$$

and similarly for the functional derivatives of $W[J]$.

In this notation, we can rewrite equations (1.3), (1.4) and (1.5) as

$$\Gamma_z = -J_z$$

$$\frac{\delta \Phi_z}{\delta J_y} = W_{zy}$$

$$\frac{\delta J_z}{\delta \Phi_y} = -\Gamma_{zy}$$

$$W_{zy} = -\Gamma_{zy}^{-1}.$$

Differentiating the last of these, we find

$$W_{zyz} = -\int_{a,b,c} \Gamma_{za}^{-1} \Gamma_{yb}^{-1} \Gamma_{zc}^{-1} \Gamma_{abc}.$$

The Schwinger-Dyson equation (3.1) becomes

$$-\Gamma_z = K^2(\partial_z^2 + m^2)\Phi_z + \frac{\lambda K^4}{6}\Phi_z^3 \qquad (3.2)$$

$$+ \frac{\lambda K^4}{2}(i\Gamma_{zz}^{-1})\Phi_z + \frac{\lambda K^4}{6}\int_{a,b,c} \Gamma_{za}^{-1} \Gamma_{zb}^{-1} \Gamma_{zc}^{-1} \Gamma_{abc}.$$

(3.2) contains the full content of the quantum theory. Ideally, one would

1) solve this functional differential equation for Γ_z, and then 2) reconstruct

$\Gamma[\Phi]$ by the formula

$$\Gamma[\Phi] = \Gamma[0] + \int_0^1 ds \int_z \Phi_z \Gamma_z[s\Phi]. \qquad (3.3)$$

(This formula follows by noting that

$$\frac{d}{ds}\Gamma[s\Phi] = \int_z \Phi_z \Gamma_z[s\Phi].$$

Note the similarity of (3.3) to Wess and Zumino's low-energy effective action, derived by integrating the anomaly [31].)

Unfortunately, reality usually falls far short of the ideal. It is ordinarily impossible to carry out step (1) above; (3.2) is too hard to solve. The standard procedure is to solve it perturbatively, by iteration and truncation. This generates the loop-expansion, which I will now discuss more formally.

2 The Loop Expansion

First, let us see what is involved in the iterative solution of the Schwinger-Dyson equation (3.2). Functionally differentiating, we have

$$-\Gamma_{zy} = K^2(\partial_z^2 + m^2)\delta_{zy} + \frac{\lambda K^4}{2}\Phi_z^2\delta_{zy} \tag{3.4}$$

$$+ \frac{\lambda K^4}{2}(i\Gamma_{zz}^{-1})\delta_{zy} - \frac{\lambda K^4}{2}\Phi_z\left(i\int_{a,b}\Gamma_{za}^{-1}\,\Gamma_{zb}^{-1}\,\Gamma_{aby}\right)$$

$$+ \frac{\lambda K^4}{6}\int_{a,b,c}\Gamma_{za}^{-1}\,\Gamma_{zb}^{-1}\,\Gamma_{zc}^{-1}\,\Gamma_{abcy}$$

$$- \frac{\lambda K^4}{2}\int_{a,b,c,d,e}\Gamma_{zc}^{-1}\,\Gamma_{ae}^{-1}\,\Gamma_{dey}\,\Gamma_{zb}^{-1}\,\Gamma_{zc}^{-1}\,\Gamma_{aby}$$

$$-\Gamma_{zyz} = \lambda K^4\,\Phi_z\,\delta_{zy}\delta_{zz} + \ldots$$

Clearly, it is tiresome just to write out even the first few terms of the infinite family of equations that can be generated in this way. The loop-expansion organizes this mess by giving a graphical interpretation to the equations and by providing a systematic procedure for truncating them.

The graphical interpretation is as follows:

the "blob" means $\Gamma[\Phi]$;

the "dot" • means $S[\Phi]$.

Each line attached to either a blob or a dot indicates a functional derivative. Also, we define a special blob for the propagator:

 means $\Gamma^{-1}_{xy}[\Phi]$.

I will not bother to indicate numerical coefficients. The Schwinger-Dyson equation and its functional derivatives, (3.2) and (3.4), can then be compactly written:
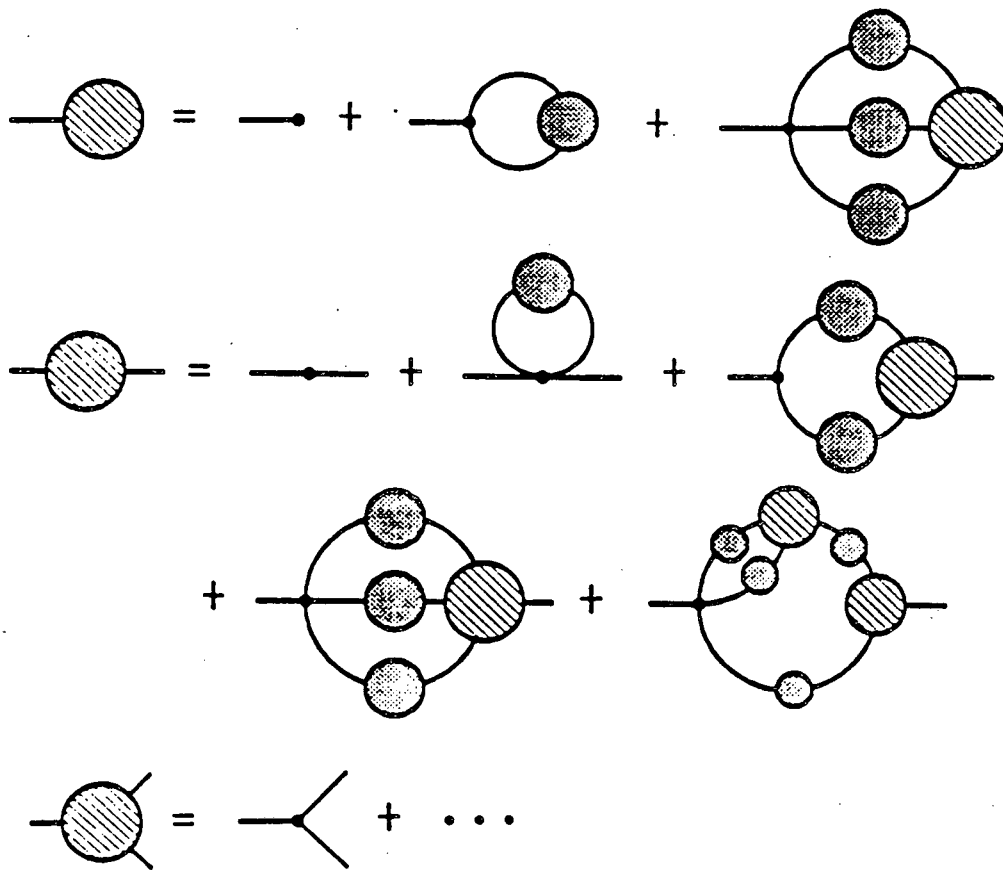
Sketch (3.1).

There is one additional fact we need, the identity

$$\Gamma_{zy}^{-1} = \int_{a,b} \Gamma_{za}^{-1} \, \Gamma_{ab} \, \Gamma_{by}^{-1},$$

which can be written graphically:

Sketch (3.2).

This equation allows us to systematically improve a given approximation for the propagator.

The simplest approximation of the propagator is
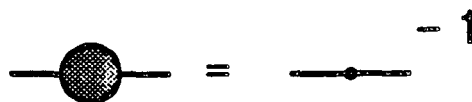
Sketch (3.3).

With this approximation, it is simple to expand Γ_z to an arbitrary number of loops. For example, to two loops
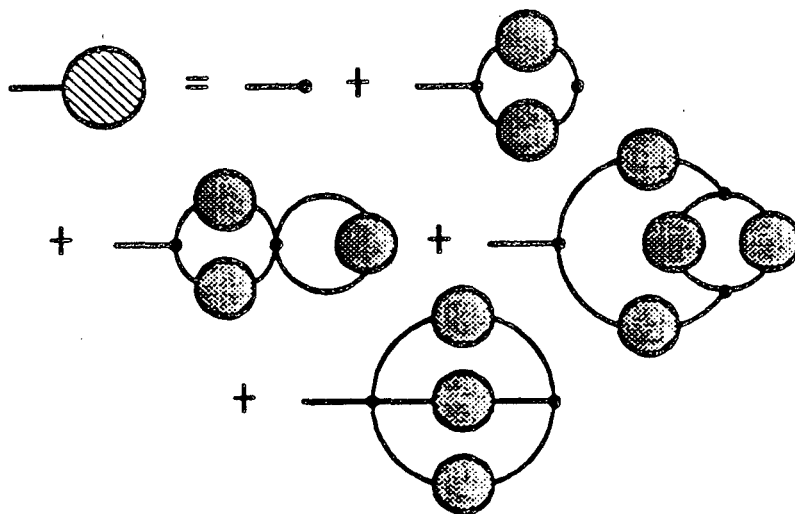
Sketch (3.4).

3 A Special Case

It is now trivial to find a Schwinger-Dyson equation for the effective potential. We simply replace Φ_z by $\hat{\Phi} = $ constant in equation (3.2). I will use $\hat{\Gamma}_{zy}$ to denote $\Gamma_{zy}(\hat{\Phi})$, etc. Then we have

$$V'(\hat{\Phi}) = m^2 K^2 \hat{\Phi} + \frac{\lambda K^4}{6} \hat{\Phi}^3 + \frac{\lambda K^4}{2} \left(i \hat{\Gamma}_{zz}^{-1}\right) \hat{\Phi} + \frac{\lambda K^4}{6} \int_{a,b,c} \hat{\Gamma}_{za}^{-1} \hat{\Gamma}_{zb}^{-1} \hat{\Gamma}_{zc}^{-1} \hat{\Gamma}_{abc} .$$

This equation is *exact*. As in the general case, it generates a loop-

expansion which must be truncated at some order. I will do some sample calculations in the following sections.

IV   The One-loop Effective Potential and Beyond

1   A One-loop Calculation

At the one-loop level, our Schwinger-Dyson equation is very simple:
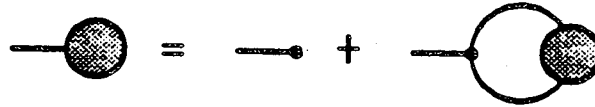
Sketch (4.1).

Algebraically, this works out to be

$$V'(\hat{\Phi}) = m_1^2 K_1^2 \hat{\Phi} + \frac{\lambda K_1^4}{6} \hat{\Phi}^3 + \frac{\lambda K_0^4}{2} \hat{\Phi} \left(i\hat{\Gamma}_{zz}^{-1} \right). \qquad (4.1)$$

Let me comment on the notation. I *must* renormalize m^2; I *choose* to renormalize K^2, but not λ. Thus, m^2 and K^2 are unknown constants that will be fixed by my renormalization conventions. Expanding in $\hbar$:

$$m^2 = m_R^2 + \hbar \, \delta m_1^2 + \hbar^2 \, \delta m_2^2 + \dots$$

$$K^2 = 1 + \hbar \, \delta K_1^2 + \hbar^2 \, \delta K_2^2 + \dots$$

The leading terms are the classical values; higher order terms represent corrections from the loop-expansion. Indeed, the $\hbar^n$ correction comes from the n-loop diagrams. In my notation, m_n^2 and K_n^2 represent a truncation of the above series to order $\hbar^n$.

Now consider the Schwinger-Dyson equation (3.4) for $\Gamma_{zy}(\hat{\Phi})$:

$$-\hat{\Gamma}_{zy} = \left[K^2(\partial_z^2 + m^2) + \frac{\lambda K^4}{2}\left(\hat{\Phi}^2 + i\hat{\Gamma}_{zz}^{-1} \right) \right] \delta_{zy} + \ldots$$

Graphically, this is
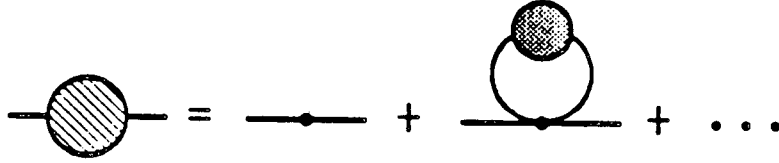
Sketch (4.2).

The propagator $\hat{\Gamma}_{zy}^{-1}$ is obtained by inverting this. At tree-level, we have

$$-\hat{\Gamma}_{zy} = (\partial_z^2 + \mu^2)\delta_{zy} \tag{4.2a}$$

$$\mu^2(\hat{\Phi}) = m_R^2 + \tfrac{1}{2}\lambda\hat{\Phi}^2 = U''(\hat{\Phi}). \tag{4.2b}$$

So the "tree-level" propagator is

$$\hat{\Gamma}_{zy}^{-1} = \int \frac{d^2p}{(2\pi)^2} \frac{e^{-ip\cdot(z-y)}}{p^2 - \mu^2 + i\epsilon}. \tag{4.2c}$$

Performing the Wick rotation,

$$i\hat{\Gamma}_{zz}^{-1} = \int_E \frac{d^2p}{(2\pi)^2} \frac{1}{p^2 + \mu^2},$$

where E denotes Euclidean space. The above integral is log-divergent. It is convenient to define a whole family of integrals

$$J_n(\mu^2) \equiv \int_E \frac{d^2p}{(2\pi)^2} \frac{1}{(p^2 + \mu^2)^n}.$$

For $n \geq 2$, these are finite and satisfy the property

$$\frac{\partial J_n}{\partial (\mu^2)} = -n J_{n+1}.$$ (4.3)

I will take this property to hold for J_1 also. (If one regulates all the J_n in some way, then (4.3) is true for all n in the limit in which the regulator is removed.) It is easy to compute

$$J_n(\mu^2) = \frac{1}{4\pi(n-1)(\mu^2)^{n-1}} \qquad \text{where } n \geq 2.$$

Thus we have

$$
\begin{aligned}
i\hat{\Gamma}_{zz}^{-1} = J_1(\mu^2) &= J_1(m_R^2) + \int_{m_R^2}^{\mu^2} ds \, \frac{\partial J_1}{\partial s}(s) \\
&= J_1(m_R^2) - \int_{m_R^2}^{\mu^2} ds \, \frac{1}{4\pi s} \\
&= J_1(m_R^2) - \frac{1}{4\pi} \log\left(\frac{\mu^2}{m_R^2}\right).
\end{aligned}
$$ (4.4)

So we can rewrite (4.1) as

$$
\begin{aligned}
V'(\hat{\Phi}) &= m_1^2 K_1^2 \hat{\Phi} + \frac{\lambda K_1^4}{6} \hat{\Phi}^3 + \tfrac{1}{2}\lambda J_1(\mu^2)\hat{\Phi} \\
&= \left[m_1^2 K_1^2 + \tfrac{1}{2}\lambda J_1(m_R^2) \right] \hat{\Phi} + \frac{\lambda K_1^4}{6} \hat{\Phi}^3 - \frac{\lambda \hat{\Phi}}{8\pi} \log\left(\frac{\mu^2}{m_R^2}\right).
\end{aligned}
$$ (4.5)

I would now like to renormalize the mass. This can be done for both the symmetric and broken phases simultaneously.

Let F be the non-negative value of $\hat{\Phi}$ for which V takes a minimum. I.e.,

$$V'(F) = 0 \qquad \text{defines } F.$$

The renormalization prescription is

$$m_R^2 \equiv V''(F)$$

$$= m_1^2 K_1^2 + \tfrac{1}{2}\lambda J_1(m_R^2) + \tfrac{1}{2}\lambda K_1^4 F^2 - \frac{\lambda}{8\pi}\log\left(\frac{\mu_F^2}{m_R^2}\right) - \frac{\lambda F g}{8\pi\mu_F^2}\,, \quad (4.6)$$

where we define

$$\mu_F^2 \equiv \mu^2(F)$$

$$g \equiv \frac{\partial\mu^2}{\partial\hat{\Phi}}(F)\,.$$

Solving for m_1^2 and substituting into (4.5), we have

$$V'(\hat{\Phi}) = m_R^2\hat{\Phi} + \frac{\lambda K_1^4}{6}(\hat{\Phi}^2 - 3F^2)\hat{\Phi} - \frac{\lambda\hat{\Phi}}{8\pi}\log\left(\frac{\mu^2}{\mu_F^2}\right) + \frac{\lambda F g\hat{\Phi}}{8\pi\mu_F^2}\,. \quad (4.7)$$

This result is actually more general than I have indicated in the derivation. In the following subsections, I will analyze this equation and expose its broader setting.

2   The One-loop Symmetric Case

In the symmetric phase, $F = 0$, and (4.7) reduces to

$$V'(\hat{\Phi}) = m_R^2\hat{\Phi} + \frac{\lambda K_1^4}{6}\hat{\Phi}^3 - \frac{\lambda\hat{\Phi}}{8\pi}\log\left(\frac{\mu^2}{\mu_F^2}\right)\,. \quad (4.8)$$

Differentiating this,

$$V'' = m_R^2 + \frac{\lambda K_1^4}{2}\hat{\Phi}^2 - \frac{\lambda}{8\pi}\left[\log\left(\frac{\mu^2}{\mu_F^2}\right) - \frac{\hat{\Phi}}{\mu^2}\frac{\partial\mu^2}{\partial\hat{\Phi}}\right]\,. \quad (4.9)$$

I will now show that $K_1^2 = 1$. To one-loop, Γ_{xy} is given by
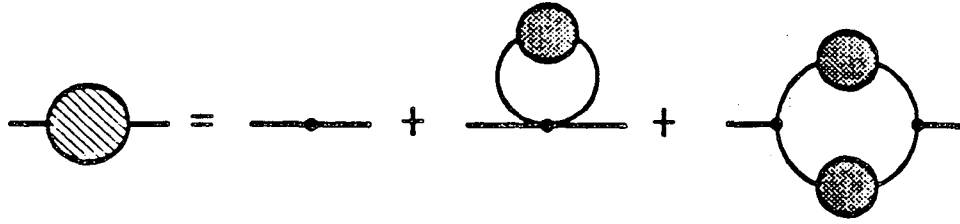
Sketch (4.3).

To compute K_1^2, we need to evaluate this at $\hat{\Phi} = 0$, which means that the third diagram on the right vanishes. We then have

$$-\hat{\Gamma}_{xy}(0) = \left[K_1^2(\partial_x^2 + m_1^2) + \tfrac{1}{2}\lambda \left(i\hat{\Gamma}_{xx}^{-1}(0) \right) \right] \delta_{xy}$$

$$= \left(K_1^2 \partial_x^2 + \text{constant} \right) \delta_{xy} .$$

K_1^2 is to be chosen so that the coefficient of ∂_x^2 is 1. Hence, $K_1^2 = 1$.

Now recall that $\mu^2(\hat{\Phi}) = m_R^2 + \tfrac{1}{2}\lambda\hat{\Phi}^2$. Hence $\mu_F^2 = m_R^2$. So

$$V'(\hat{\Phi}) = m_R^2\hat{\Phi} + \frac{\lambda}{6}\hat{\Phi}^3 - \frac{\lambda\hat{\Phi}}{8\pi} \log\left(\frac{m_R^2 + \tfrac{1}{2}\lambda\hat{\Phi}^2}{m_R^2} \right)$$

which is easily integrated:

$$V(\hat{\Phi}) = V(0) + m_R^2\hat{\Phi}^2 + \frac{\lambda}{24}\hat{\Phi}^4 - \frac{1}{8\pi}\left[\mu^2 \log\left(\frac{\mu^2}{m_R^2} \right) - \tfrac{1}{2}\lambda\hat{\Phi}^2 \right] .$$

This is the standard one-loop result in two dimensions.

3 The Gaussian Approximation

Recall that the perturbative expansion follows from the truncation of the Schwinger-Dyson equation for the inverse propagator:
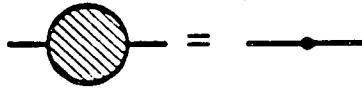
Sketch (4.4).

This provides a powerful temptation to improve this radical truncation, since *any* improvement will yield non-perturbative results. The simplest improvement is to write
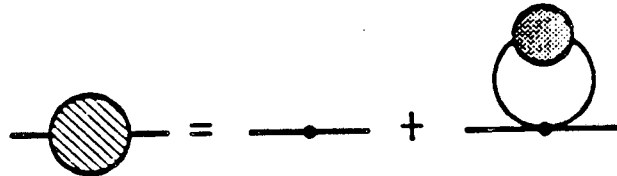
Sketch (4.5).

This yields the equation

$$-\hat{\Gamma}_{xy} = \left[\partial_x^2 + \mu^2(\hat{\Phi})\right] \delta_{xy}$$

where

$$\mu^2(\hat{\Phi}) = m_1^2 + \tfrac{1}{2}\lambda\hat{\Phi}^2 + \tfrac{1}{2}\lambda(i\hat{\Gamma}_{xx}^{-1}) \,.$$

This is very similar to the perturbative case, (4.2), except that $\mu^2(\hat{\Phi})$ is now a different function of $\hat{\Phi}$. The renormalization runs exactly as before. The results of Subsection 4.1 are still valid, and using (4.4), (4.6) and (4.7),

we have

$$V'(\hat{\Phi}) = m_R^2 \hat{\Phi} + \frac{\lambda}{6} \hat{\Phi}^3 - \frac{\lambda \hat{\Phi}}{8\pi} \log\left(\frac{\mu^2}{\mu_F^2}\right) , \qquad (4.10)$$

where

$$\mu^2(\hat{\Phi}) = m_R^2 + \tfrac{1}{2}\lambda \hat{\Phi}^2 - \frac{\lambda}{8\pi} \log\left(\frac{\mu^2}{\mu_F^2}\right) . \qquad (4.11)$$

It follows that $\mu_F^2 = \mu^2(0) = m_R^2$. One can show graphically that the transcendental equation (4.11) has a unique solution μ^2 for each value of $\hat{\Phi}$, when $m_R^2 \neq 0$.

The above procedure is not really new. It reproduces the results of the Gaussian approximation. Only the derivation above is new; I have given this derivation to help motivate further improvements and to show how little work needs to be done to implement them.

It is possible to integrate $V'(\hat{\Phi})$ in (4.10) analytically. However, let me point out that the numerical solution is somewhat easier (and remains tractable for the improved approximations I intend to develop throughout the rest of this thesis). There are three steps:

1. Compute $\mu^2(\hat{\Phi})$ numerically, using (4.11).

2. Substitute μ^2 into $V'(\hat{\Phi})$, in (4.10).

3. Integrate $V'(\hat{\Phi})$ numerically.

Computer plots are given at the end of this section. But first, I will generalize the above procedure to find a new and improved result.

4 The Self-consistent Approximation

In the previous subsection, I motivated the Gaussian approximation by appealing to the truncated Schwinger-Dyson equation for Γ_{xy}, described by Sketch (4.5). Suppose that I could solve the full equation, given in Sketch (3.1). The answer would certainly *not* be of the form $(\partial_x^2 + \mu^2)\delta_{xy}$. Instead, it would have an infinite number of derivative terms

$$-\hat{\Gamma}_{xy} = \left[V''(\hat{\Phi}) + Z(\hat{\Phi})\partial_x^2 + \ldots\right]\delta_{xy}.$$

This equation is exact, but unusable; I will therefore severely truncate it:

$$-\hat{\Gamma}_{xy} = \left[\partial_x^2 + V''(\hat{\Phi})\right]\delta_{xy}. \tag{4.12}$$

This is *again* of the same form as the perturbative inverse propagator (4.2). Writing

$$\mu^2(\hat{\Phi}) = V''(\hat{\Phi}), \tag{4.13a}$$

$$\hat{\Gamma}_{xy}^{-1} = \int \frac{d^2p}{(2\pi)^2} \frac{e^{-ip\cdot(x-y)}}{p^2 - \mu^2 + i\epsilon}, \tag{4.13b}$$

we can take over all the perturbative results of Subsection 4.1 immediately.

Note that $\mu_F^2 = \mu^2(0) = V''(0) = m_R^2$. So (4.8) and (4.9) become

$$V'(\hat{\Phi}) = m_R^2\hat{\Phi} + \tfrac{1}{6}\lambda\hat{\Phi}^3 - \frac{\lambda\hat{\Phi}}{8\pi}\log\left(\frac{\mu^2}{m_R^2}\right) \tag{4.14a}$$

$$\mu^2(\hat{\Phi}) = m_R^2 + \tfrac{1}{2}\lambda\hat{\Phi}^2 - \frac{\lambda}{8\pi}\left[\log\left(\frac{\mu^2}{m_R^2}\right) - \frac{\hat{\Phi}}{\mu^2}\frac{\partial\mu^2}{\partial\hat{\Phi}}\right]. \tag{4.14b}$$

There is no hope of an analytical solution to (4.14), but a numerical solution is not difficult. (4.14b) is a first-order differential equation for $\mu^2(\hat{\Phi})$. It can be solved and substituted into (4.14a), which can then be numerically integrated to yield $V(\hat{\Phi})$.

The boundary condition for (4.14b) is just the symmetry requirement

$$\frac{\partial(\mu^2)}{\partial\hat{\Phi}}(0) = V'''(0) = 0.$$

It is necessary to use a fairly good numerical routine for solving the differential equation. I used a sixth-order predictor-corrector Adams-Moulton algorithm. Results are plotted at the end of this section and discussed in the next subsection.

A few comments are necessary here. From now on, I will call (4.13) the self-consistent approximation. This approximation to the propagator is the only non-perturbative element in the scheme. Γ_{xyz} and higher functional derivatives are still to be computed perturbatively. The close resemblance of (4.13) to (4.2) enables the usual renormalization procedure to go through unhindered.

5   A Comparison

I have plotted the results of four approximations (tree, one-loop, Gaussian, and self-consistent) in Figures (4.1) through (4.12). $\tilde{\lambda}$ ranges from 6 to 600. (This range is unreasonably broad; I will discuss the reliability of our re-

sults in Section 6.) Note that the perturbative and Gaussian approximations show a phase transition (which can be shown analytically to be first-order) at $\tilde{\lambda}_{crit} \approx 40 - 60$. (The precise value is unimportant. A first-order phase transition is forbidden, and anyway these approximations yield non-convex potentials, so they are wrong on two counts.)

The self-consistent results are interesting, for two reasons. First, they are convex. Second, for large $\tilde{\lambda}$, they show a very flat well, reminiscent of the lattice results of Calloway and Maloof [4]. The well is not completely flat, as we see on magnification of Fig. (4.11) to Fig. (4.12). The reason is quite simple. Our renormalization conditions put the minimum of V at $\hat{\Phi} = 0$, with $V''(0) = m_R^2$. Convexity then keeps V from flattening out. This is similar to the analyticity constraint on the lattice calculation, which prevented a true flat well from emerging.

Nearly identical reasoning shows that we are unable to see a phase transition in the self-consistent approximation. By convexity, V has only one minimum. Our renormalization prescription locates that minimum at $\hat{\Phi} = 0$.

Nevertheless, for large $\tilde{\lambda}$, the self-consistent $V(\hat{\Phi})$ looks rather suspicious, as though it were struggling to exhibit a phase-transition under impossible circumstances. We know that the phase transition occurs at $\tilde{\lambda} \to \infty$. Our results (if we can believe them) are entirely consistent with this fact. I will discuss the trustworthiness of all of our approximations in Section 6.
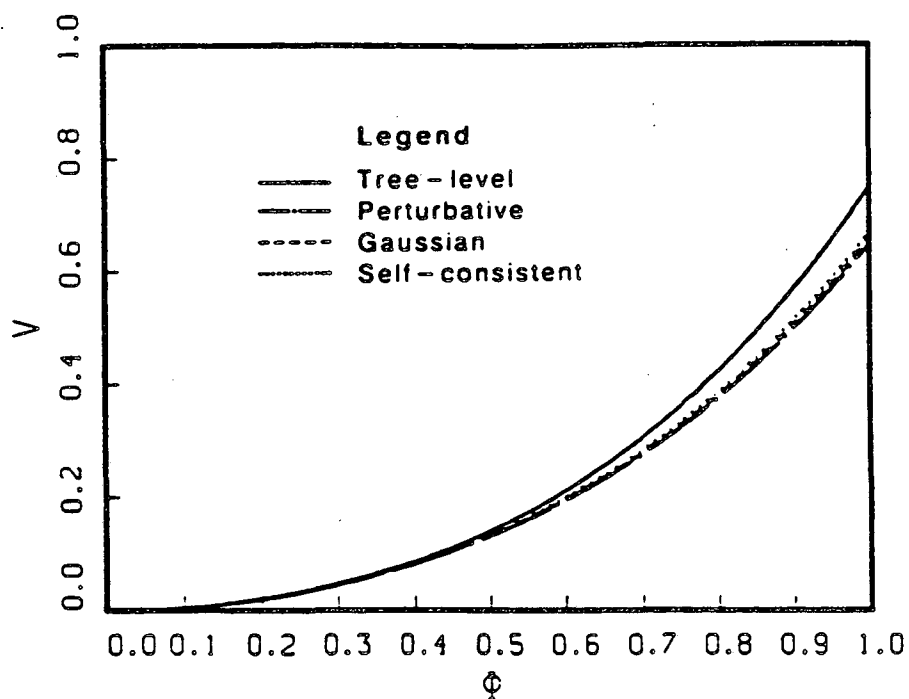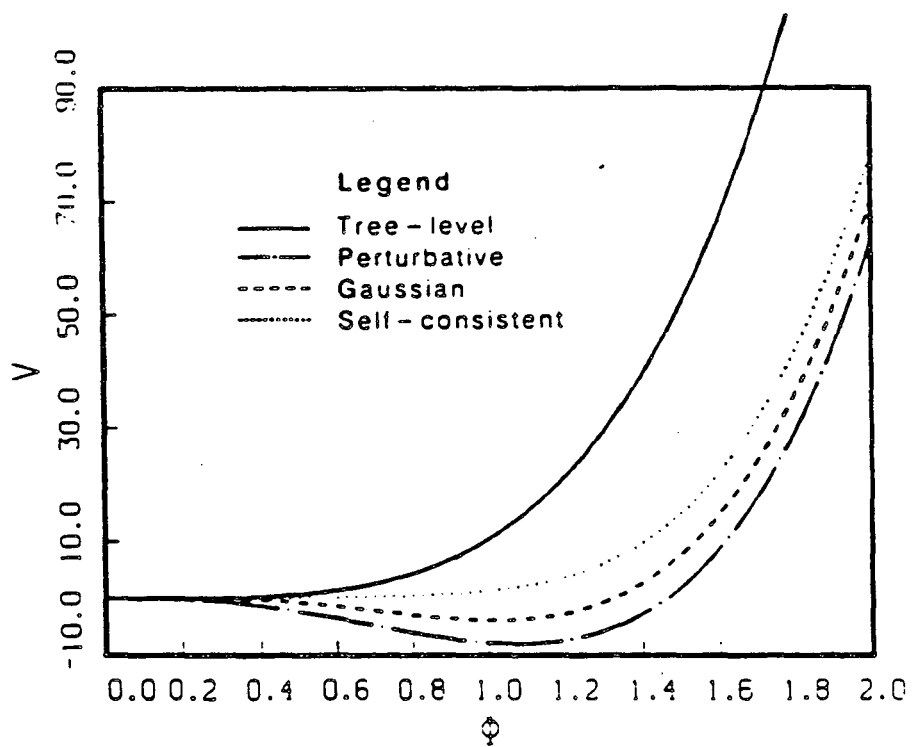
Figure (4.1): Plot of $V(\Phi)$ at $\bar{\lambda} = 6$.
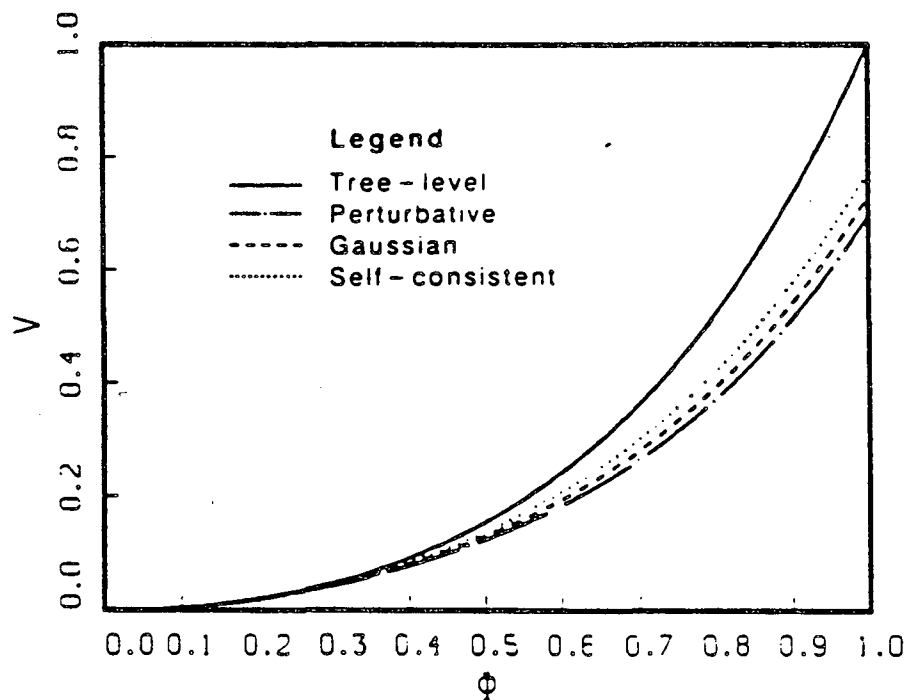
Figure (4.2): Plot of $V(\Phi)$ at $\bar{\lambda} = 12$.
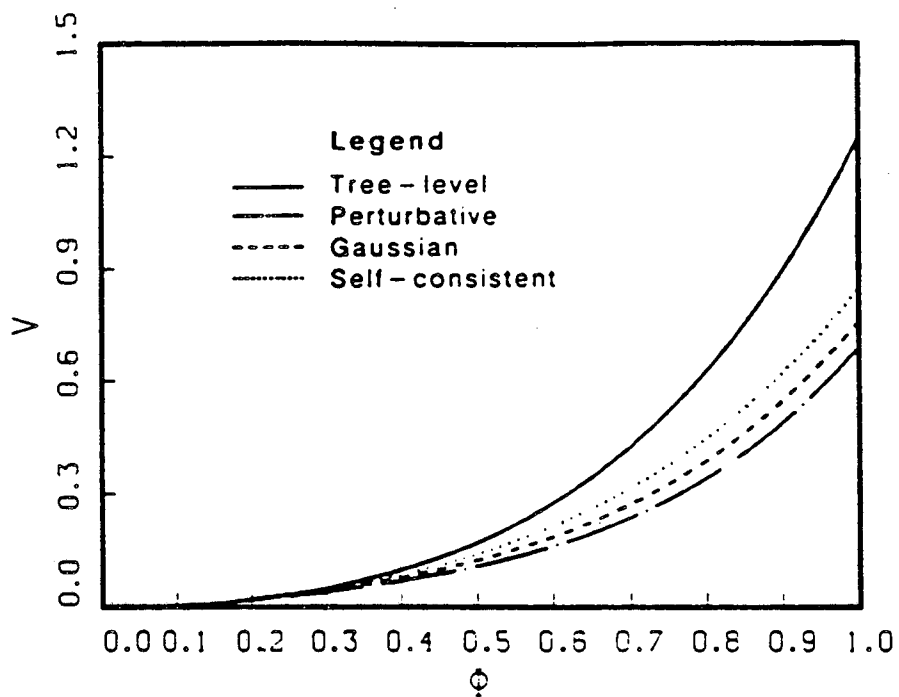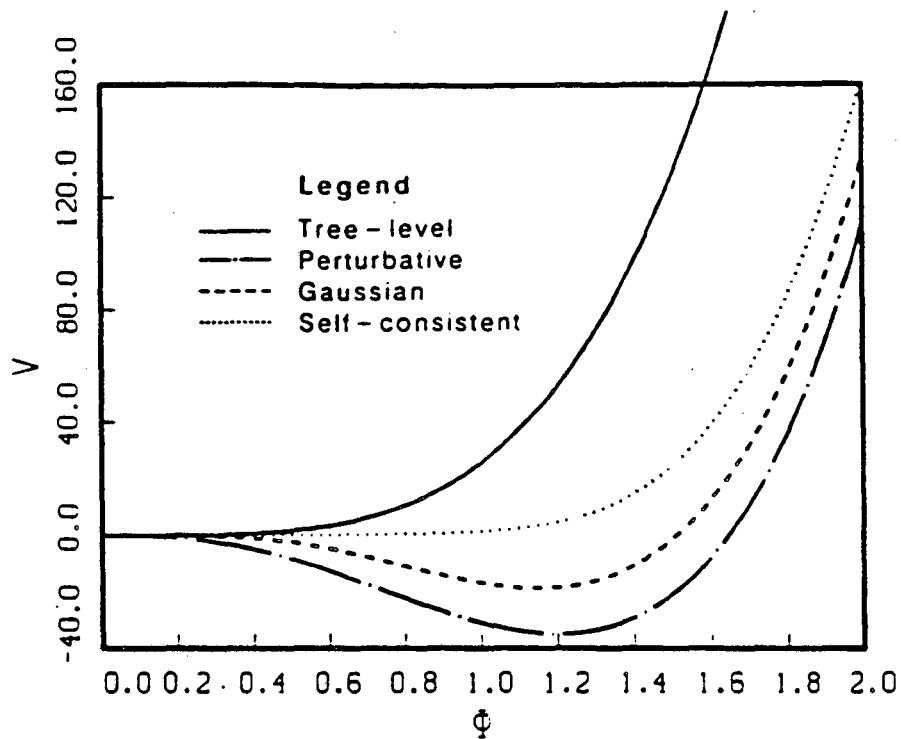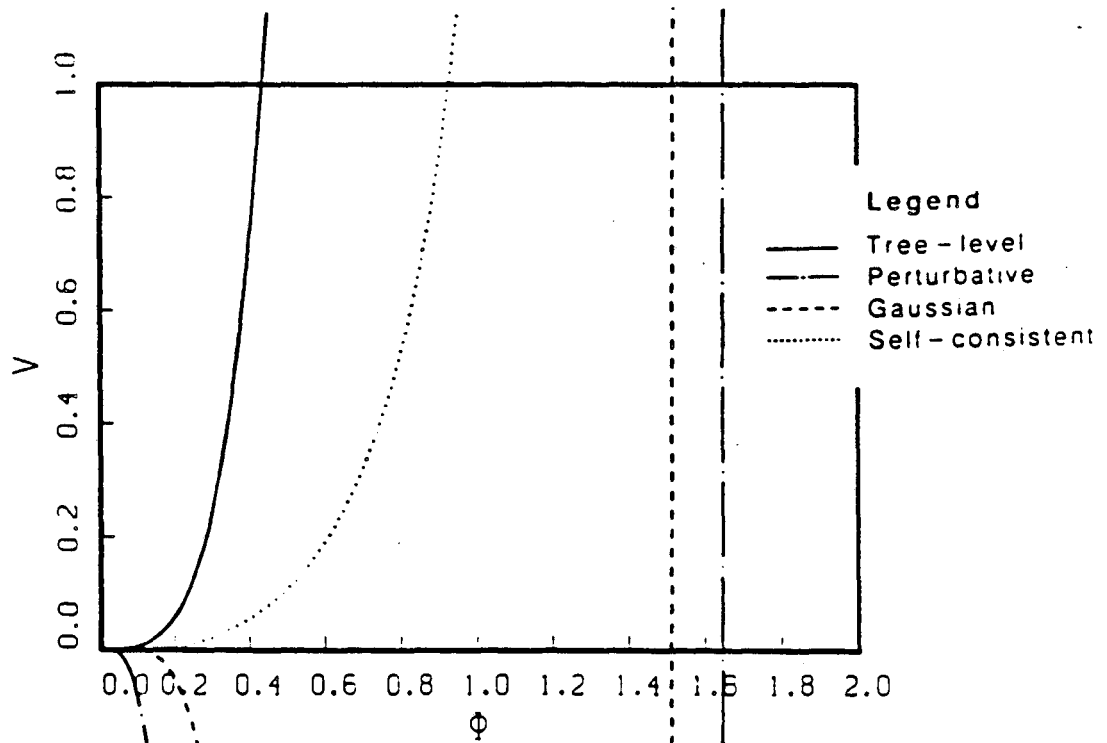
Figure (4.3): Plot of $V(\Phi)$ at $\tilde{\lambda} = 18$.
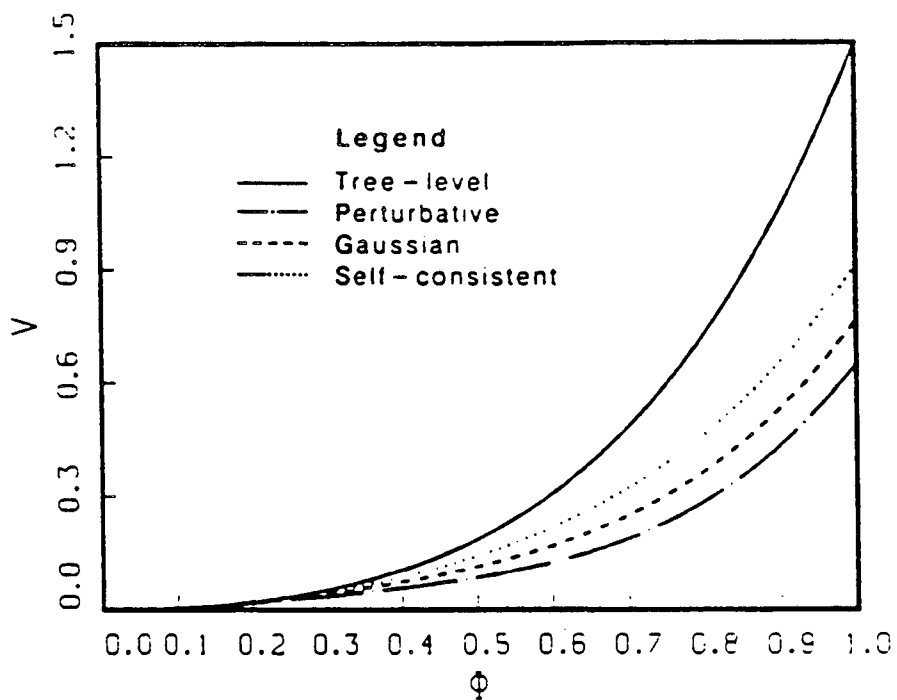
Figure (4.4): Plot of $V(\Phi)$ at $\tilde{\lambda} = 24$.
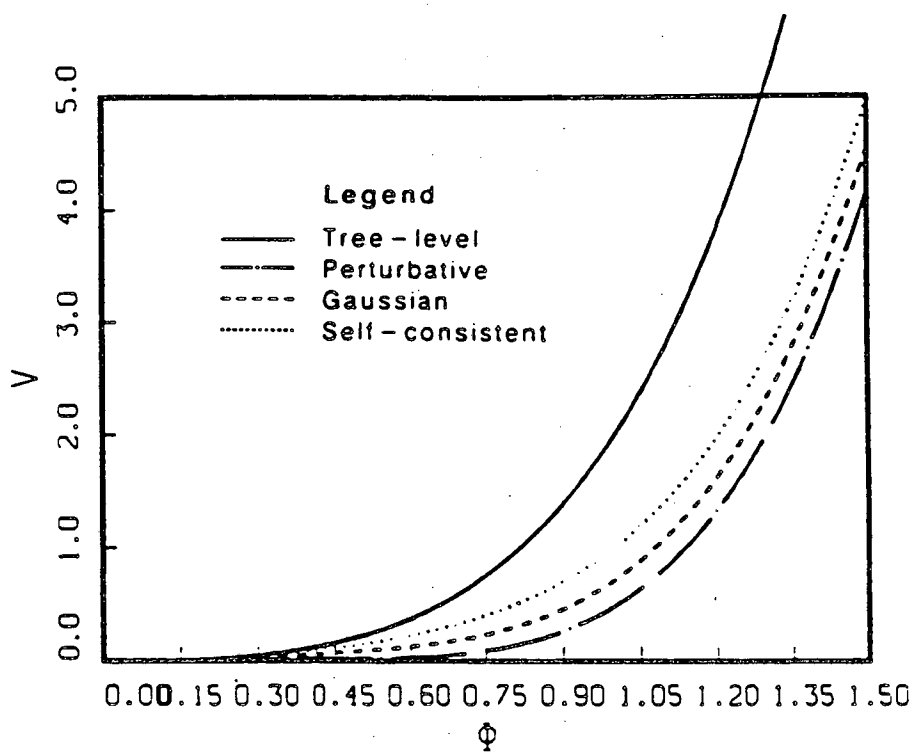
Figure (4.5): Plot of $V(\Phi)$ at $\bar{\lambda} = 36$.
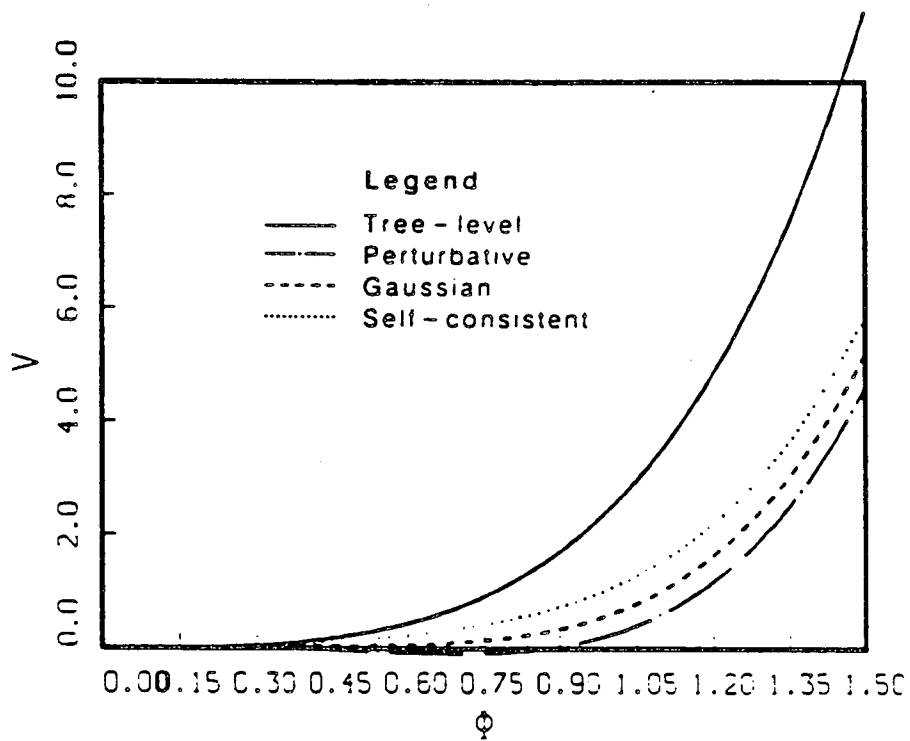
Figure (4.6): Plot of $V(\Phi)$ at $\bar{\lambda} = 48$.
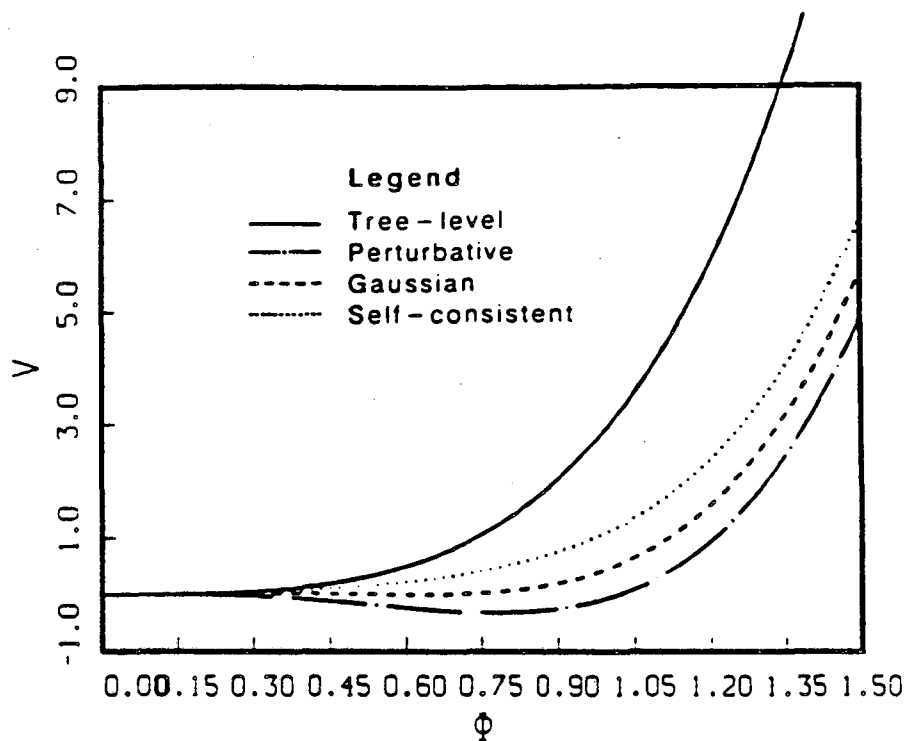
Figure (4.7): Plot of $V(\Phi)$ at $\bar{\lambda} = 60$.
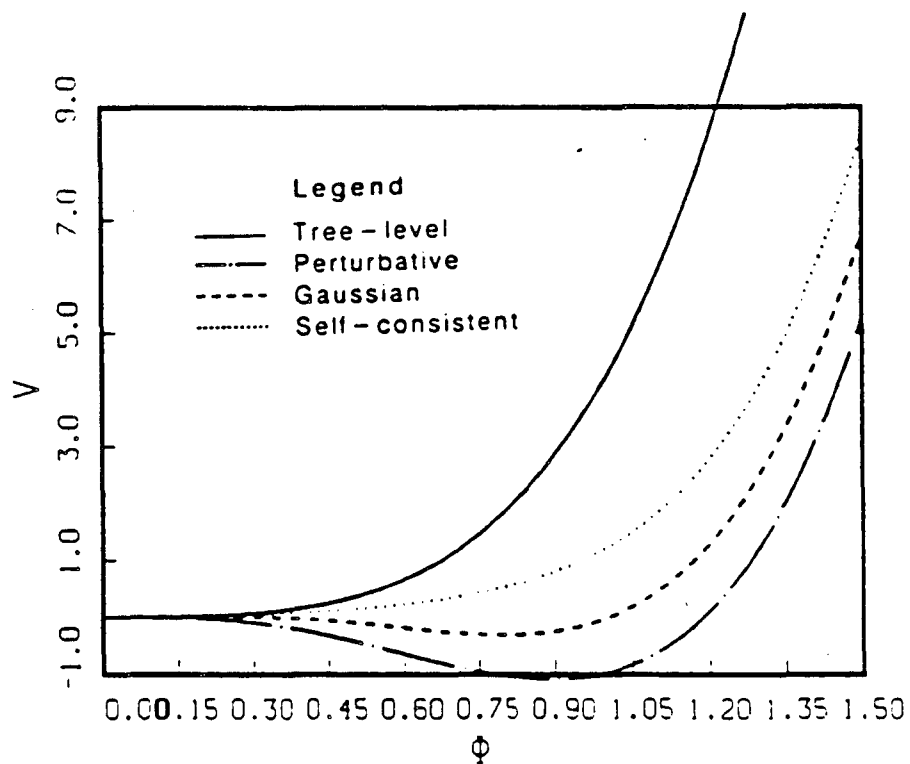
Figure (4.8): Plot of $V(\Phi)$ at $\bar{\lambda} = 90$.
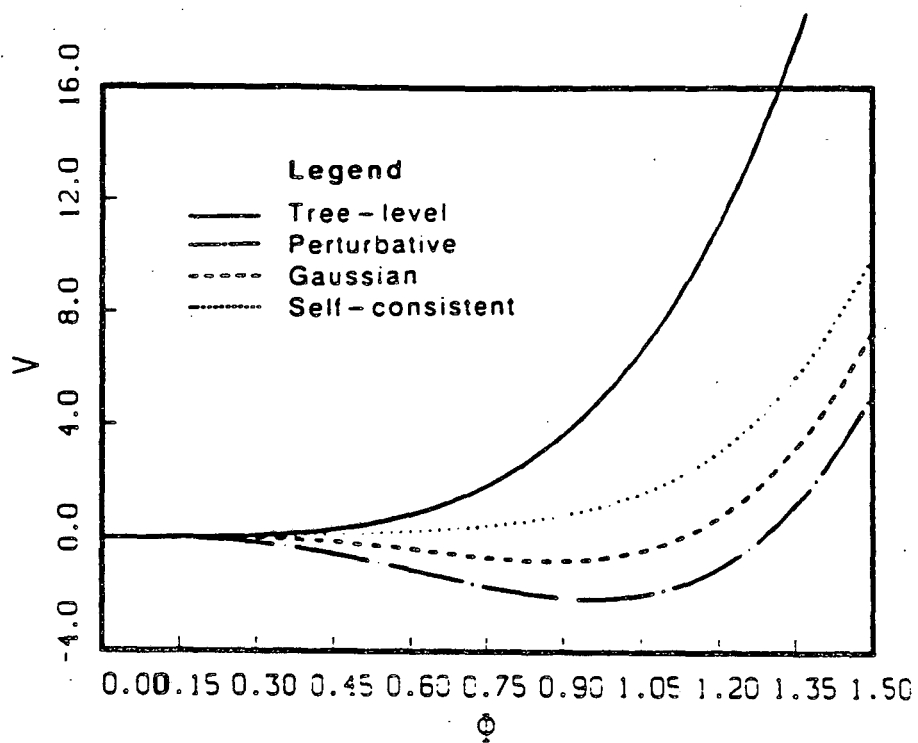
Figure (4.9): Plot of $V(\Phi)$ at $\bar{\lambda} = 120$.

Figure (4.10): Plot of $V(\Phi)$ at $\bar{\lambda} = 240$.

Figure (4.11): Plot of $V(\Phi)$ at $\tilde{\lambda} = 600$.

Figure (4.12): Magnified plot of $V(\Phi)$ at $\tilde{\lambda} = 600$.

V On Higher-Derivative Terms

1 A Sample Calculation: $Z(\Phi)$

In this section, I will consider the one-loop effective action. It is sufficient to discuss $Z(\hat{\Phi})$, the second term in the derivative expansion of Γ. Higher-order terms can be calculated with an increase in tedium. Z will be useful to us later, in the two-loop calculation.

To one loop, the Schwinger-Dyson equation for the inverse propagator is
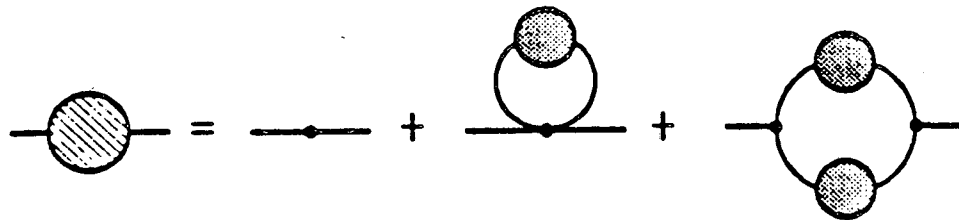
Sketch (5.1).

Algebraically, this is

$$-\hat{\Gamma}_{zy} = \left[K_1^2 \partial_z^2 + m_1^2 + \tfrac{1}{2}\lambda\left(\hat{\Phi}^2 + i\hat{\Gamma}_{zz}^{-1}\right)\right]\delta_{zy} - \tfrac{1}{2}\lambda\hat{\Phi}\left(i\int_{a,b}\hat{\Gamma}_{za}^{-1}\,\hat{\Gamma}_{zb}^{-1}\,\hat{\Gamma}_{aby}\right),$$

where

$$-\hat{\Gamma}_{aby} = \lambda\hat{\Phi}\,\delta_{ab}\delta_{ay}\,.$$

I will use the same general-purpose propagator used in Section 4:

$$\hat{\Gamma}_{zy}^{-1} = \int \frac{d^2p}{(2\pi)^2}\,\frac{e^{-ip\cdot(z-y)}}{(p^2 - \mu^2 + i\epsilon)}\,.$$

Using standard methods of Feynman integral evaluation, we find

$$-\hat{\Gamma}_{xy} = Z(\hat{\Phi})\,\partial_x^2 \delta_{xy} + \text{stuff}\,,$$

where

$$Z(\hat{\Phi}) = K_1^2 + \frac{\lambda^2 \hat{\Phi}^2}{48\pi(\mu^2)^2}\,. \tag{5.1}$$

2 Discussion of Results

The main points to note are the following:

1. Physically, we require $Z(F) = 1$, which implies that

$$K_1^2 = 1 - \frac{\lambda^2 F^2}{48\pi(\mu_F^2)^2} \simeq \left[1 + \frac{\lambda^2 F^2}{48\pi(\mu_F^2)^2}\right]^{-1}\,. \tag{5.2}$$

(K_1^2 must be positive. Higher order terms in the perturbative series would ensure positivity. I have approximated the perturbative result in (5.2) with a manifestly positive function which agrees with it to second order in λ.)

2. We have really computed three different approximations to $Z(\hat{\Phi})$, corresponding to the three choices of $\mu^2(\hat{\Phi})$ in Section 4. Thus, we have extended both the Gaussian approximation and the self-consistent approximation to the whole effective action, in the derivative expansion.

3. $Z(\hat{\Phi})$ gets large (and therefore important) when $\mu^2/(\lambda\hat{\Phi})$ gets small. In the self-consistent approximation, this happens when the well gets

flat, which happens when $\tilde{\lambda}$ gets large.

I have plotted $Z(\hat{\Phi})$ in Figures (5.1) through (5.10). Note that the self-consistent curve is higher than the Gaussian, which is higher than the perturbative, which is higher than the classical. This effect is enhanced as $\tilde{\lambda}$ increases.
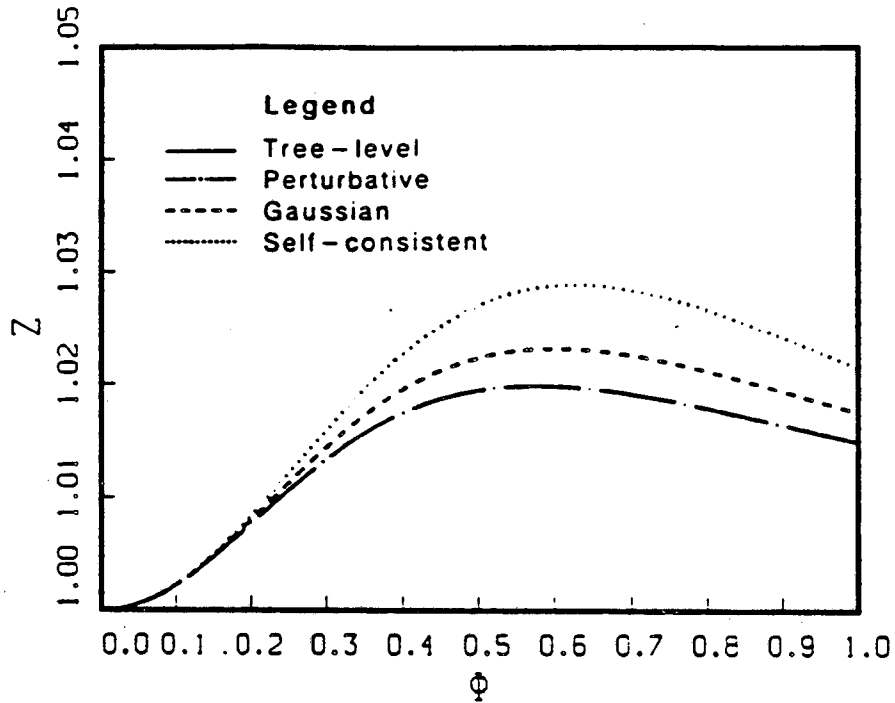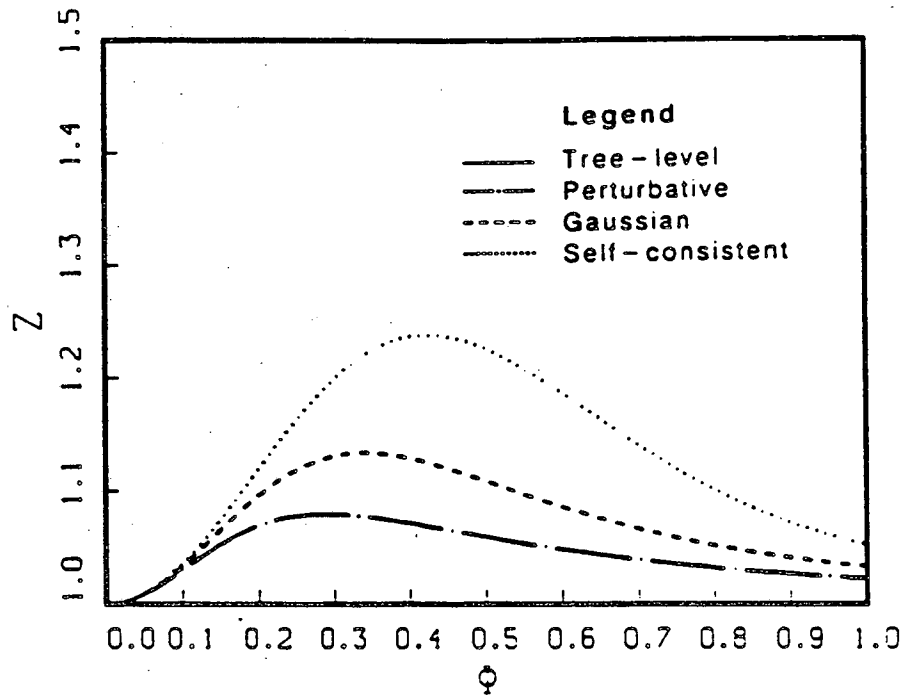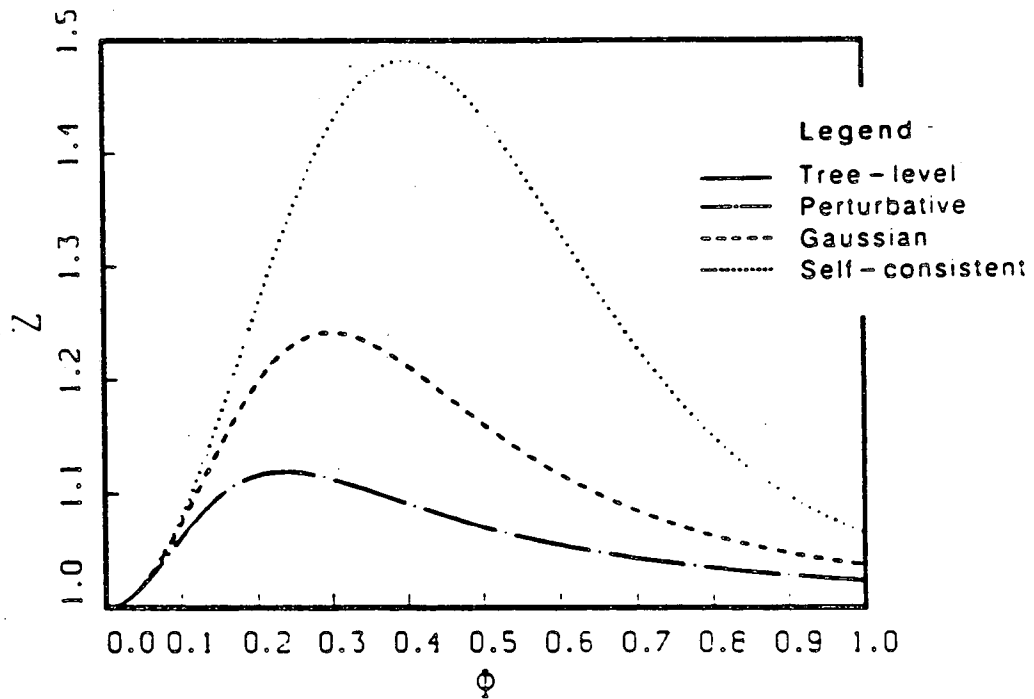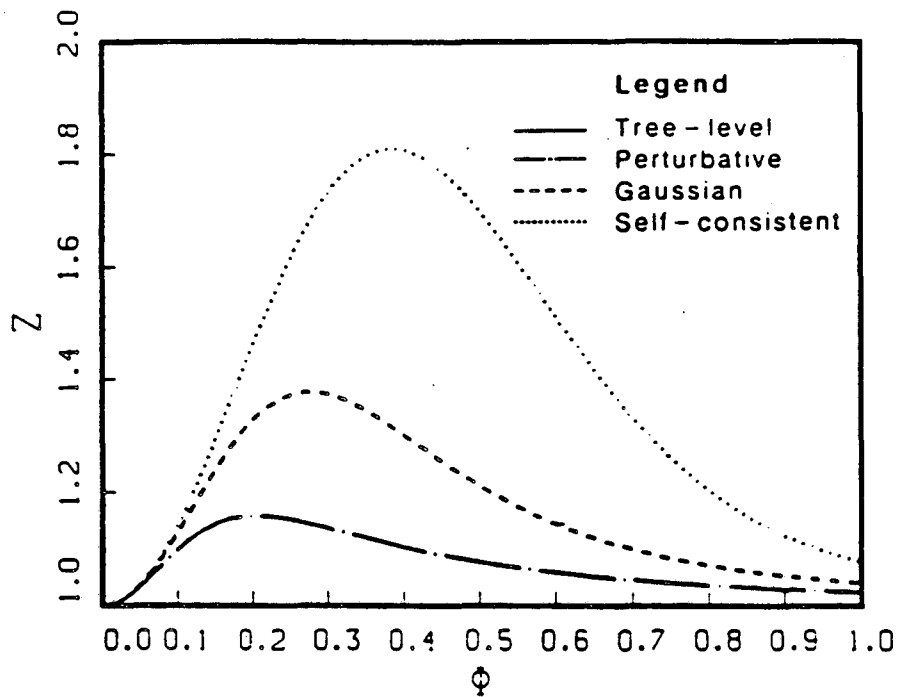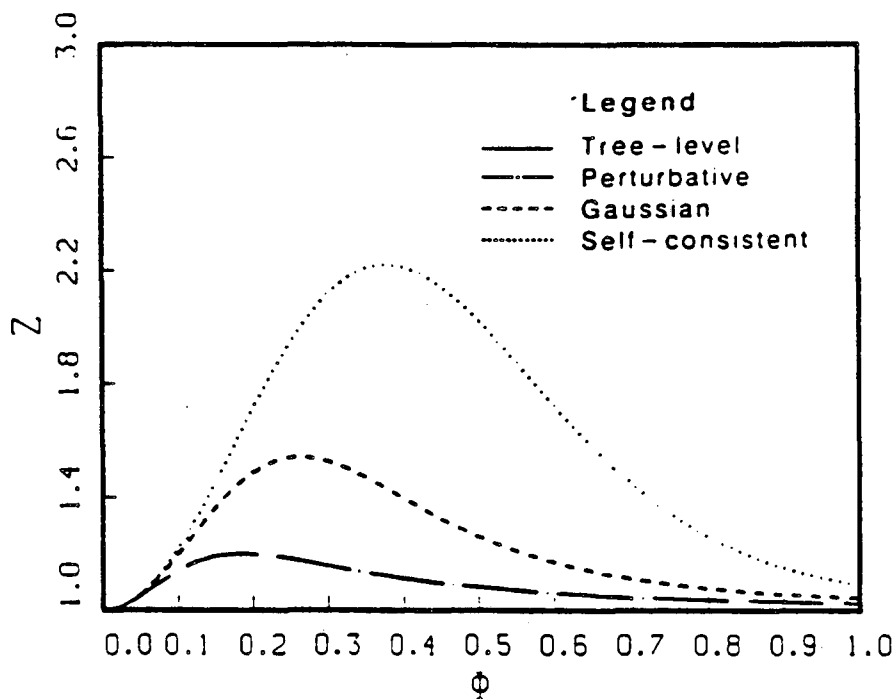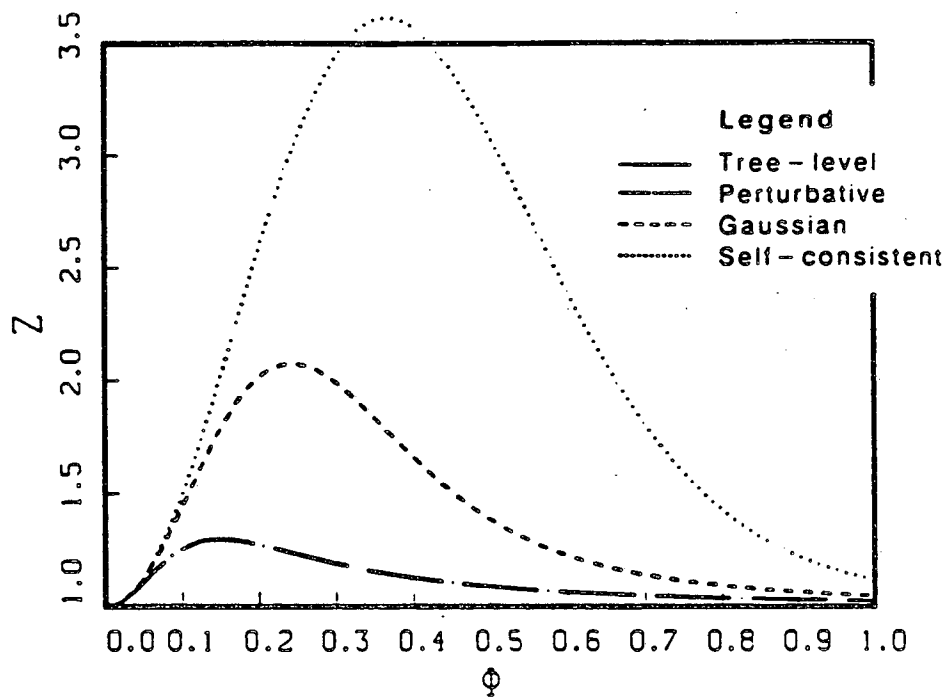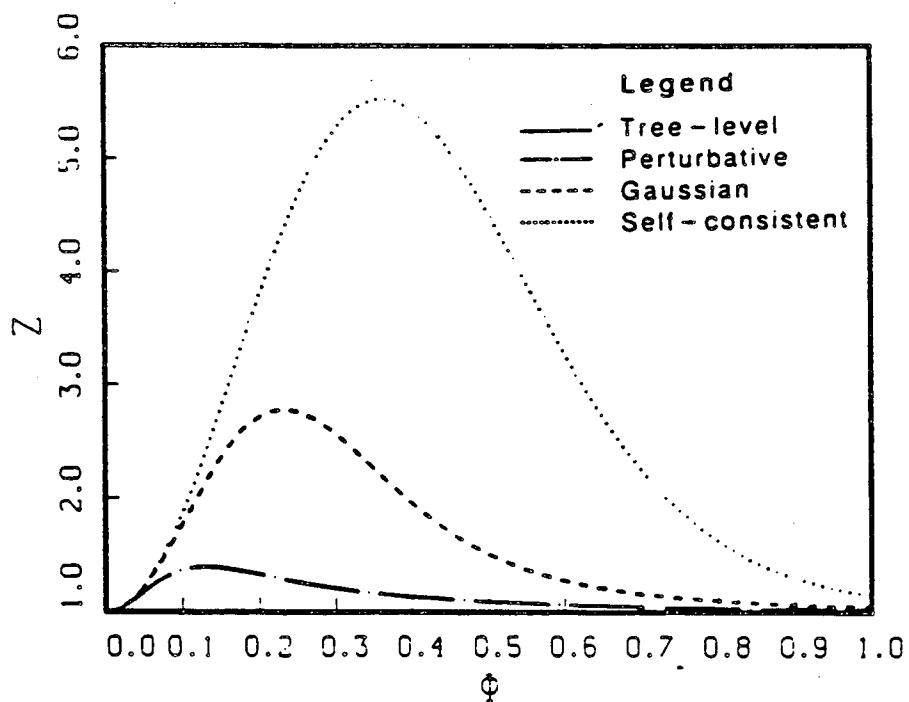
Figure (5.1): Plot of one-loop approximation to $Z(\Phi)$ for $\bar{\lambda} = 6$.
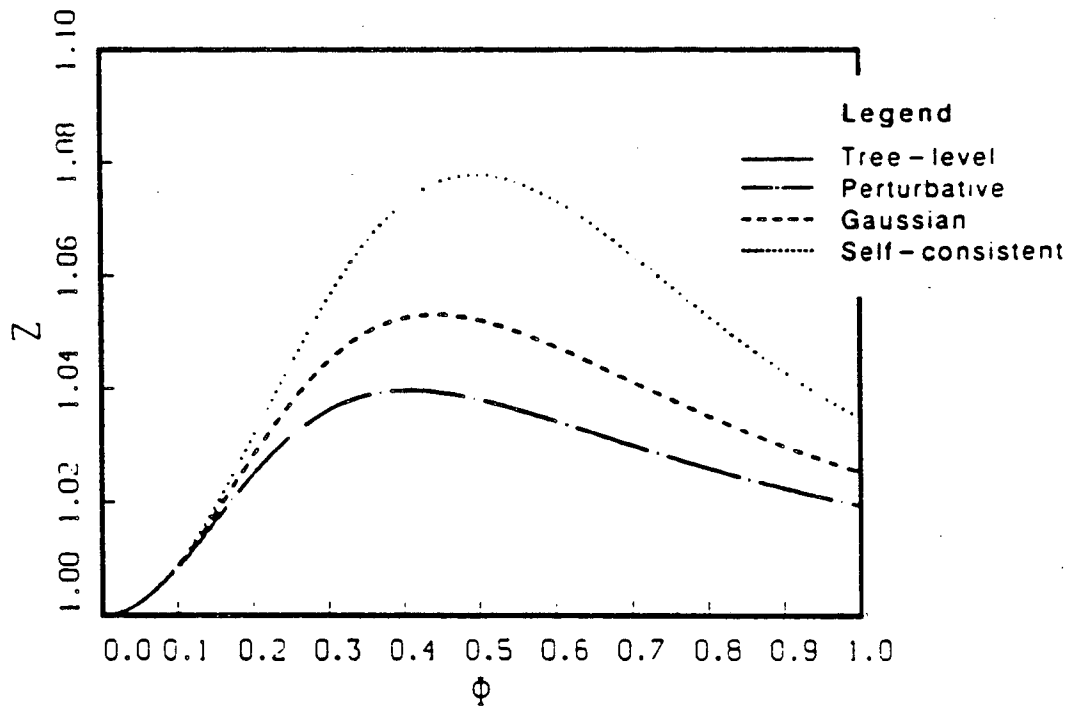
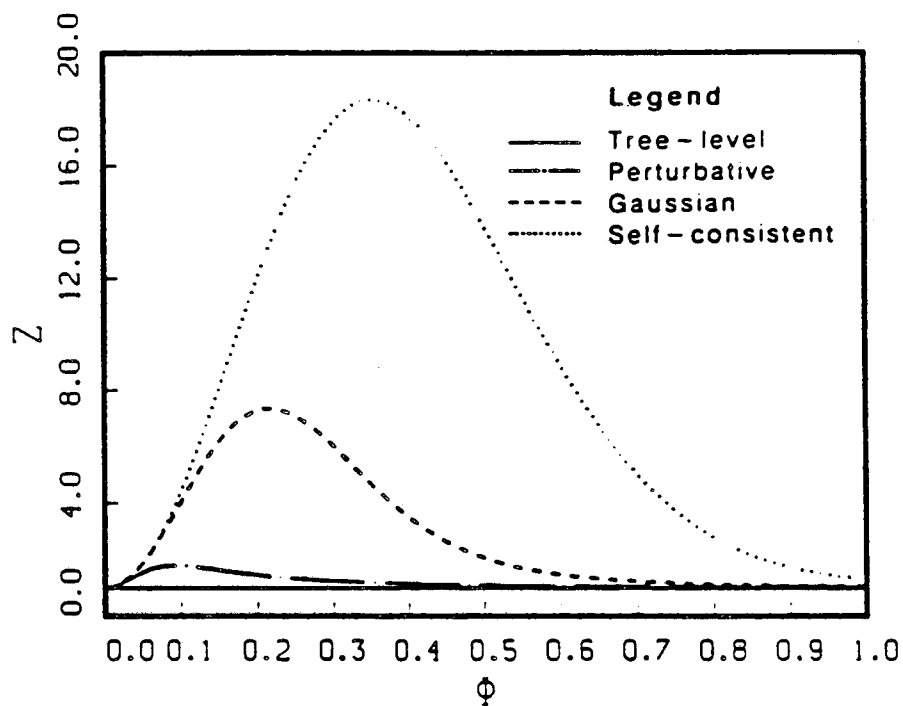Figure (5.2): Plot of one-loop approximation to $Z(\Phi)$ for $\bar{\lambda} = 12$.

Figure (5.3): Plot of one-loop approximation to $Z(\Phi)$ for $\bar{\lambda} = 24$.

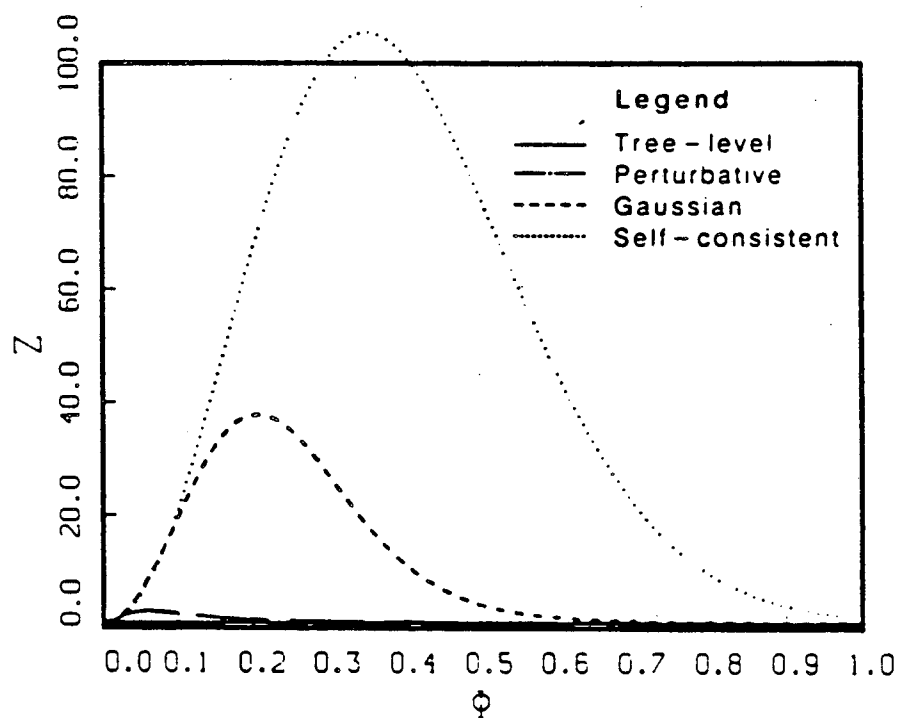Figure (5.4): Plot of one-loop approximation to $Z(\Phi)$ for $\bar{\lambda} = 36$.

Figure (5.5): Plot of one-loop approximation to $Z(\Phi)$ for $\bar{\lambda} = 48$.

Figure (5.6): Plot of one-loop approximation to $Z(\Phi)$ for $\bar{\lambda} = 60$.

Figure (5.7): Plot of one-loop approximation to $Z(\Phi)$ for $\tilde{\lambda} = 90$.

Figure (5.8): Plot of one-loop approximation to $Z(\Phi)$ for $\tilde{\lambda} = 120$.

Figure (5.9): Plot of one-loop approximation to $Z(\Phi)$ for $\tilde{\lambda} = 240$.

Figure (5.10): Plot of one-loop approximation to $Z(\Phi)$ for $\tilde{\lambda} = 600$.

VI   Improving the Two-loop Effective Potential

1   A Two-loop Calculation

In Section 4, I showed how to obtain the Gaussian and self-consistent approximations by making simple changes in the one-loop calculation. The same procedure works at n loops. In this section, I will work out the details for two loops (restricted to the symmetric phase for simplicity).

The two-loop Schwinger-Dyson equation for the effective potential is
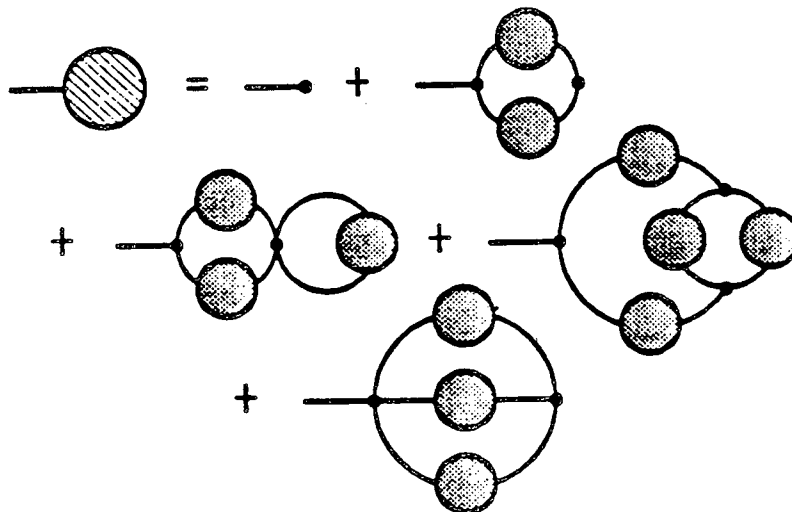
Sketch (6.1).

The algebraic expression for this, with appropriate counterterms, (and recalling $K_0 = K_1 = 1$) is

$$V'(\hat{\Phi}) = m_2^2 K_2^2 \hat{\Phi} + \frac{\lambda K_2^4}{6}\hat{\Phi}^3 + \tfrac{1}{2}\lambda \hat{\Phi}\left[-i\int_a \hat{\Gamma}_{za}^{-1}(\partial_a^2 + M^2)\hat{\Gamma}_{az}^{-1}\right]$$

$$+ \frac{\lambda^3 \hat{\Phi}^3}{4}\int_{a,b} \hat{\Gamma}_{za}^{-1}\,\hat{\Gamma}_{ab}^{-1}\,\hat{\Gamma}_{ab}^{-1}\,\hat{\Gamma}_{bz}^{-1} - \frac{\lambda^2 \hat{\Phi}}{6}\int_a \hat{\Gamma}_{za}^{-1}\,\hat{\Gamma}_{za}^{-1}\,\hat{\Gamma}_{za}^{-1},$$

where

$$\mathcal{M}^2 \equiv m_1^2 + \tfrac{1}{2}\lambda\hat{\Phi}^2 + \tfrac{1}{2}\lambda(i\hat{\Gamma}_{zz}^{-1})$$

$$= m_R^2 + \tfrac{1}{2}\lambda\hat{\Phi}^2 - \frac{\lambda}{8\pi}\log\left(\frac{\mu^2}{m_R^2}\right) \tag{6.1}$$

is a familiar object from Section 4. Using our general-purpose propagator (4.2c), a lengthy, but standard, calculation yields

$$V'(\hat{\Phi}) = \left[m_2^2 K_2^2 + \tfrac{1}{2}\lambda J_1(m_R^2) - \tfrac{1}{6}\lambda^2 I_0(m_R^2)\right]\hat{\Phi} + \frac{\lambda K_2^4}{6}\hat{\Phi}^3 \tag{6.2}$$

$$+ \frac{\lambda\hat{\Phi}}{8\pi}\left[\frac{\mathcal{M}^2 - \mu^2}{\mu^2} - \log\left(\frac{\mu^2}{m_R^2}\right)\right] + \frac{\lambda^3 Q\hat{\Phi}^3}{12(\mu^2)^2} - \frac{\lambda^2 Q\hat{\Phi}}{6}\left(\frac{1}{m_R^2} - \frac{1}{\mu^2}\right),$$

where

$$I_0(\mu^2) \equiv \int_E \frac{d^2p}{(2\pi)^2}\frac{d^2q}{(2\pi)^2}\frac{1}{(p^2+\mu^2)(q^2+\mu^2)([p+q]^2+\mu^2)}$$

is a divergent Euclidean-space integral and $Q \simeq -1.484 \times 10^{-2}$ is a numerical constant which arises as follows. Define

$$I_1(\mu^2) \equiv \frac{\partial I_0}{\partial(\mu^2)}$$

$$= -3\int_E \frac{d^2p}{(2\pi)^2}\frac{d^2q}{(2\pi)^2}\frac{1}{(p^2+\mu^2)^2(q^2+\mu^2)([p+q]^2+\mu^2)}$$

$$\equiv \frac{Q}{(\mu^2)^2}.$$

We already know from Section 4 that $\mu^2(0) = m_R^2$, so therefore (6.1) tells us that $\mathcal{M}^2(0) = m_R^2$. Mass renormalization is again simple:

$$m_R^2 = V''(0) = m_2^2 K_2^2 + \tfrac{1}{2}\lambda J_1(m_R^2) - \tfrac{1}{6}\lambda^2 I_0(m_R^2).$$
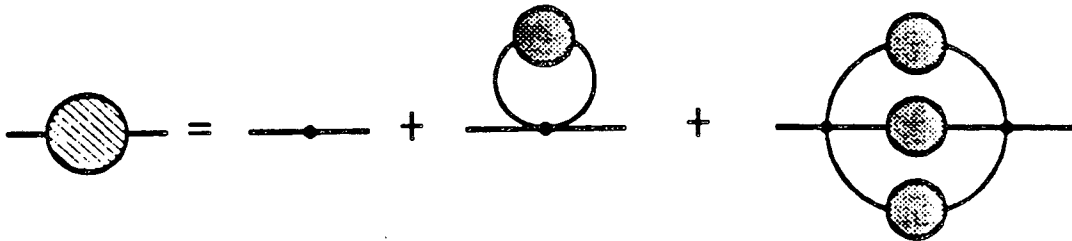
So we can rewrite (6.2) in terms of finite parameters as

$$V'(\hat{\Phi}) = m_R^2 \hat{\Phi} + \frac{\lambda K_2^4}{6} \hat{\Phi}^3 + \frac{\lambda \hat{\Phi}}{8\pi} \left[\frac{M^2 - \mu^2}{\mu^2} - \log\left(\frac{\mu^2}{m_R^2}\right) \right] \qquad (6.3)$$
$$+ \frac{\lambda^3 Q \hat{\Phi}^3}{12(\mu^2)^2} - \frac{\lambda^2 Q \hat{\Phi}}{6} \left(\frac{1}{m_R^2} - \frac{1}{\mu^2} \right).$$

It is easy to differentiate this to find $V''(\hat{\Phi})$, but the result is messy and unenlightening.

The final preliminary step is to compute K_2^2. At $\hat{\Phi} = 0$, the two-loop inverse propagator is

Sketch (6.2).

or algebraically,

$$-\hat{\Gamma}_{zy} = [K_2^2 \partial_z^2 + \text{stuff}] \delta_{zy} - \tfrac{1}{6} \lambda^2 \left(\hat{\Gamma}_{zy}^{-1} \right)^3.$$

Expanding, one eventually finds

$$-\hat{\Gamma}_{zy} = \left[\left(K_2^2 + \frac{2\theta^2 I}{3} \right) \partial_z^2 + \text{stuff} \right] \delta_{zy},$$

where I define the dimensionless constant

$$\theta \equiv \frac{\lambda}{8\pi m_R^2},$$

and

$$I \equiv \int_0^1 d\alpha \int_0^1 d\beta \frac{\beta(1-\beta)\alpha(1-\alpha)}{[\beta + \alpha(1-\alpha)(1-\beta)]^2} \simeq .11462$$

is an integral arising from the last diagram in Sketch (6.2).

We therefore find that

$$K_2^2 = 1 - \frac{2\theta^2 I}{3}. \tag{6.4}$$

Higher-order corrections would ensure positivity for K^2. I achieve this artificially, by the approximation

$$K_2^2 \simeq \left[1 + \frac{2\theta^2 I}{3}\right]^{-1},$$

which agrees with the perturbative result (6.4) to second order in λ.

2 A Systematic Approach

It is not really necessary to consider the perturbative, Gaussian and self-consistent approximations for $V(\hat{\Phi})$ and $Z(\hat{\Phi})$ in the piecemeal fashion of Sections 4 and 5. It is easier to work systematically as follows:

1. Compute $\mu^2(\hat{\Phi})$ in one of the three approximations:

   a) Perturbative: $\mu^2(\hat{\Phi}) = m_R^2 + \frac{1}{2}\lambda\hat{\Phi}^2$,

   b) Gaussian: $\mu^2(\hat{\Phi}) = m_R^2 + \frac{1}{2}\lambda\hat{\Phi}^2 - \frac{\lambda}{8\pi}\log\left(\frac{\mu^2}{m_R^2}\right)$,

   c) Self-consistent: $\mu^2(\hat{\Phi}) = V''(\hat{\Phi})$.

   (Note that (b) is an algebraic consistency condition, whereas (c) is a differential consistency condition.)

2. For (a), (b) and (c), substitute $\mu^2(\hat{\Phi})$ into $V'(\hat{\Phi})$ and integrate numerically to get $V(\hat{\Phi})$.

3. For (a), (b) and (c), substitute $\mu^2(\hat{\Phi})$ into the expression (5.1) for $Z(\hat{\Phi})$.

The results are plotted in Figures (6.1) through (6.16). I will refer to these as the two-loop approximations, although this is not strictly accurate nomenclature for the results for $Z(\hat{\Phi})$. I discuss these plots in the next subsection.

3   Can We Trust Our Results?

So far, I have consciously ignored the nagging question of the reliability of the various approximations. It has traditionally been difficult to handle this issue with precision.

The usual answer to the question in perturbation theory is that the results are 1) reliable, if $\tilde{\lambda} \ll 24$, 2) questionable for $\tilde{\lambda} \approx 24$, and 3) unreliable for $\tilde{\lambda} \gg 24$. This answer is somewhat vague; what do $\ll$, $\approx$, and $\gg$ really mean?

I believe that a better criterion is possible, based on visual comparison of the various approximations of V. This criterion is subjective, but less so than the $\ll$ / $\approx$ / $\gg$ trichotomy given above. Let us see how this criterion works out in practice, by examining our one-loop and two-loop results.

Consider, for example the one-loop and two-loop plots of V at $\tilde{\lambda} = 12$, Figures (4.2) and (6.3). The one-loop results agree among themselves very

well, as well as agreeing with the two-loop curves. Clearly, any one of these curves could be labelled "reliable".

Making similar comparisons, one observes a gradual decline in the reliability as $\bar{\lambda}$ increases up to about 21. At $\bar{\lambda} = 22$, the two-loop self-consistent curve charts its own course, and the other two-loop curves are substantially different from their one-loop cousins. For $\bar{\lambda} \gtrsim 24$, the two-loop self-consistent curve cannot be computed (for reasons to be explained in a moment). Observe that the one-loop perturbative and Gaussian predictions of a first-order phase transition at $\bar{\lambda} \sim 50$ now look far less likely, as we know they should. If we must stop at two loops, we should probably label all graphs with $\bar{\lambda} \gtrsim 22$ at least questionable, if not totally unreliable.

Why has the two-loop self-consistent approximation failed so abruptly for $\bar{\lambda} \gtrsim 22$? I have already anticipated the answer in Section 5. Consider the graphs of $Z(\hat{\Phi})$ from the previous section, Figures (5.1) through (5.10), and the plots of $Z(\hat{\Phi})$ in the first ten figures at the end of this section. Note how the self-consistent curve rises high above the other two approximations when $\bar{\lambda}$ gets large. Z becomes important here! In the next subsection, I will show how to take this effect into account.

4 Further Improvements

Recall the exact equation

$$-\hat{\Gamma}_{zy} = \left[V''(\hat{\Phi}) + Z(\hat{\Phi})\partial_z^2 + \ldots\right]\delta_{zy}.$$

In the self-consistent approximation, we set the dots to zero and Z to

one. This second approximation was not *really* necessary. Without it,

$$\hat{\Gamma}_{zy}^{-1} = \frac{1}{Z(\hat{\Phi})}\int\frac{d^2p}{(2\pi)^2}\frac{e^{-ip\cdot(z-y)}}{\left(p^2 - \frac{V''}{Z} + i\epsilon\right)}. \qquad (6.5)$$

Note that this is a very dangerous propagator! It can introduce field-

dependent divergences. For example,

$$i\hat{\Gamma}_{zz}^{-1} = \frac{1}{Z(\hat{\Phi})}J_1(V''/Z)$$

is a divergent quantity multiplied by a function of $\hat{\Phi}$. Presumably, an exact

calculation of $\hat{\Gamma}_{zy}^{-1}$ would evade this problem, but that is little consolation.

For the moment, we are stuck with the approximate propagator above, so

we will have to restrict its use to finite diagrams (or subdiagrams). In the

two-loop calculation, the only such diagram is
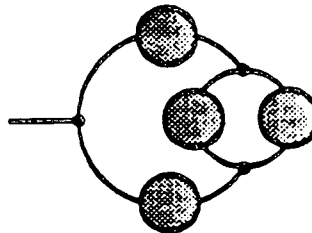
Sketch (6.3).

The net effect of using the improved propagator, (6.5), here is to multiply this diagram by a factor $1/Z^2$. This affects only one term in our previous computation of $V'(\hat{\Phi})$. In (6.3) one finds the following replacement:

$$\frac{\lambda^3 Q \hat{\Phi}^3}{12(\mu^2)^2} \rightarrow \frac{\lambda^3 Q \hat{\Phi}^3}{12(\mu^2)^2 Z^2} .$$

[A technical note: The calculation of $Z(\hat{\Phi})$ in Section 5 was also finite. What happens if we recompute $Z(\hat{\Phi})$ using our new, improved propagator, (6.5)? The answer is that nothing happens. All diagrams get multiplied by 1, and we again get equation (5.1).]

One can again perform the numerical calculations outlined in Subsection 6.2 to obtain improved estimates of $\mu^2(\hat{\Phi})$, $V(\hat{\Phi})$ and $Z(\hat{\Phi})$. I will refer to the newly computed $V(\hat{\Phi})$ and $Z(\hat{\Phi})$ as the improved two-loop approximations. I have plotted $V(\hat{\Phi})$ and $Z(\hat{\Phi})$ in Figures (6.11) through (6.24). $\tilde{\lambda}$ varies from 6 to 57; above 57, the self-consistent approximation again fails to exist. The changes are most striking for the self-consistent approximation. The Gaussian and self-consistent curves for $V(\hat{\Phi})$ are now quite close together over the full range of $\tilde{\lambda}$ for which the self-consistent approximation exists, and I think we can reasonably label them "reliable". Moreover, the improved two-loop perturbative curve looks fairly reliable. Comparing these curves to the previous results in Section 4, it seems that even the one-loop self-consistent curve can be re-assessed as being somewhat reliable *at least* up to $\tilde{\lambda} \approx 57$, while the other one-loop results become increasingly poor.
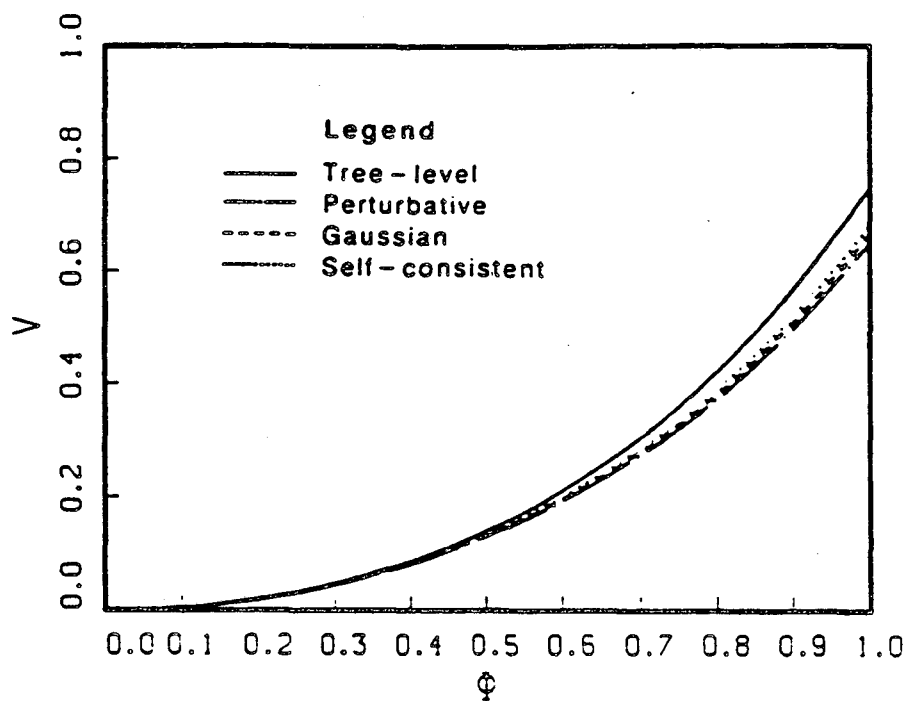
Figure (6.1): Plot of two-loop approximation to $V(\Phi)$ at $\tilde{\lambda} = 6$.
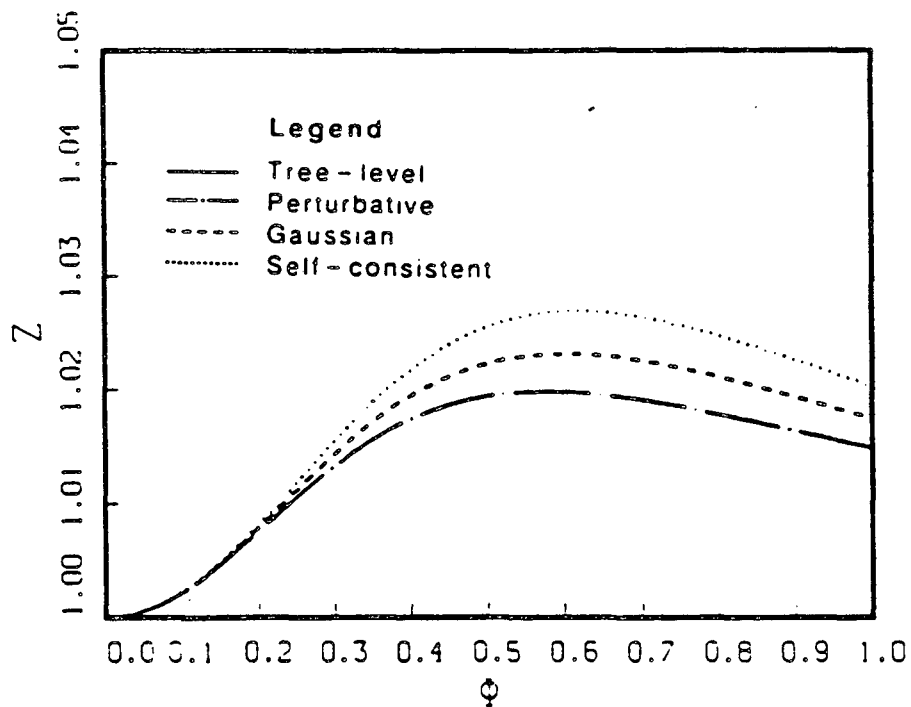

Figure (6.2): Plot of two-loop approximation to $Z(\Phi)$ at $\tilde{\lambda} = 6$.
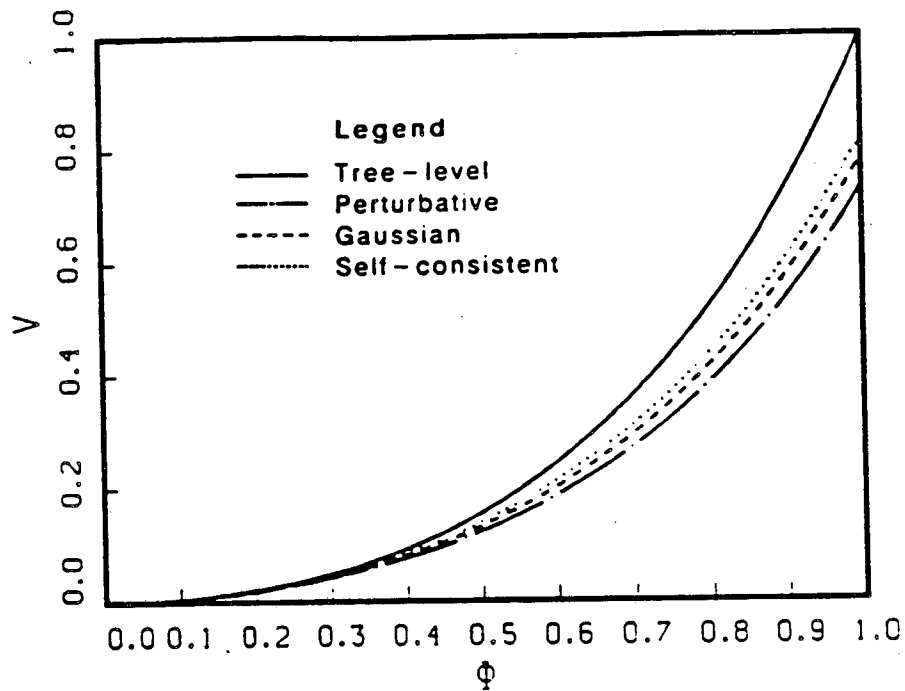
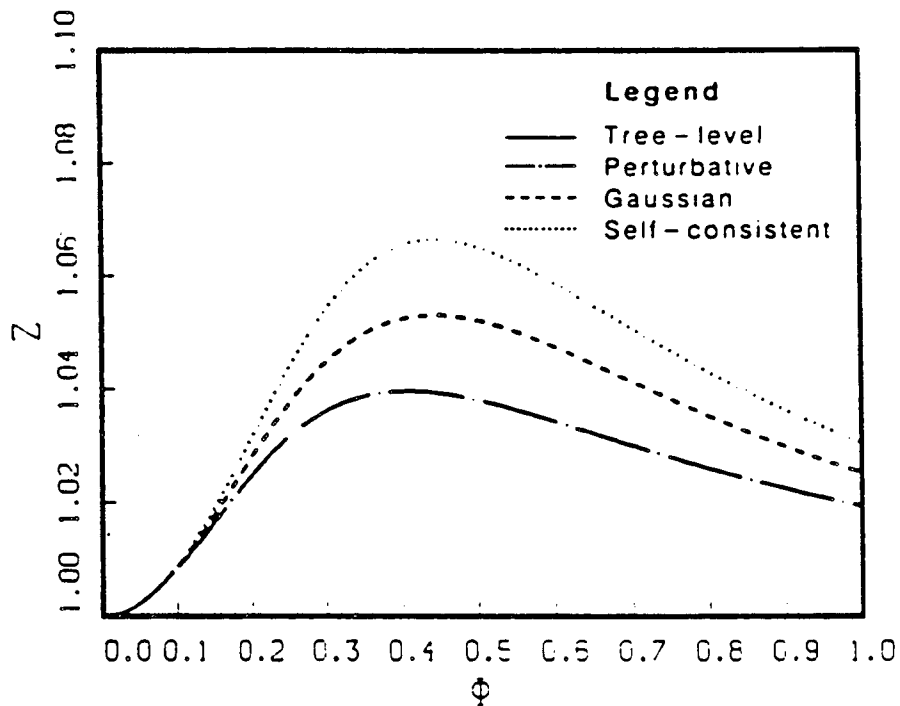Figure (6.3): Plot of two-loop approximation to $V(\Phi)$ at $\tilde{\lambda} = 12$.

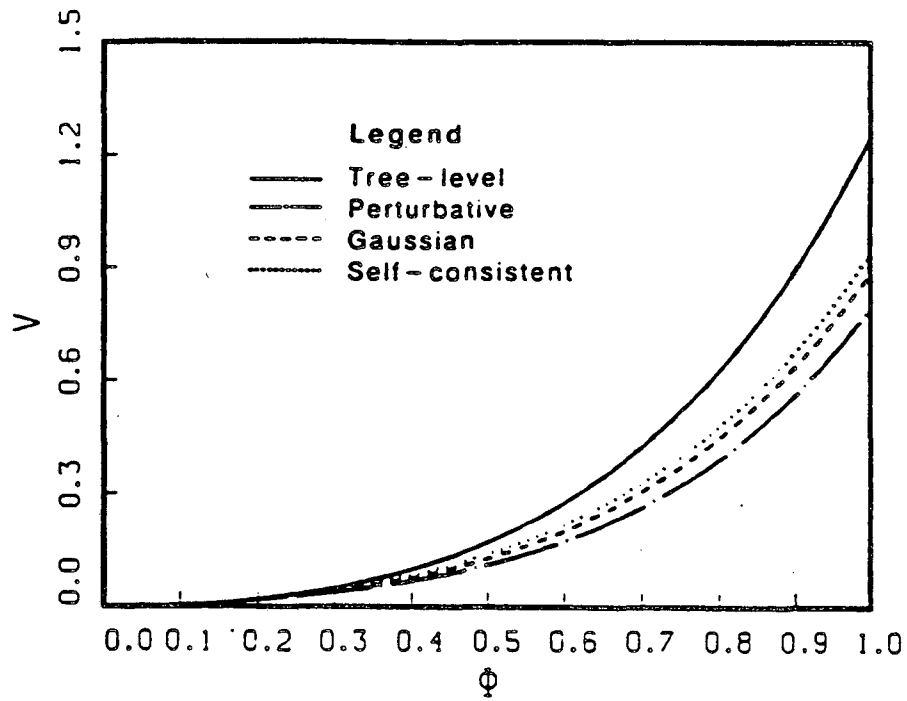Figure (6.4): Plot of two-loop approximation to $Z(\Phi)$ at $\tilde{\lambda} = 12$.

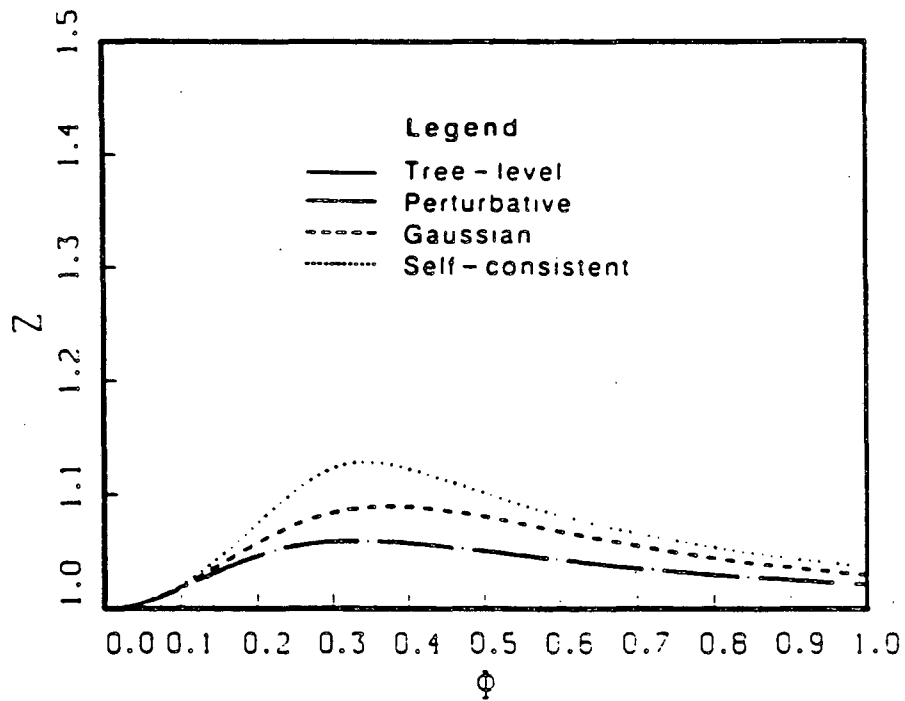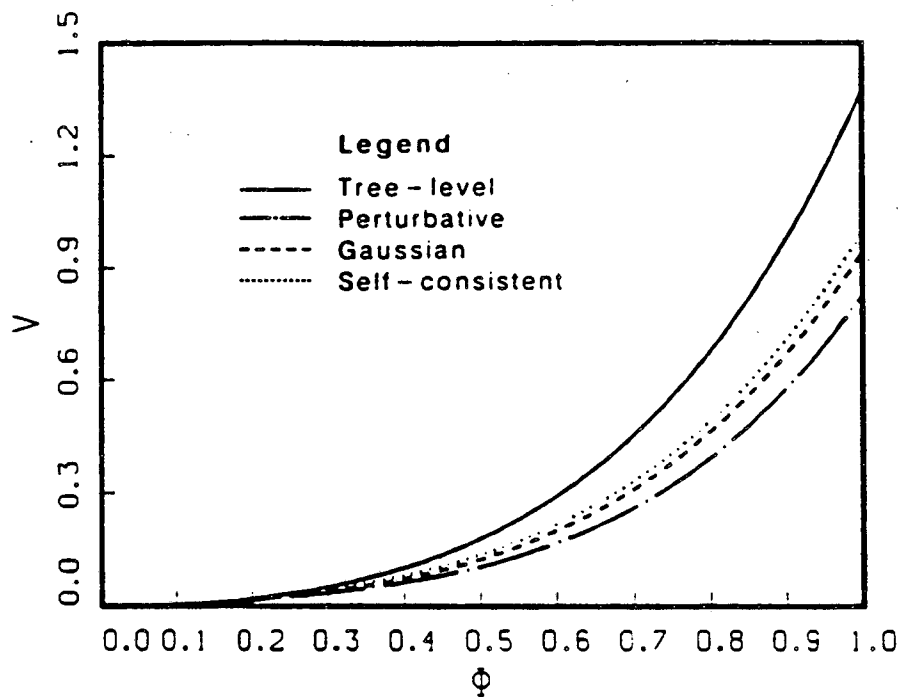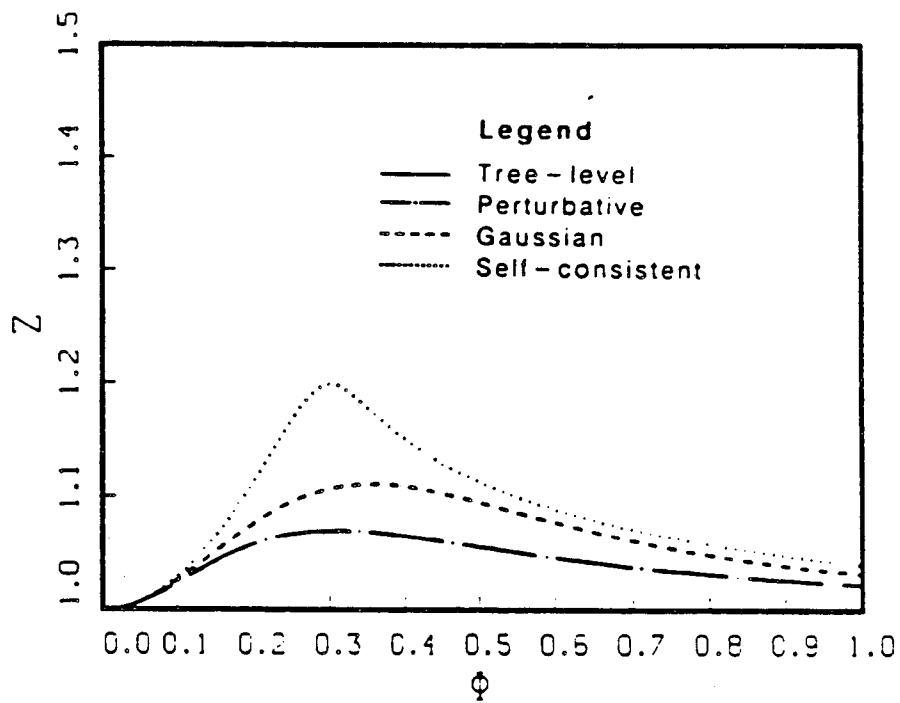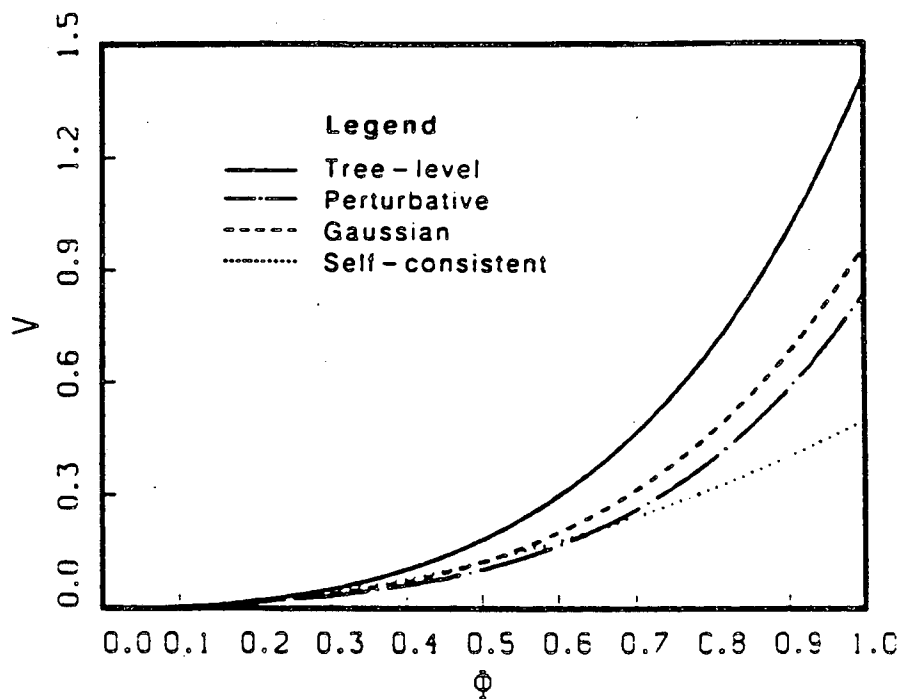Figure (6.5): Plot of two-loop approximation to $V(\Phi)$ at $\tilde{\lambda} = 18$.

Figure (6.6): Plot of two-loop approximation to $Z(\Phi)$ at $\tilde{\lambda} = 18$.

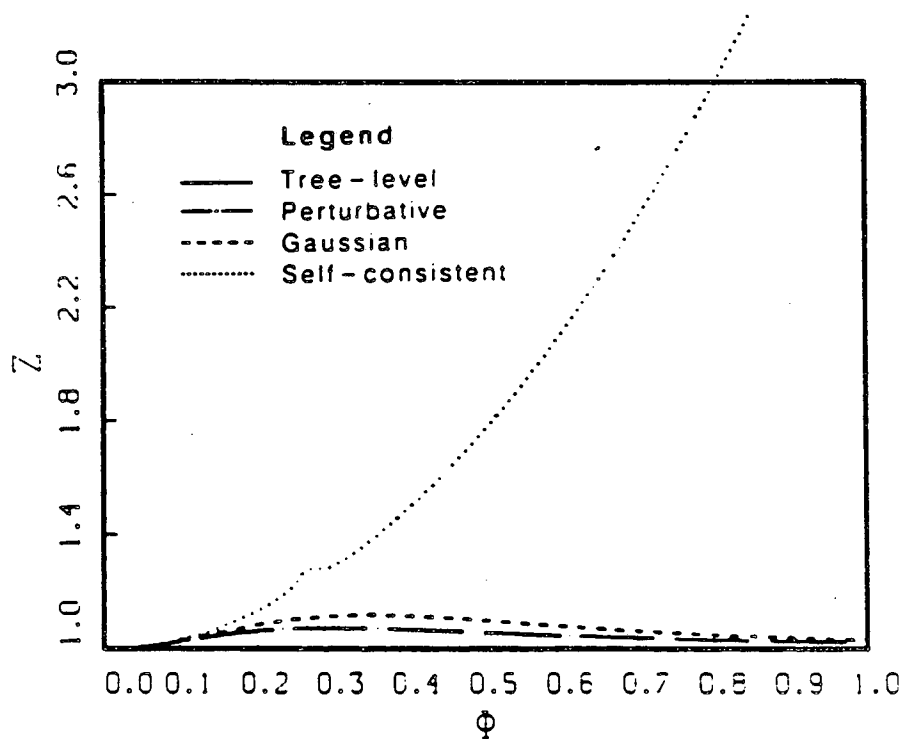Figure (6.7): Plot of two-loop approximation to $V(\Phi)$ at $\bar{\lambda} = 21$.

Figure (6.8): Plot of two-loop approximation to $Z(\Phi)$ at $\bar{\lambda} = 21$.

Figure (6.9): Plot of two-loop approximation to $V(\Phi)$ at $\bar{\lambda} = 22$.

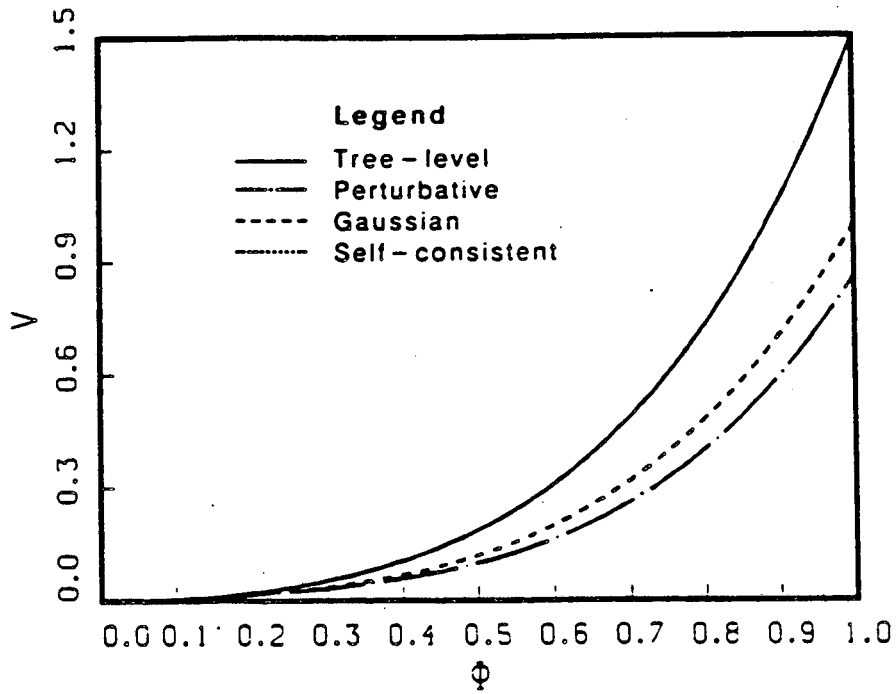Figure (6.10): Plot of two-loop approximation to $Z(\Phi)$ at $\bar{\lambda} = 22$.

Figure (6.11): Plot of two-loop approximation to $V(\Phi)$ at $\bar\lambda = 24$. (The self-consistent approximation does not exist.)
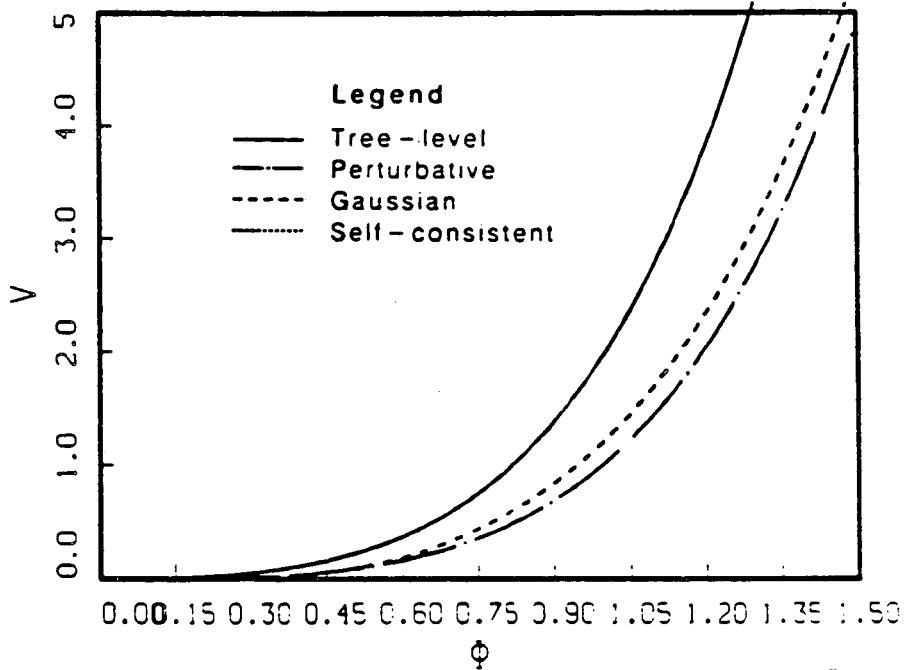

Figure (6.12): Plot of two-loop approximation to $V(\Phi)$ at $\bar\lambda = 36$. (The self-consistent approximation does not exist.)
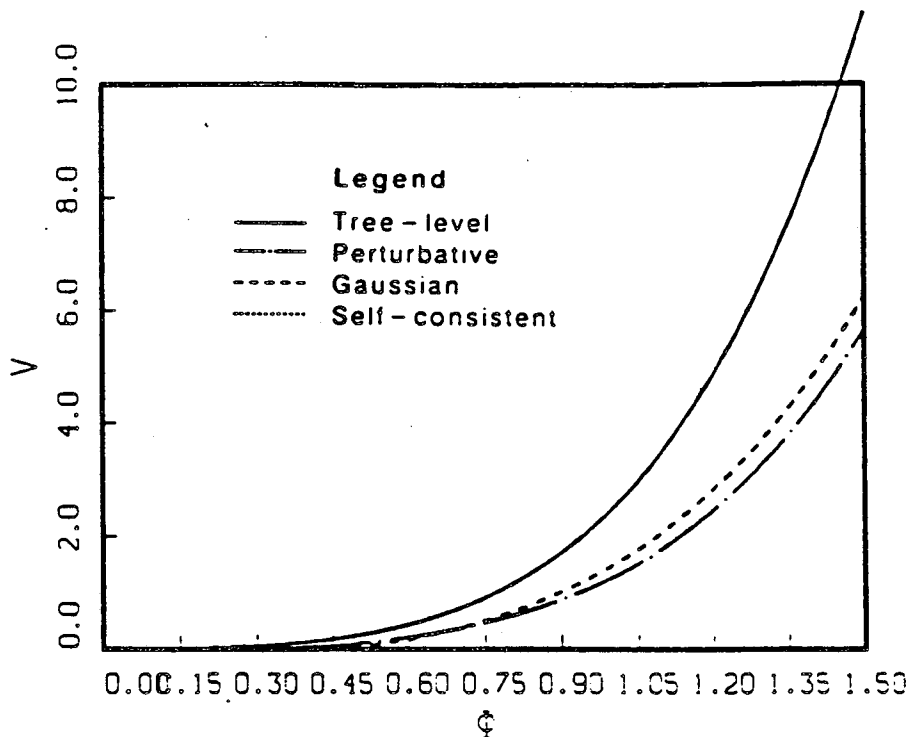
Figure (6.13): Plot of two-loop approximation to $V(\Phi)$ at $\bar{\lambda} = 48$. (The self-consistent approximation does not exist.)
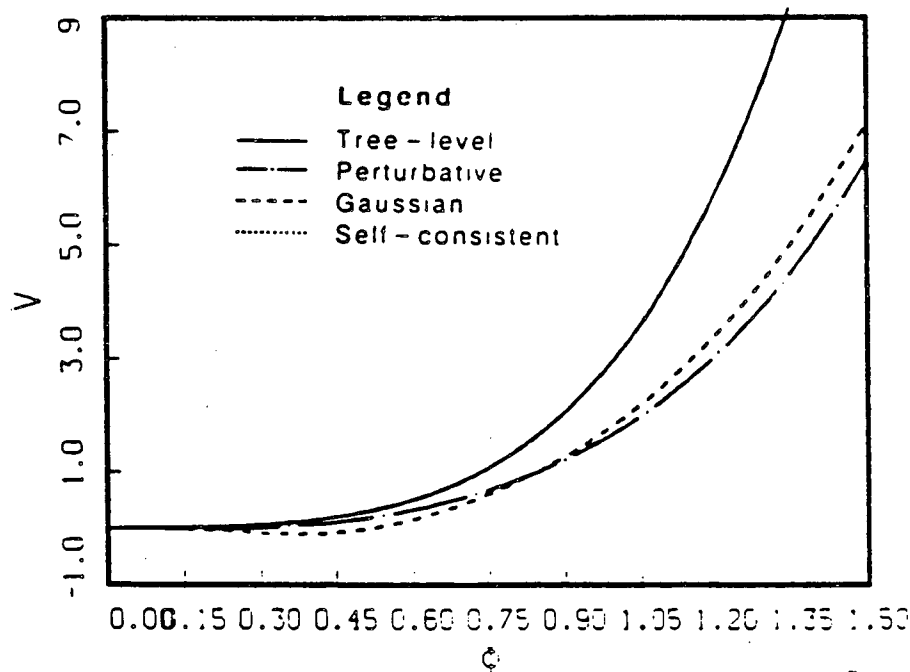

Figure (6.14): Plot of two-loop approximation to $V(\Phi)$ at $\bar{\lambda} = 60$. (The self-consistent approximation does not exist.)
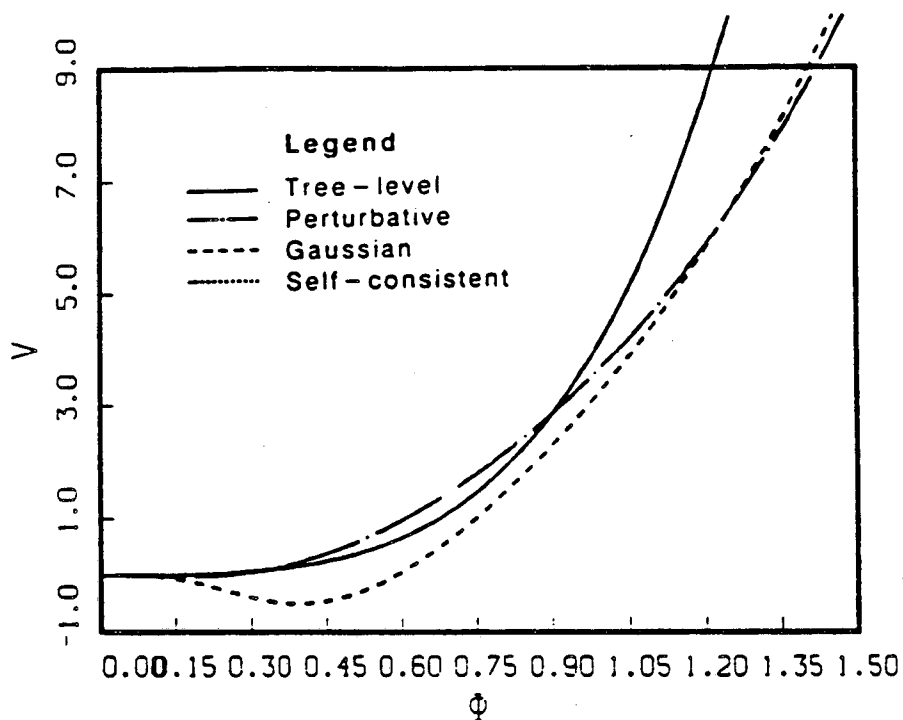
Figure (6.15): Plot of two-loop approximation to $V(\Phi)$ at $\tilde{\lambda} = 90$. (The self-consistent approximation does not exist.)
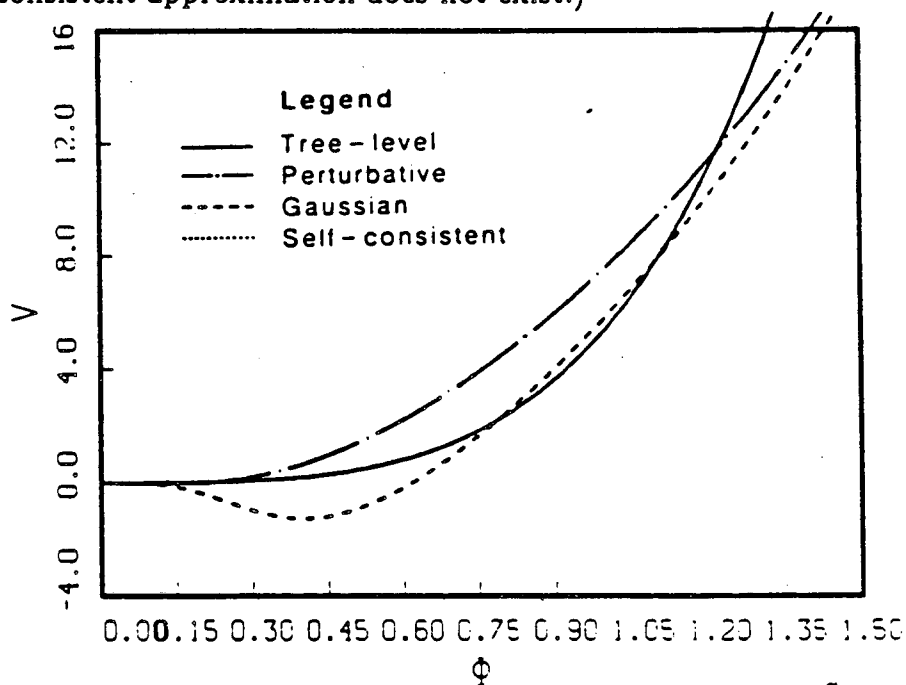

Figure (6.16): Plot of two-loop approximation to $V(\Phi)$ at $\tilde{\lambda} = 120$. (The self-consistent approximation does not exist.)
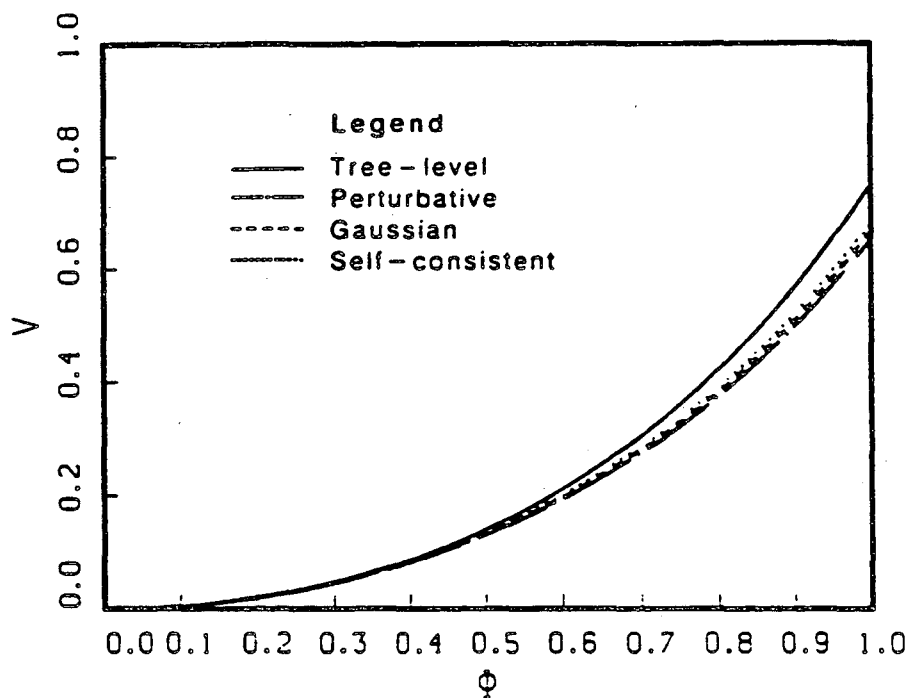
Figure (6.17): Plot of improved two-loop approximation to $V(\Phi)$ at $\tilde{\lambda} = 6$.

Figure (6.18): Plot of improved two-loop approximation to $Z(\Phi)$ at $\tilde{\lambda} = 6$.
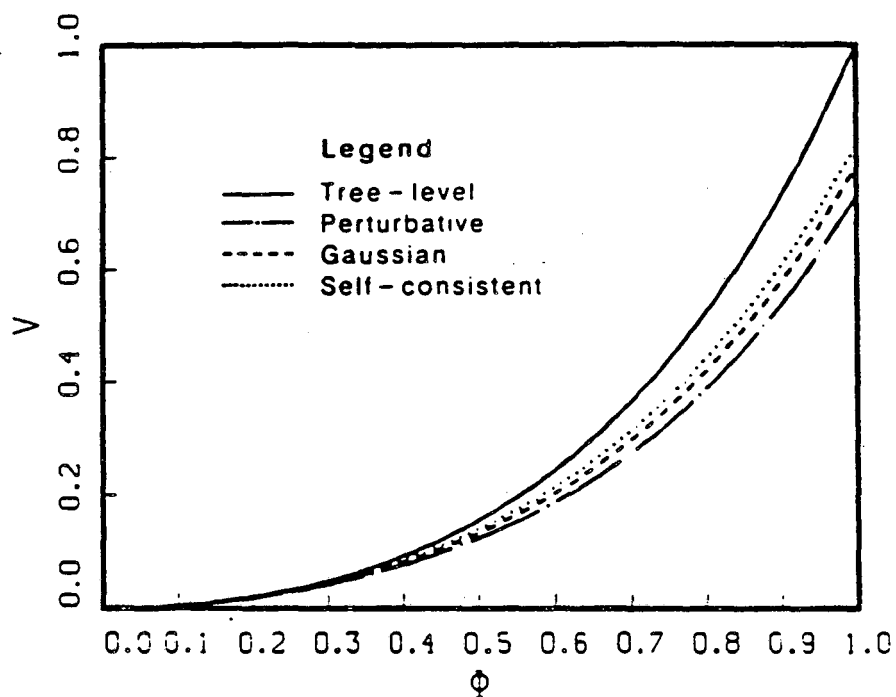
Figure (6.19): Plot of improved two-loop approximation to $V(\Phi)$ at $\tilde{\lambda} = 12$.
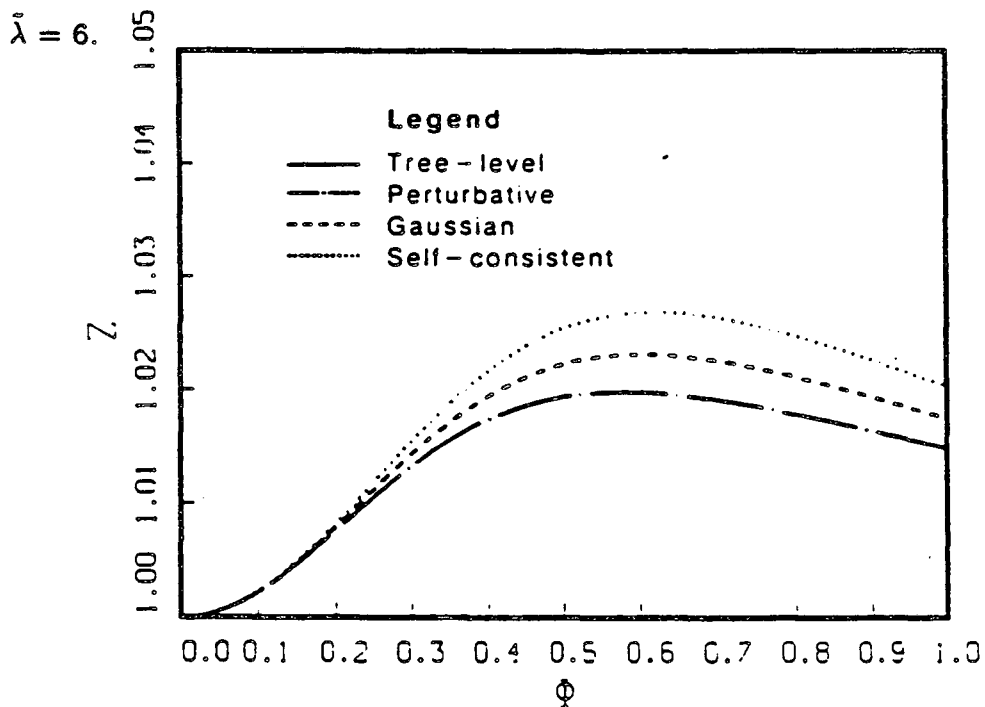

Figure (6.20): Plot of improved two-loop approximation to $Z(\Phi)$ at $\tilde{\lambda} = 12$.
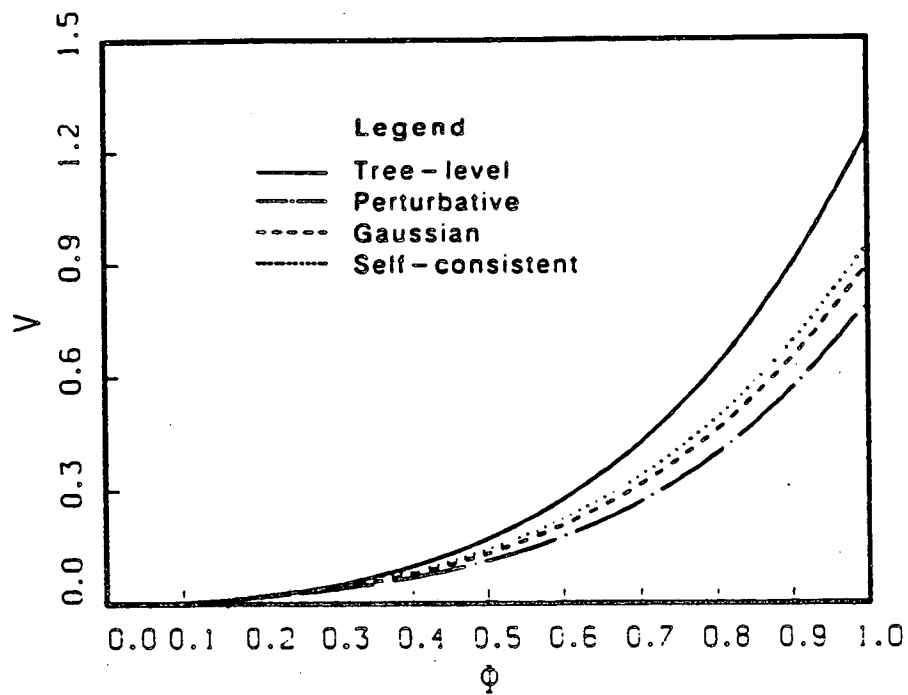
Figure (6.21): Plot of improved two-loop approximation to $V(\Phi)$ at $\tilde{\lambda} = 18$.

Figure (6.22): Plot of improved two-loop approximation to $Z(\Phi)$ at $\tilde{\lambda} = 18$.

Figure (6.23): Plot of improved two-loop approximation to $V(\Phi)$ at $\tilde{\lambda} = 24$.

Figure (6.24): Plot of improved two-loop approximation to $Z(\Phi)$ at $\tilde{\lambda} = 24$.

Figure (6.25): Plot of improved two-loop approximation to $V(\Phi)$ at $\tilde{\lambda} = 36$.

Figure (6.26): Plot of improved two-loop approximation to $Z(\Phi)$ at $\tilde{\lambda} = 36$.

Legend

— Tree – level
—·— Perturbative
----- Gaussian
·········· Self – consistent

Figure (6.27): Plot of improved two-loop approximation to $V(\Phi)$ at $\tilde{\lambda} = 48$.

Legend

— Tree – level
—·— Perturbative
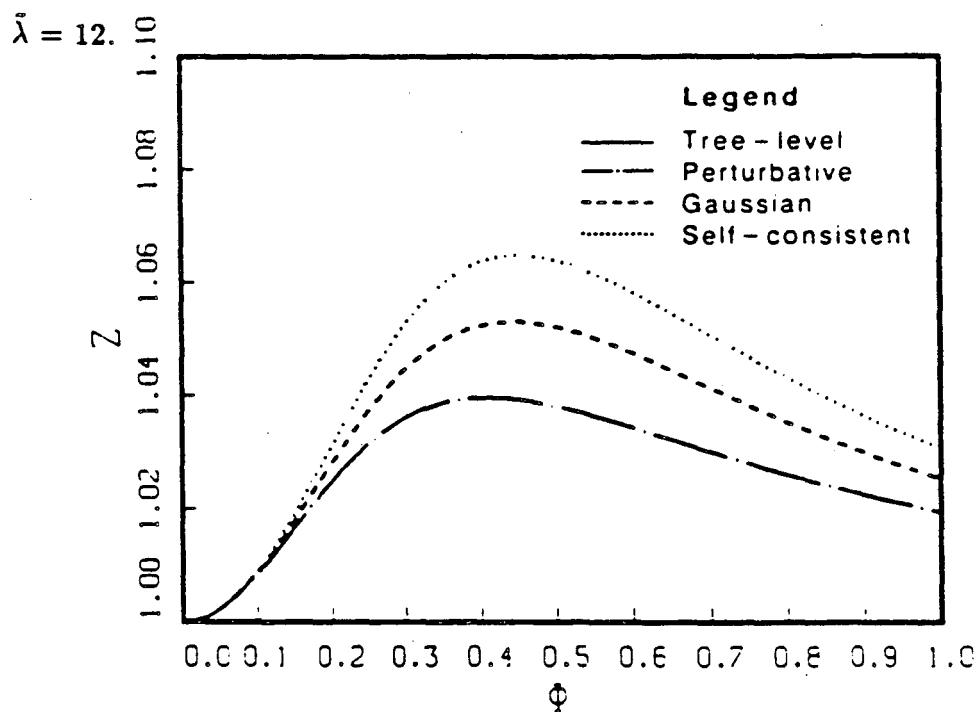----- Gaussian
——— Self – consistent

Figure (6.28): Plot of improved two-loop approximation to $Z(\Phi)$ at

$\tilde{\lambda} = 48$.
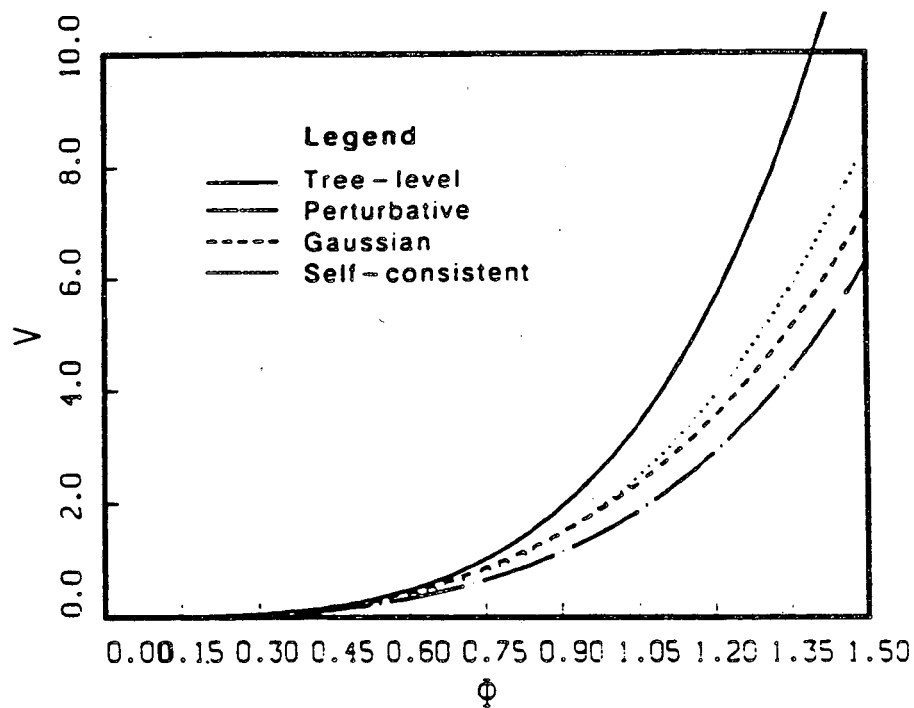
Figure (6.29): Plot of improved two-loop approximation to $V(\Phi)$ at $\tilde{\lambda} = 57$.
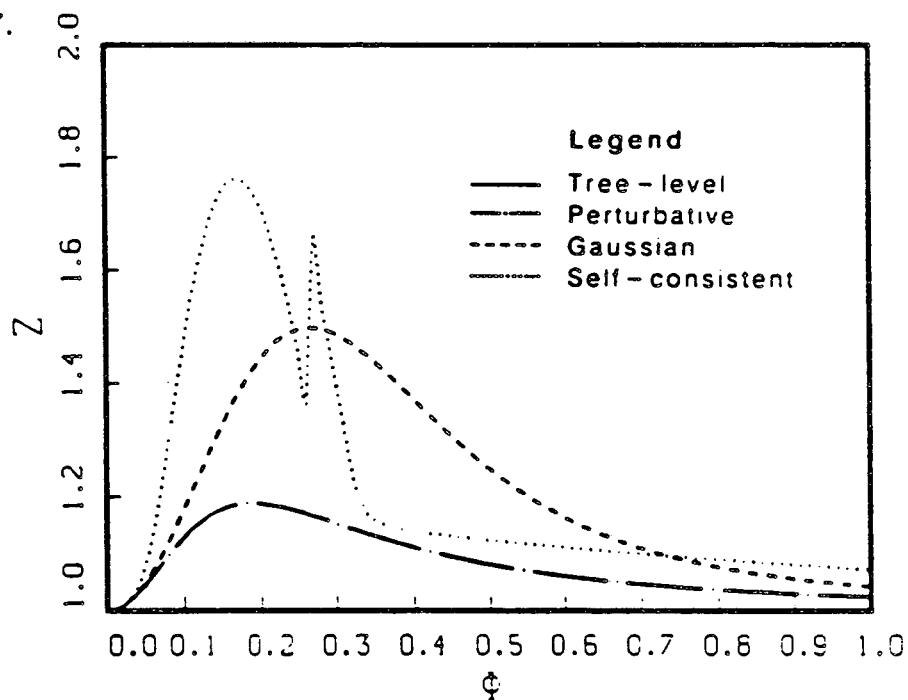
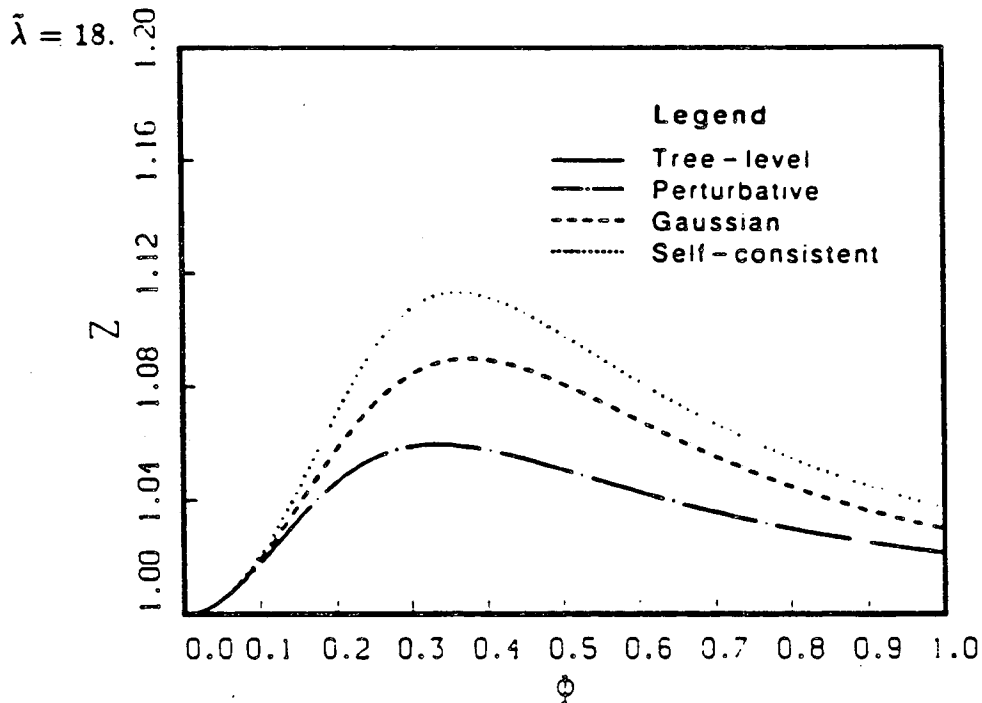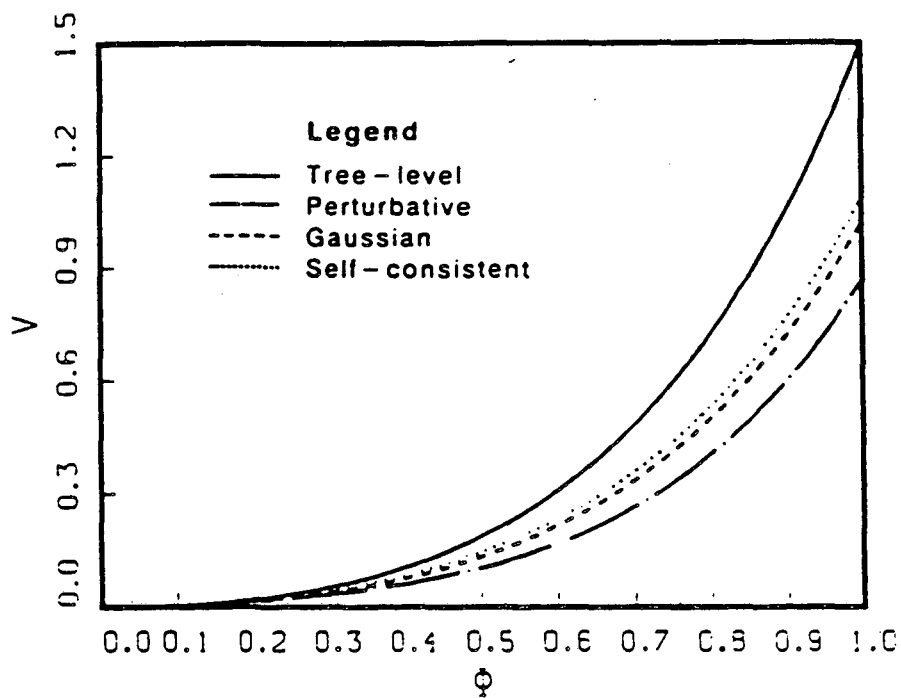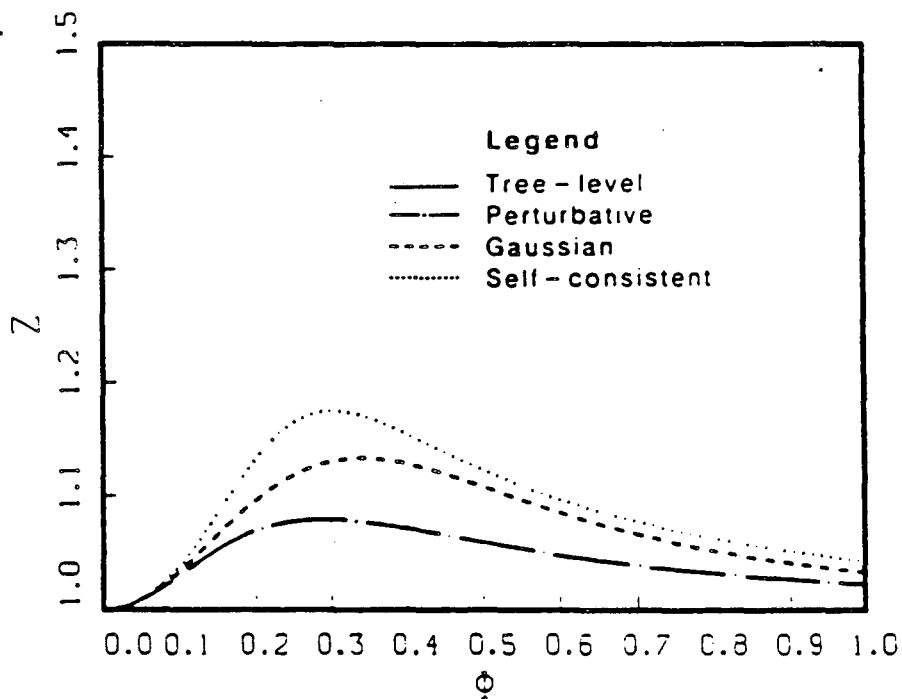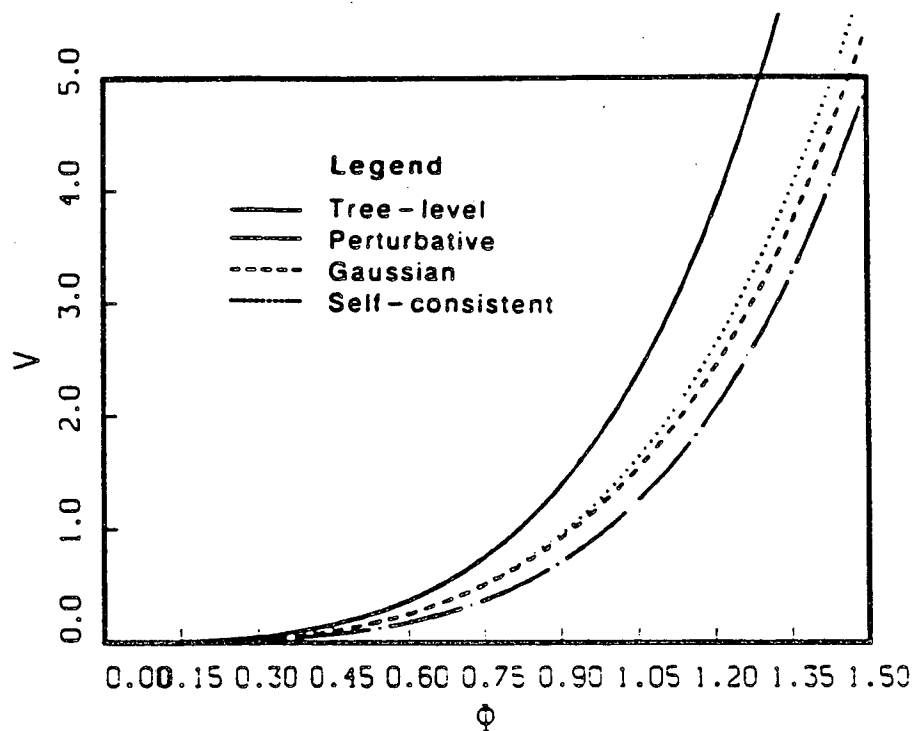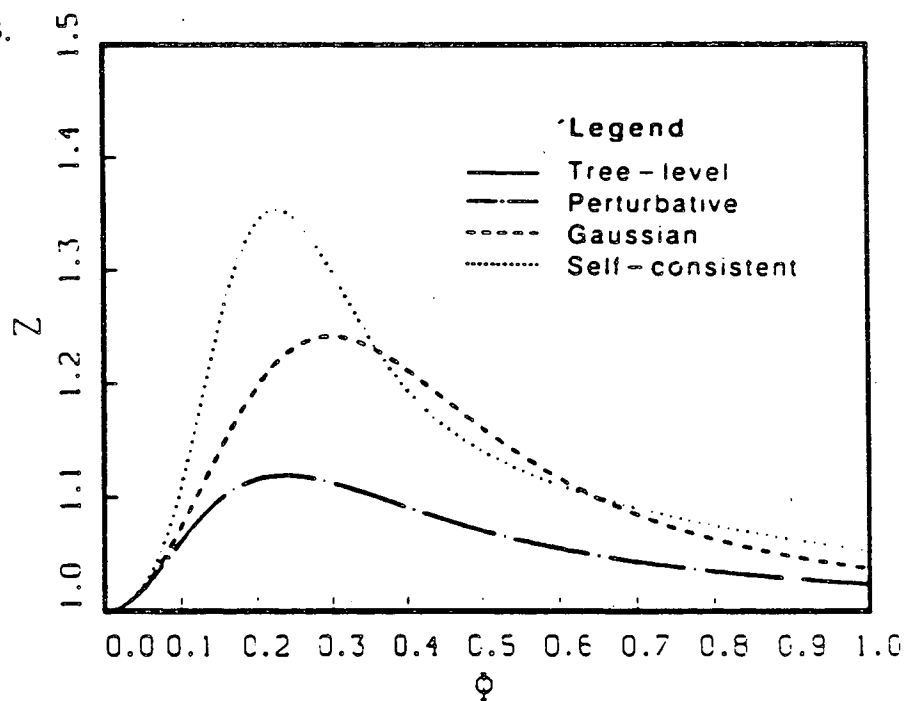Figure (6.30): Plot of improved two-loop approximation to $Z(\Phi)$ at $\tilde{\lambda} = 57$.
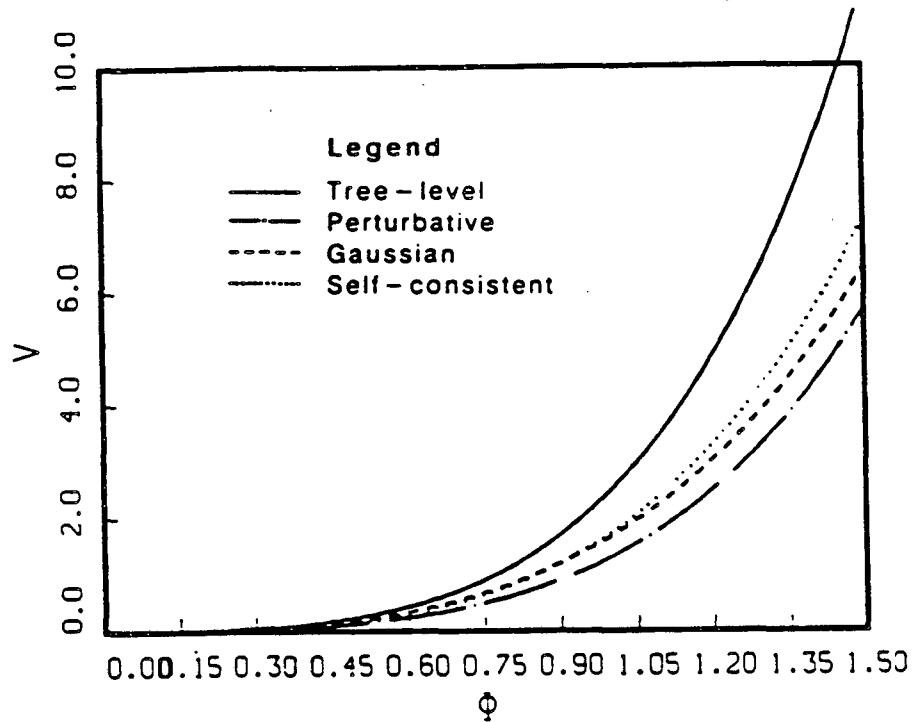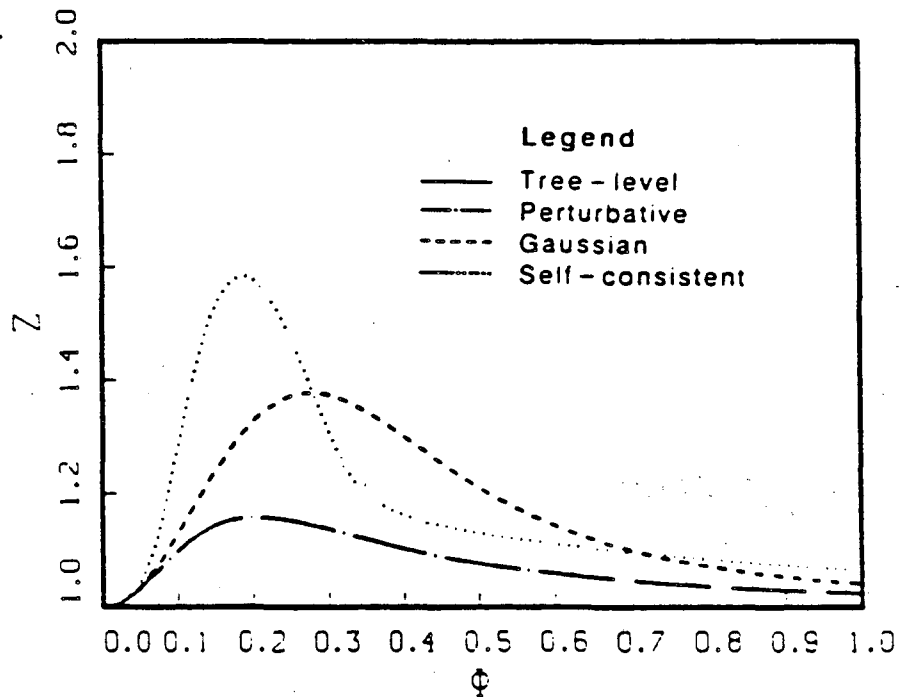
VII   The Broken-Symmetry Case

1   Some Preliminaries

The analysis of the broken phase is somewhat more complicated than the symmetric phase. For this reason, I will only consider the one-loop case.

In Section 4, I showed that the one-loop, all-purpose expression for $V'(\hat{\Phi})$ is (4.7), which I rewrite here for convenience:

$$V'(\hat{\Phi}) = m_R^2 \hat{\Phi} + \frac{\lambda K_1^4}{6} \left(\hat{\Phi}^2 - 3F^2 \right) \hat{\Phi} + \frac{\lambda F g \hat{\Phi}}{8\pi \mu_F^2} - \frac{\lambda \hat{\Phi}}{8\pi} \log \left(\frac{\mu^2}{\mu_F^2} \right) . \qquad (7.1)$$

The condition that $V(\hat{\Phi})$ assumes a minimum at F implies

$$0 = V'(F) = m_R^2 F - \tfrac{1}{3}\lambda K_1^4 F^3 + \frac{\lambda g F^2}{8\pi \mu_F^2} .$$

(One must be wary of spurious solutions to this equation, which make $V(\hat{\Phi})$ a local maximum at F.) For the broken-symmetry case, $F \neq 0$ and this implies the relation

$$m_R^2 = \tfrac{1}{3}\lambda K_1^4 F^2 - \frac{\lambda g F}{8\pi \mu_F^2} . \qquad (7.2)$$

(This is analogous to the tree-level result $m_R^2 = \tfrac{1}{3}\lambda F^2$.) Without loss of generality, we can assume that $F > 0$. (7.2) allows us to simplify the expression of $V'(\hat{\Phi})$ in (7.1):

$$V'(\hat{\Phi}) = \frac{\lambda K_1^4}{6} \left(\hat{\Phi}^2 - F^2 \right) \hat{\Phi} - \frac{\lambda \hat{\Phi}}{8\pi} \log \left(\frac{\mu^2}{\mu_F^2} \right) . \qquad (7.3)$$

We have already calculated K_1^2 for the broken phase, (5.2):

$$K_1^2 \simeq \left[1 + \frac{\lambda^2 F^2}{48\pi(\mu_F^2)^2}\right]^{-1}.$$ (7.4)

Clearly, $K_1^2 \simeq 1$ if $\lambda F/\mu_F^2$ is small compared to 48π. We will see retrospectively that this condition holds for the perturbative and Gaussian approximations, so for the next two subsections, I will set $K_1^2 = 1$. This makes the algebra somewhat simpler.

In the next three subsections, I derive equations for $\mu^2(\hat{\Phi})$, to supplement (7.3) and (7.4). I also check whether $K_1^2 \simeq 1$ is a valid approximation. Actual calculations will be deferred to Subsection 7.5.

2 The Perturbative Approximation

The classical potential $U(\hat{\Phi})$ can be written in the form

$$U(\hat{\Phi}) = \frac{\lambda}{24}\left(\hat{\Phi}^2 - F^2\right)^2 + \text{constant.}$$

The loop-expansion is specified by

$$\mu^2(\hat{\Phi}) \equiv U''(\hat{\Phi}) = \tfrac{1}{6}\lambda\left(3\hat{\Phi}^2 - F^2\right).$$ (7.5)

We then have

$$\mu_F^2 = \mu^2(F) = \tfrac{1}{3}\lambda F^2$$

$$g = \frac{\partial\mu^2}{\partial\hat{\Phi}}(F) = \lambda F.$$

Inserting these into our equation for m_R^2, (7.2), we have

$$m_R^2 = \lambda \left[\frac{F^2}{3} - \frac{3}{8\pi} \right].$$

Note that $m_R^2 \neq \mu_F^2$, unlike the symmetric case. Clearly m_R^2 is positive only for $F > \sqrt{9/(8\pi)} \simeq .599$. This is a consequence of the spurious first-order phase-transition, which we already saw in the symmetric phase calculations in Section 4.

We also compute

$$\frac{\lambda F}{\mu_F^2} = \frac{3}{F},$$

which is certainly much smaller than 48π in the allowed region for F. So $K_1^2 \simeq 1$ is a good approximation.

Note that $\mu^2(\hat{\Phi}) > 0$ only for $\hat{\Phi}^2 > \frac{1}{3}F^2$. This implies that $V(\hat{\Phi})$ will be complex for $\hat{\Phi}^2 < \frac{1}{3}F^2$, a fact which remains true to every finite order in perturbation theory.

3 The Gaussian Approximation

For the Gaussian approximation in the broken phase, we cannot use the simple expression (4.11) for $\mu^2(\hat{\Phi})$. It is easy to derive the correct expression, using the Schwinger-Dyson equation
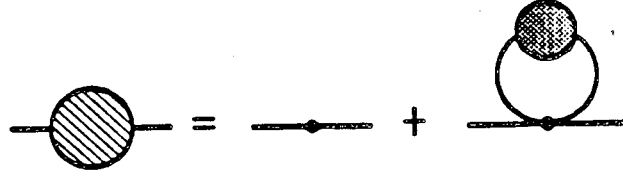
Sketch (7.1).

Algebraically, this is

$$-\hat{\Gamma}_{zy} = K_1^2(\partial_z^2 + m_1^2)\delta_{zy} + \tfrac{1}{2}\lambda K_1^4 \hat{\Phi}^2 \,\delta_{zy} + \tfrac{1}{2}\lambda \left(i\hat{\Gamma}_{zz}^{-1}\right)\delta_{zy}.$$

Setting $K_1^2 = 1$, and copying our previous result (4.6) for m_1^2, we find that

$$\mu^2(\hat{\Phi}) = m_R^2 + \tfrac{1}{2}\lambda\left(\hat{\Phi}^2 - F^2\right) - \frac{\lambda}{8\pi}\log\left(\frac{\mu^2}{\mu_F^2}\right) + \frac{\lambda g F}{8\pi\mu_F^2}.$$

Again, we find $m_R^2 \neq \mu_F^2$. We can simplify μ_F^2, using (7.2), to obtain

$$\mu^2(\hat{\Phi}) = \tfrac{1}{6}\lambda\left(3\hat{\Phi}^2 - F^2\right) - \frac{\lambda}{8\pi}\log\left(\frac{\mu^2}{\mu_F^2}\right), \qquad (7.6)$$

from which we find

$$\mu_F^2 = \tfrac{1}{3}\lambda F^2.$$

This is just like the perturbative case. So, again

$$\frac{\lambda F}{\mu_F^2} = \frac{3}{F},$$

and $K_1^2 = 1$ will be a valid approximation if F should happen to be restricted to be fairly large (i.e., $F^2 \gg 1/(16\pi)$). Such a condition does hold, due

to the spurious first-order phase-transition in the Gaussian approximation.

I will sketch the derivation here. From (7.6), one can compute

$$g = \frac{\partial \mu^2}{\partial \hat{\Phi}}(F) = \frac{\lambda F}{1 + \frac{3}{8\pi F^2}} .$$

Inserting this into (7.2), one finds

$$m_R^2 = \frac{\lambda F^2}{3} \left[1 - \frac{9}{8\pi F^2 + 3} \right] ,$$

which is positive only when $F^2 \geq 3/(4\pi)$, (i.e., $|F| > .489$). So clearly,
$F^2 \gg 1/(16\pi)$, and hence, $K_1^2 \simeq 1$ is valid.

4 The Self-consistent Approximation

As usual in the self-consistent approximation, we require $\mu^2(\hat{\Phi}) = V''(\hat{\Phi})$.
This fixes $\mu_F^2 = \mu^2(F) = m_R^2$. We have to solve the differential equation
obtained by differentiating (7.3):

$$\mu^2(\hat{\Phi}) = V''(\hat{\Phi})$$

$$= \tfrac{1}{6}\lambda K_1^4 \left(3\hat{\Phi}^2 - F^2 \right) - \frac{\lambda}{8\pi} \left[\log\left(\frac{\mu^2}{m_R^2} \right) + \frac{\hat{\Phi}}{\mu^2} \frac{\partial \mu^2}{\partial \hat{\Phi}} \right]. \qquad (7.7)$$

But, in order to solve this, we need to use the boundary condition

$$\frac{\partial \mu^2}{\partial \hat{\Phi}}(F) = g.$$

In the previous two subsections, we specified the function $\mu^2(\hat{\Phi})$, from
which we computed the constants μ_F^2 and g. Here the situation is reversed:

we must specify g so that the function $\mu^2(\hat{\Phi})$ and the constant μ_F^2 can be computed. What physical principle will enable us to specify g? After a fair amount of trial and error, I have concluded that the best procedure is to choose g so that μ_F^2 comes out the same as it did in the previous two subsections, namely

$$\mu_F^2 = \tfrac{1}{3}\lambda F^2.$$

Since we also have $\mu_F^2 = m_R^2$, this means that

$$\tilde{\lambda} \equiv \frac{\lambda}{m_R^2} = \frac{3}{F^2}. \tag{7.8}$$

Note that this is the classical result. Also, in the limit $F \to 0$, we have $\tilde{\lambda} \to \infty$, as it must, according to the rigorous field theory results. Our equations (7.2) and (7.4) can be rewritten

$$K_1^2 \simeq \left(1 + \frac{3}{16\pi F^2}\right)^{-1}$$

$$\tilde{g} = \frac{8\pi F}{3}(K_1^4 - 1), \tag{7.9}$$

where $\tilde{g}$ is the rescaled quantity

$$\tilde{g} \equiv \frac{g}{m_R^2}.$$

Regarding F as the independent variable, (7.8) and (7.9) determine all the unknown quantities. We are now free to integrate (7.7), the differential equation for $\mu^2(\hat{\Phi})$, insert the solution into (7.3) and integrate to find the

self-consistent effective potential. I will do this in the next subsection, but first, I would like to make some observations.

1. Our equations (7.8) and (7.9) are physically sensible for all values of $F > 0$. Hence the phase transition is *not* first order.

2. As $F \to 0$, the expression for K_1^2 in (7.9) approaches zero. It is certain that this approximation becomes increasingly unreliable for small F. We could establish a reliability rating of some sort, if we took the trouble to do a two-loop calculation. Lacking this, I will make the rough guess that our approximation for K_1^2 is bad when $F^2 \lesssim 3/(16\pi)$, (i.e., $F \lesssim .25$). This corresponds to a value of $\tilde{\lambda} \gtrsim 50$. We already saw in Section 6 that such large values of $\tilde{\lambda}$ can yield reasonably accurate results in the one-loop self-consistent approximation for the symmetric phase of the model.

5 A Comparison

As before, it is an easy numerical problem to compute $\mu^2(\hat{\Phi})$, substitute into $V'(\hat{\Phi})$ and integrate to obtain the effective potential in each of our three approximations. I have plotted the results for various values of F in Figures (7.1) through (7.6). The graphs show the properties I reported in Section 2 for the perturbative and Gaussian approximations. The perturbative results are non-convex and have a domain where they are complex. The Gaussian

results are real, but not convex. Both show a first-order phase-transition near $F \sim .5$. (For F smaller than the respective critical values, the graphs show a local maximum at $\Phi = F$, corresponding to the unphysical situation $m_R^2 < 0$.)

The self-consistent results show the following features:

1. V is convex and real.

2. There is a phase-transition of order greater than 1, as $\tilde{\lambda} \to \infty$.

3. V exhibits a hard wall on the "inner side", while it agrees well with the perturbative and Gaussian results (when these exist) on the "outer side".

Finally, we must make some judgement on the reliability of the three approximations. From the graphs, it seems clear that one should distinguish two regions, $\hat{\Phi}^2 > F^2$ and $\hat{\Phi}^2 < F^2$. When the perturbative approximation exists, (i.e., for $|F| > .599$), and when the Gaussian approximation exists, (i.e., for $|F| > .489$), the various approximations agree fairly well for $\hat{\Phi}^2 > F^2$. The agreement improves strongly as F^2 increases. Clearly, all of these approximations should be judged somewhere between fairly reliable and very reliable, on this domain of $\hat{\Phi}$. On the other hand, the three approximations disagree badly for $\hat{\Phi}^2 < F^2$. As we know from the discussion in Section 2, these are all "wrong"; the true potential is flat here. Our computations analytically continue V from the non-trivial domain into the flat

region, giving the potential of metastable field configurations. These analytic continuations are all very different; lacking two-loop results, we can not label any of them reliable. (However, the perturbative and Gaussian approximations are very unlikely to be better than the self-consistent approximation.)
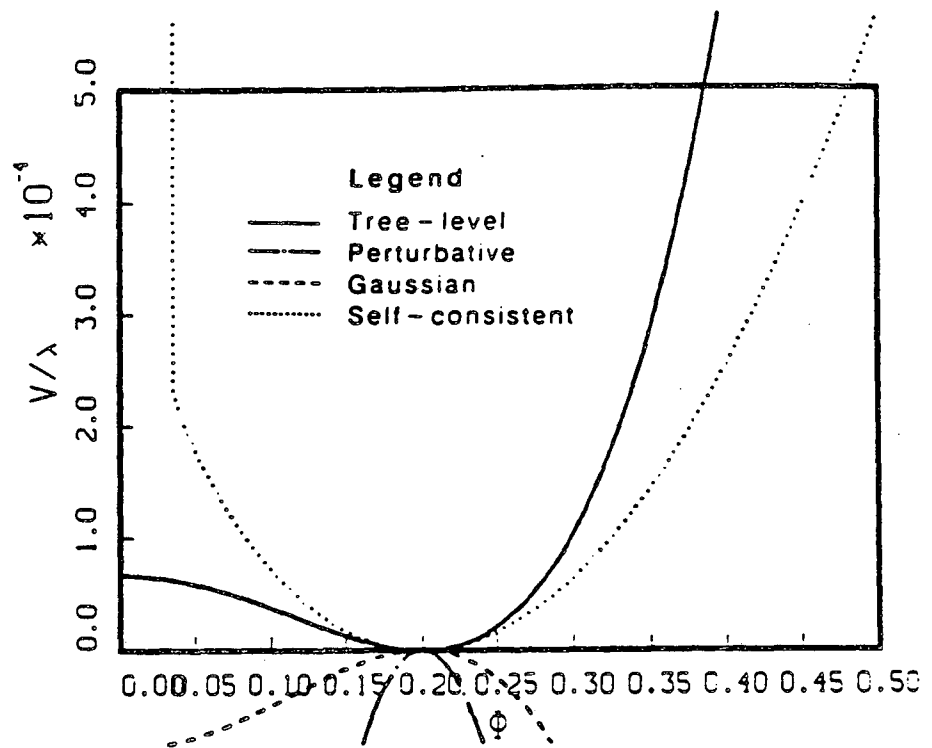
Figure (7.1): Plot of one-loop approximation to $V(\Phi)$, in the broken phase, at $F = .2$.

Figure (7.2): Plot of one-loop approximation to $V(\Phi)$, in the broken phase, at $F = .4$.

Figure (7.3): Plot of one-loop approximation to $V(\Phi)$, in the broken phase, at $F = .6$.
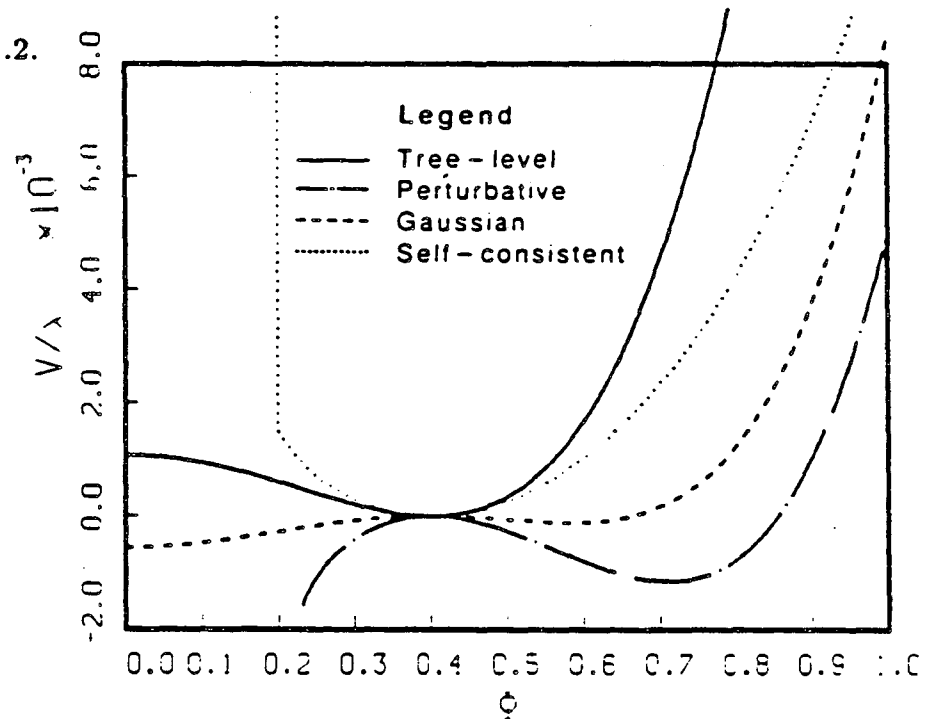

Figure (7.4): Plot of one-loop approximation to $V(\Phi)$, in the broken phase, at $F = .8$.
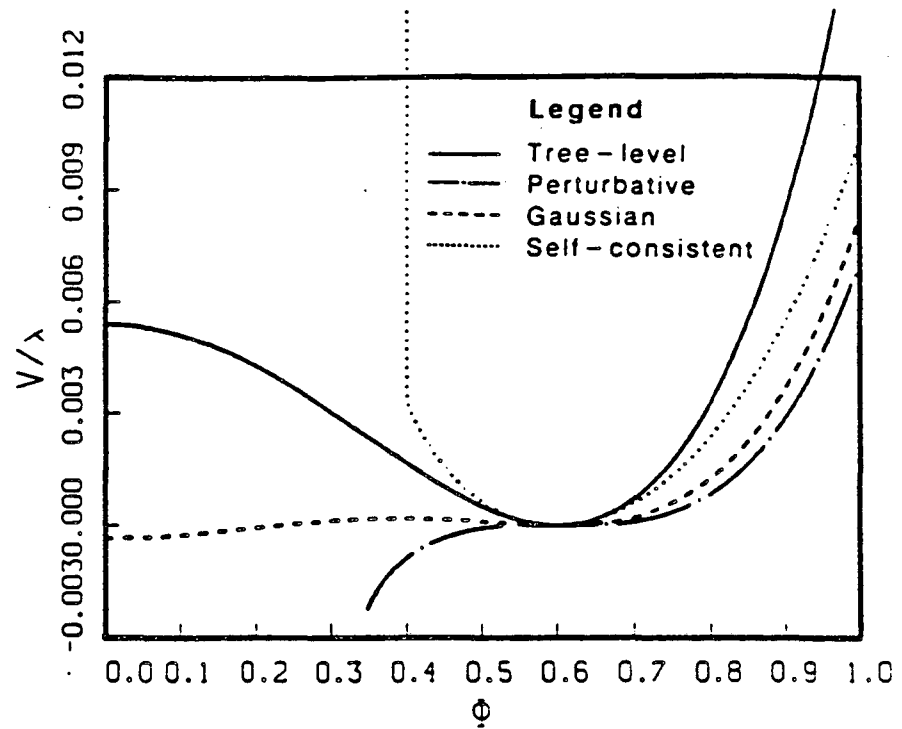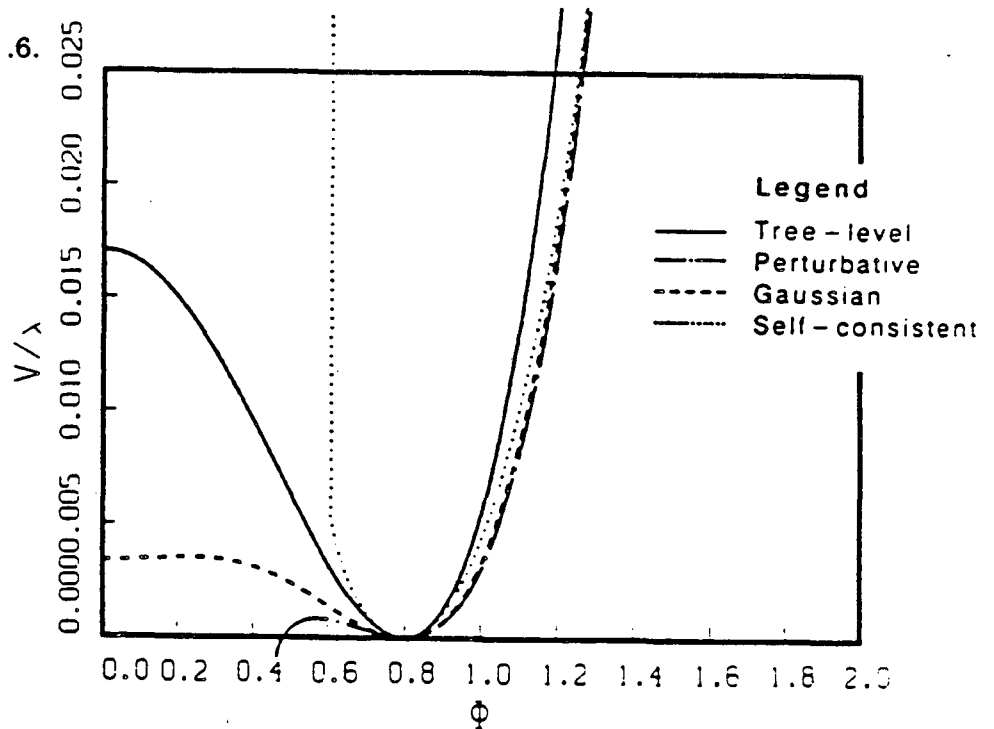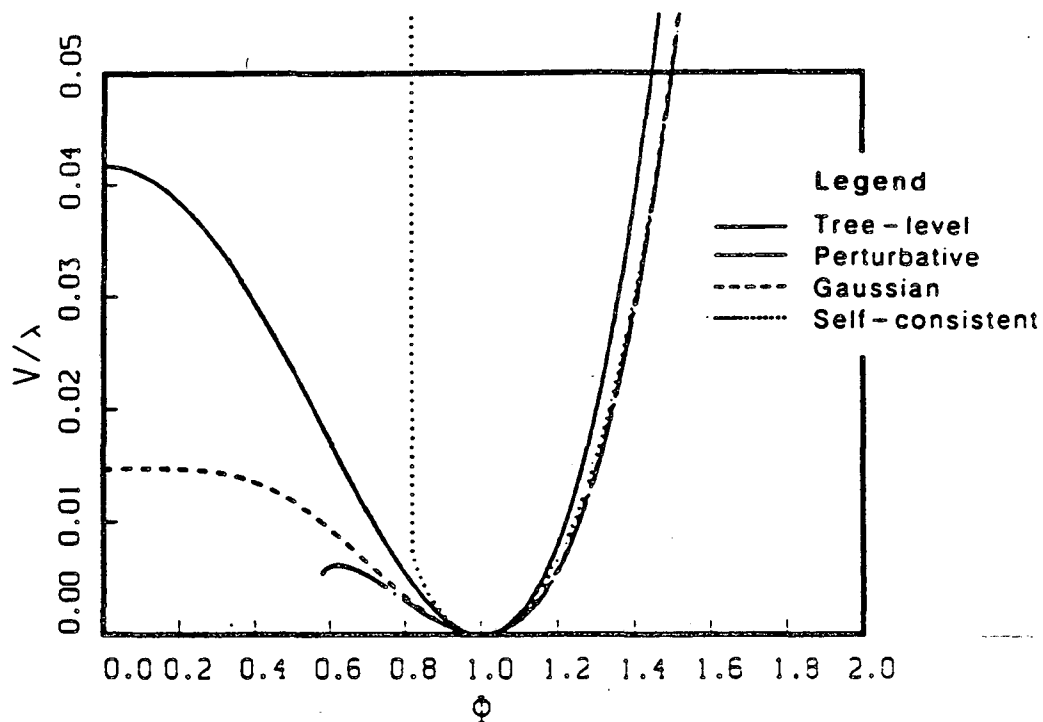
Figure (7.5): Plot of one-loop approximation to $V(\Phi)$, in the broken phase, at $F = 1$.
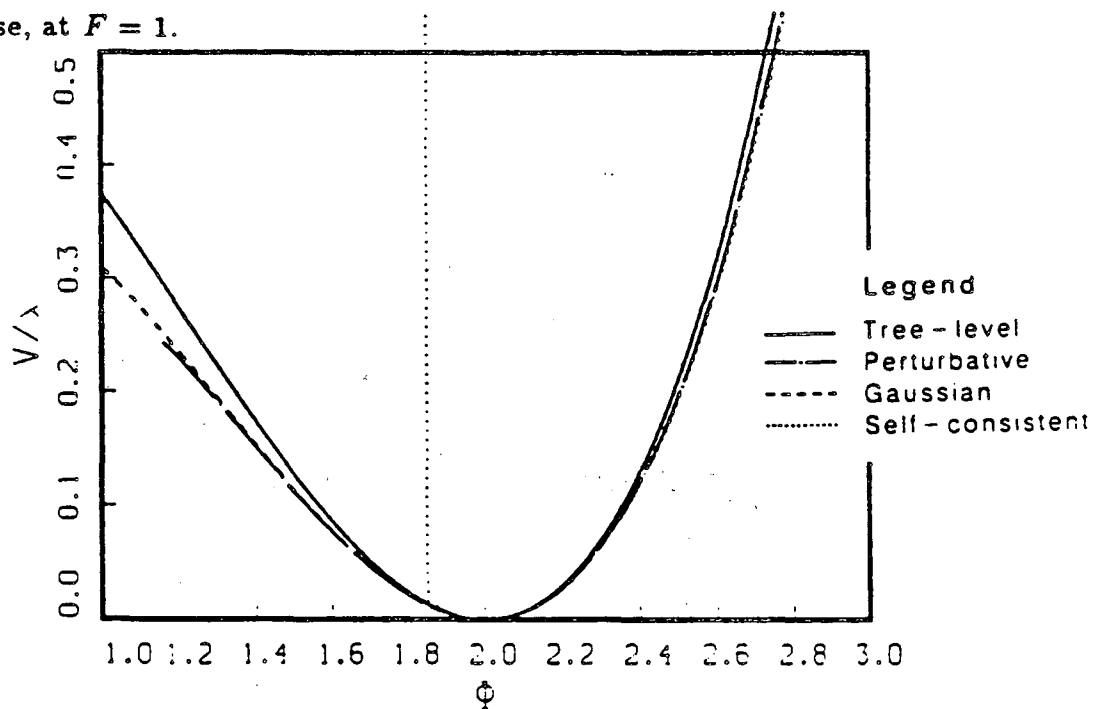

Figure (7.6): Plot of one-loop approximation to $V(\Phi)$, in the broken phase, at $F = 2$.

VIII   Conclusion

1   A Look Backward

In this subsection, I will briefly review this thesis.

Sections 1, 2 and 3 were devoted to reviewing, respectively, the effective action, ϕ_2^4 theory, and the Schwinger-Dyson equations.

In Section 4, I began by computing the well-known one-loop effective potential for ϕ_2^4 using an intentionally methodical procedure. I then showed that this procedure could be used to obtain almost instantly the Gaussian approximation, a well-known non-perturbative tool.

The fact that a perturbative procedure could be souped-up to yield non-perturbative information motivated me to look for improvements. I found several. These improvements fall into three categories:

1. Development of a better propagator, the self-consistent propagator, (which filled out Section 4).

2. Extension to higher-order terms in the derivative expansion, with $Z(\Phi)$ as the prototype, (which occupied all of Section 5).

3. Extension to higher orders in the loop-expansion, exemplified by a two-loop calculation, (which took up the first two subsections of Section 6).

It is important to note that these improvements can be mixed. One could, for

example, use the self-consistent propagator to compute $Z(\Phi)$ to two loops.

A large number of numerical results are plotted at the ends of Sections 4, 5 and 6. My purpose in displaying these graphs was to test the reliability of the various approximations. Comparison of the plots suggested an improved, self-consistent, two-loop procedure for the effective potential which appears to be reliable up to around $\tilde{\lambda} \sim 50$. Surprisingly, even the one-loop self-consistent effective potential turned out to be fairly accurate for this range of $\tilde{\lambda}$. This analysis rounded out Section 6.

In Section 7, I examined the broken-symmetry phase of the model using the perturbative, Gaussian and self-consistent propagators in the one-loop approximation. Again, the self-consistent propagator came out the clear winner. It correctly yielded a convex effective potential and a second-order phase transition, contrary to the perturbative and Gaussian propagators.

Some general comments are in order here. We have learned nothing new about ϕ_2^4. But we *have* learned some interesting facts about field theory in general. We have learned how to make systematic improvements in the Gaussian approximation. More importantly, (in my opinion), we have found a new non-perturbative technique, the self-consistent approximation, which seems to work very well even at the one-loop level. It has the important property that the self-consistent effective potential is automatically convex (when it exists). In the symmetric phase, it correctly approaches a flat-

bottomed well, while in the broken phase, it correctly shows a second-order phase transition. (However, in neither phase can accurate calculations be made at the critical point, $\tilde{\lambda} \to \infty$.)

I conclude that the self-consistent approximation is visibly superior to the Gaussian approximation, which in turn is unquestionably better than the perturbative approximation. Moreover, both approximations can be systematically improved to stay ahead of the perturbative approximation to all orders in the loop-expansion.

2   A Look Forward

In this subsection, I will discuss some possible future applications of the techniques I have developed here. I will consider in turn applications to the effective potential, and applications to higher-order terms in the derivative expansion of the effective action.

First, it should be clear that the techniques of this paper apply immediately to any massive scalar theory. In particular, ϕ_3^6 theory, the Liouville model and the sine-Gordon model would be straightforward. (A partial step has already been made for the sine-Gordon model, with surprisingly clean results [16, 12].) It would also be interesting to examine ϕ_4^4, to see whether Stevenson's (one-loop) Gaussian results can be improved. I believe that nonlinear σ-models could also be studied, by introducing Lagrange multipliers

into the action to eliminate the constraints. Also, it would not be too difficult to check the conclusions of Coleman and Weinberg [5] for scalar electrodynamics. This has already been done using the Gaussian approximation [32], so it would only be necessary to work out the details for the self-consistent approximation.

We have seen that one can improve the loop-expansion by modifying the propagator. Is it possible to get further improvements by also modifying the vertices? For example, one might try

$$\Gamma_{xyz} = V'''(\Phi)\delta_{xy}\delta_{xz}, \quad \text{etc.}$$

This does not seem to work very well. There are two reasons for this. For one thing, it introduces field-dependent divergences, just as we saw when we used $\mu^2 = V''/Z$ in Section 6. Thus, one can really only use this improved vertex in finite subdiagrams. A more compelling difficulty is that the differential equation for V'' becomes second-order and highly non-linear. The headaches involved in solving this equation seem to outweigh the (as yet unseen) advantages it might have.

An ambitious task would be to extend my techniques to gauge theories. This is non-trivial. In QCD, for example, it would be ill-advised to compute the effective potential in terms of the mean quark and gluon fields. Instead of these, one should use as variables the quark and gluon condensates $\langle \bar{\psi}\psi \rangle$ and $\langle \mathrm{Tr}F^2 \rangle$, which have proven so useful in the QCD sum-rule approach [33,

34]. Furthermore, the momentum dependence of the propagator is certain to be far more complicated than that in the simple model considered in this thesis.

Turning now to higher-order terms in the derivative expansion of the effective action, we note that the standard method of computation [35] is somewhat clumsy. Recent work has made the calculation easier (see, e.g., [36] and the many references contained therein), but the results are restricted to one-loop. The procedure I have outlined in Section 5 is more convenient than that of Ref. [35], but I am unsure how it compares to the more recent methods. In any event, my method can be easily modified to yield non-perturbative results, as we have seen repeatedly throughout this thesis.

Ultimately, one would like to work out a low-energy effective action for QCD, describing mesons and (via the Skyrme model [37, 38]) baryons. One can easily write down the most general form of such an effective action. One can even decide which terms are the most important, via the large-N expansion [39, 40]. However, the coefficients of these terms cannot yet be computed theoretically; they are determined phenomenologically, by comparison to the scattering data. Lattice methods may well be the only way of calculating these coefficients. However, it would be better if there were a less numerically intensive technique available. Some form of the accelerated loop-expansion might prove useful in approaching this problem.

References

[1] G. Jona-Lasinio, Nuov. Cim. 34 (1964), 1790.

[2] R.W. Haymaker and J. Perez-Mercader, Phys. Rev. D27 (1983), 1948.

[3] K. Symanzik, Comm. Math. Phys. 16 (1970), 48.

[4] D.J.E. Calloway and D.J. Maloof, Phys. Rev. D27, (1983), 406.

[5] S. Coleman and E. Weinberg, Phys. Rev. D7 (1973), 1888.

[6] . R. Jackiw, Phys. Rev. D9 (1974), 1686.

[7] J.M. Cornwall, R. Jackiw and E. Tomboulis, Phys. Rev. D10 (1974), 2428.

[8] T. Barnes and G.I. Ghandour, Phys. Rev. D28 (1980), 924.

[9] R. Jackiw in "Theories and Experiments in High-Energy Physics" (Orbis Scientiae II), edited by B. Korsunoglu, A. Perlmutter and S.M. Widmayer, (Plenum, New York), 1975, p. 371.

[10] P.M. Stevenson, Phys. Rev. D30 (1984), 1712; Phys. Rev. D32 (1985), 1389; P.M. Stevenson and I. Roditi, Phys. Rev. D33 (1986), 2305.

[11] M. Altenbokum and U. Kaulfuss, preprint ILL-(TH)-86-13, (1986).

[12] U. Kaulfuss, M. Altenbokum, preprint ILL-(TH)-31, (1986).

[13] C.S. Hsue, H. Kümmel and P. Ueberholz, Phys. Rev. D32 (1985), 1435.

[14] W.A. Bardeen and M. Moshe, Phys. Rev. D28 (1983), 1372.

[15] S. Coleman, Phys. Rev. D11 (1975), 2088.

[16] R. Ingermanson, Nucl. Phys. B266 (1986), 620.

[17] R. Ingermanson, preprint LBL-20844, (1986).

[18] M. Altenbokum, U. Kaulfuss, J.J.M. Verbaarschot, preprint ILL-(TH)-33, (1986).

[19] Y. Fujimoto, L. O'Raifeartaigh and G. Parravacini, Nucl. Phys. B212 (1983), 268.

[20] R.H. Brandenberger, Rev. Mod. Phys. 57, (1985), 1.

[21] J. Taron and R. Tarrach, preprint UBFT-FP-11-85, (1985).

[22] M. Consoli and A. Ciancitto, Nucl. Phys. B254 (1985), 653.

[23] A.J. Niemi and G.W. Semenoff, Phys. Rep. 135 (1986), 101.

[24] S. Coleman, Comm. Math. Phys. 31 (1973), 259.

[25] S.-J. Chang, Phys. Rev. D13 (1976), 2778.

[26] B. Simon and R.B. Griffiths, Comm. Math. Phys. 33, (1973), 145.

[27] S.-J. Chang, Phys. Rev. D12 (1975), 1071.

[28] S.D. Drell, M. Weinstein and S. Yankielowicz, Phys. Rev. D14 (1976). 487.

[29] J.S. Langer, Ann. Phys. (N.Y.) 41 (1967), 108; 54 (1969), 258.

[30] For the modern development given here, and references to the original

papers by Dyson and by Schwinger, see, e.g., C. Itzykson and J.-B. Zuber, "Quantum Field Theory", (McGraw Hill), 1980, p. 475.

[31] J. Wess and B. Zumino, Phys. Lett. 37B (1971), 95.

[32] P. Cea, Phys. Lett. 165B (1985), 197.

[33] L.J. Reinders, H. Rubinstein and S. Yazaki, Phys. Rep. 127 (1985), 1.

[34] M.A. Shifman, A.I. Vainshtein and V.I. Zakharov, Nucl. Phys. B147 (1970), 385; 448.

[35] J. Iliopoulos, C. Itzykson and A. Martin, Rev. Mod. Phys. 47 (1975), 1.

[36] J. Zuk, Phys. Rev. D33 (1986), 3645.

[37] T.H.R. Skyrme, Proc.Roy. Soc. A260 (1961), 127.

[38] G.S. Adkins, C.R. Nappi and E. Witten, Nucl. Phys. B228 (1983), 552.

[39] G. t'Hooft, Nucl. Phys. B72 (1974), 461; Nucl. Phys. B75 (1974). 461.

[40] E. Witten, Nucl. Phys. B160 (1979), 57.